UNIVERSITY OF CALIFORNIA
SANTA CRUZ

ROLE OF IRON AND ISCR IN THE REGULATION OF *YERSINIA PSEUDOTUBERCULOSIS* PATHOGENESIS

A dissertation submitted in partial satisfaction
of the requirements for the degree of

DOCTOR OF PHILOSOPHY

in

MOLECULAR, CELLULAR, and DEVELOPMENTAL BIOLOGY

by

Leah Schwiesow

June 2017

The Dissertation of Leah Schwiesow is approved:

_____
Professor Fitnat Yildiz

_____
Professor Martha Zúñiga

_____
Professor Donald Smith

_____
Professor Victoria Auerbuch Stone

_____
Tyrus Miller
Dean of Graduate Studies

TABLE OF CONTENTS

LIST OF FIGURES AND TABLES

Chapter 1

Chapter 2

Chapter 3

Chapter 4

ABSTRACT

Leah Schwiesow

Role of Iron and IscR in the Regulation of *Yersinia pseudotuberculosis* Pathogenesis

Previous studies suggested that the transcription factor, IscR, positively regulates the main virulence determinant in *Yersinia pseudotuberculosis*: the type III secretion system (T3SS). IscR in *E. coli* is an iron-sulfur [2Fe-2S] cluster coordinating global transcriptional regulator that has been shown to bind different DNA target sequences dependent upon [2Fe-2S] coordination. When bound to a [2Fe-2S] cluster, Holo-IscR can bind both a Motif I or Motif II IscR binding site, however, clusterless IscR, or Apo-IscR, can only bind a Motif II site. Given that the Fe-S cluster status of IscR changes in response to environmental signals such as oxygen tension, iron levels, and oxidative stress, we hypothesized that *Yersinia pseudotuberculosis* senses changes in these signals within the host through IscR to optimize expression of virulence factors. The first part of this work used two mouse models of hereditary hemochromatosis to determine how altered iron environments influence *Yersinia pseudotuberculosis* pathogenesis and T3SS expression in the host. We and others found that although the T3SS is required to cause disease in healthy mice, it is less critical in mice with hereditary hemochromatosis, suggesting that *Yersinia* pathogenesis is fundamentally different in these iron overloaded animals. The second goal of my dissertation research was to determine the role of IscR in processes potentially important for

virulence in *Yersinia pseudotuberculosis* and independent of the T3SS. We showed that IscR plays a role in regulation of a heme uptake system in *Yersinia pseudotuberculosis* and is involved in *Yersinia pseudotuberculosis* survival in blood. The third and final goal of this work was was to determine the impact of the IscR Motif II site in the promoter of *lcrF*, the *Yersinia* T3SS master regulator, on type III secretion and virulence. Our data show that suggest that this site is essential for optimal environmental control of the *lcrF* promoter by IscR *in vivo* .

DEDICATION AND ACKNOWLEDGEMENTS

I would like to thank my advisor Vicki Auerbuch Stone- You have been an extremely supportive advisor and great example of a professional scientist. You pushed me when I needed to be pushed, and allowed me to become a more independent scientist when I was ready. Working in your lab under your guidance has set me up for a future in a career I'm really excited about, and I will be forever grateful.

I would like to thank my parents- You have always been supportive of my graduate career regardless of whether you understood it or not- and you always were willing to talk to me on the phone when I was having a bad day even though you were 700 miles away.

I would like to thank all my past and current lab mates- All of you were always there with smart scientific ideas when I was in a rut and made my time in the lab fun.

Lastly, I would like to thank my husband, Omar- I simply do not know how I would have gotten through graduate school without you and I'm excited to start the next chapter of our lives. I love you.

Chapters 1, 2, and 3 of this dissertation are multi-author works. I am responsible for all the figures except: Figure 1 of Chapter 1, Figure 2 of Chapter 2 and Figures 2, 3, 4

and 5 of Chapter 3. Chapter 2 of this dissertation is a co-first author work and I contributed work equally on Figures 1, 3, and 4.

CHAPTER 1

The *Yersinia* Type III Secretion System Regulator, LcrF

By Leah Schwiesow, Hanh Lam, Petra Dersch and Victoria Auerbuch

ABSTRACT

Many Gram-negative pathogens express a type III secretion system to enable growth and survival within a host. The three human pathogenic *Yersinia* species, *Y. pestis*, *Y. pseudotuberculosis*, and *Y. enterocolitica*, encode the Ysc T3SS whose expression is controlled by an AraC-like master regulator called LcrF. In this review, we discuss LcrF structure and function as well as the environmental cues and pathways known to regulate LcrF expression. In addition, we discuss similarities between LcrF control of the Ysc T3SS and T3SS regulation in several other pathogens in response to temperature, oxygen tension, and iron availability.

INTRODUCTION

There are three *Yersinia* species pathogenic to humans. *Y. pestis* is the causative agent of bubonic and pneumonic plague, and is transmitted through the flea vector or through airborne transmission from one mammalian host to another (1). In contrast, the enteropathogenic *Yersinia*, *Y. enterocolitica* and *Y. pseudotuberculosis*, grow in the environment, but can be transmitted to mammalian hosts through ingestion of contaminated food or water (1). *Y. enterocolitica* and *Y. pseudotuberculosis* cause a typically self-limiting mesenteric lymphadenitis or gastroenteritis in otherwise healthy individuals, but can cause a serious blood-borne infection in people with iron overload disorders such as hereditary hemochromatosis (2). In addition, sequelae following enteropathogenic *Yersinia* infection, such as erythema nodosum and reactive arthritis, have also been reported (3-5).

Human pathogenic *Yersinia* species share in common a virulence plasmid, called pCD1 in *Y. pestis* and pYV in enteropathogenic *yersiniae*, encoding the Ysc type III secretion system (T3SS) essential for causing disease (6). These 70 kb plasmids encode dozens of T3SS structural genes, five or six T3SS effector proteins called Yops and their dedicated chaperones, as well as genes encoding proteins involved in regulating expression and function of the T3SS. One of these regulatory proteins, LcrF, serves as the *Yersinia* T3SS master regulator, controlling transcription of a large number of plasmid-encoded genes. Several environmental cues may influence expression of LcrF itself, possibly enabling *Yersinia* to control T3SS expression during transition from one niche to another. Recent reviews have highlighted important advances in our understanding of T3SS structure and modulation of the innate immune response by T3SS effector proteins (7). In this review, we focus on LcrF expression and activity as well as how LcrF influences *Yersinia* pathogenesis, and provide a comparison to T3SS master regulators found in other pathogens.

LCRF HISTORY, STRUCTURE, AND FUNCTION

It has long been appreciated that human pathogenic *Yersinia* encoding T3SS genes require millimolar concentrations of calcium to grow at 37˚C, and this phenomenon was termed the low-calcium response, or Lcr (8, 9). The absence of calcium in combination with a shift to 37˚C triggers secretion of T3SS effector proteins, mimicking the effect of host cell contact. The reason behind why calcium ions are involved in regulation of Yop secretion remains unclear. However, a number of T3SS

genes were originally named for the low-calcium response, as mutations in these genes were shown to alter the Lcr phenotype (10, 11).

LcrF was first identified in *Y. pestis* by Goguen and colleagues as a gene required for thermal induction of several pCD1 genes (12). Using a similar approach, VirF, the *Y. entercolitica* LcrF homolog, was discovered (13). Lastly, while sequence analysis of *Y. pestis*, *Y. enterocolitica*, and *Y. pseudotuberculosis* virulence plasmids revealed evidence of several rearrangements, the low-calcium response at 37˚C was found to be highly conserved in all three species, suggesting the presence of LcrF in *Y. pseudotuberculosis* as well (14). In this review, we will refer to the regulator as LcrF unless specifically referring to the *Y. enterocolitica* VirF homolog.

LcrF/VirF is a 30 kD AraC-like protein that shares homology with AraC in its carboxy terminal DNA-binding region (15). AraC is well known in *Escherichia coli* for its role as a DNA-binding transcriptional regulator (reviewed in (16)). Early on, *Y. pestis* LcrF and *Y. enterocolitica* VirF were shown to bind directly to sequences in the *yopE* and *yopH* promoters using gel shift assays (17). The amino-terminal domains for AraC-like proteins have been shown to be involved in self-association. Additionally, the amino-terminal domain of several AraC-like proteins binds cofactors that influence the ability of the protein to regulate transcription (16). For example, binding of the cofactor arabinose to *E. coli* AraC induces a conformational change, allowing AraC to activate transcription (16). It is thought that LcrF exists as a dimer in solution through self-association of its amino-terminal domain; however,

unlike *E. coli* AraC, the amino-terminal domain of LcrF has not been shown to bind additional cofactors.

As in all other AraC family transcriptional regulators, the carboxy-terminal DNA-binding region of LcrF contains two helix-turn-helix (HTH) domains (18). Like all HTH domains, the recognition helix binds specific DNA residues within the major groove (19). DNA binding sites of LcrF and its homologs have been experimentally investigated in a number of studies (15-17, 20, 21). The first study using DNase protection assays on promoters of genes activated by LcrF/VirF suggested a common DNA binding motif: TTTTaGYcTgTat, where capital letters represent more highly conserved residues and Y stands for C or T (17). Wattiau and Cornelis identified this 'half site' upstream of several T3SS genes. However, these proposed LcrF binding sites were highly variable in terms of distance from the transcriptional start site, directionality, and distance of half-sites from each other (17). In a recent analysis, King et al. observed that the C-terminal domain HTH DNA binding domain of LcrF/VirF is nearly identical to the DNA-binding region of the homologous AraC-like master regulator of the *Pseudomonas aeruginosa* T3SS, the protein ExsA (18). The authors further showed that *Y. pestis* LcrF binds and activates ExsA-dependent promoters in *P. aeruginosa*. Similarly, ExsA was able to induce T3SS genes in *Y. pestis* in the absence of LcrF (18). Both LcrF and ExsA were shown to interact with a common nucleotide sequence motif (AaAAAnwnMygrCynnnmYTGyaAk), which is also recognized by activators of T3SS genes from *Photorhabdus luminescencs, Aeromonas hydrophilus*, and *Vibrio parahaemolyticus* (W stands for A or T; M, A or

C; Y, C or T; R, A or G; K, G or T with uppercase letters representing more highly conserved residues)(18, 21, 22).

To reconcile these two dissimilarly presented LcrF consensus binding sites, we attempted to align the promoter regions of genes known to be controlled by LcrF. First, all previously identified LcrF binding site sequences from the *virA*, *virB*, *virC*, *yopE*, *lcrG*, and *yopH* promoters, as well as known ExsA binding sites from *P. aeruginosa* were input into MEME motif discovery to identify a consensus motif (23). The resulting motif was subsequently used to search against the virulence plasmids of the three human pathogenic *Yersinia* species to identify all putative LcrF binding sites using FIMO (Find Individual Motif Occurrences), where motifs were called with a p-value threshold less than 0.0001 (24). Alignment of LcrF binding sites of selected genes (Figure 1A) shows a 5'- AAAA - N_{5-10} - GNCT - N_{15-19} - TGANA - 3' motif located 20 to 21 bp upstream of the predicted -10 TATA box for most genes. This consensus motif is similar to that of ExsA described above. Sequences containing these motifs 20-21 bp upstream of the -10 TATA box overlap well with regions found experimentally to bind LcrF or ExsA (Figure 1A, underlined) (15-17, 20, 21)). In the case of the *yopH* and *sycE* genes, a second 5'- AAAA - N_{5-10} - GNCT - N_{15-19} - TGANA -3' motif was found further upstream and coincided with regions previously shown to be weakly bound by LcrF (Figure 1A, dashed underlines) (17)).

A closer look at the *yopE* promoter revealed surprising features that required clarification. A putative LcrF binding site within the *yopE* promoter was not located 20 to 21 bp upstream of a -10 TATA box (Figure 1B), as are the majority of putative

LcrF sites, but overlaps the annotated translational start site of *yopE* (Figure 1A). The -10 region of *yopE* is, however, probably located 30 bp upstream of the translational start site, which is 12 bp upstream of the transcriptional start site (black arrow in Figure 1B) (25). Because of this departure from other known LcrF binding sites, whether this putative LcrF binding site is functional remains to be justified. Interestingly, Wattiau and Cornelis identified two different regions further upstream from *Y. enterocolitica yopE* that were protected by VirF during DNAse I footprinting (Figure 1B in blue boxes)(17). These regions contain sequences that are the reverse complement of the 5'- AAAA - N_{5-10} - GNCT - N_{15-19} - TGANA -3' motif. Because *sycE* and *yopE* are located in close proximity but are transcribed in opposite directions, we propose that the two protected regions upstream of *yopE*, one strongly bound by VirF (underlined by solid line in Figure 1B) and the other weakly bound (underlined by dashed lines in Figure 1B) (17), are in fact LcrF binding motifs on the reverse DNA strand, belonging to the *sycE* promoter. This LcrF binding site phenomenon of two adjacent, co-regulated but divergent genes can also be evidenced in the case of *virA* and *virB* (blue solid-line box, Figure 1A).

Putative LcrF binding sites appear in a number of locations in the virulence plasmids of *Yersinia*. As shown in Figure 1A, a 5'- AAAA - N_{5-10} - GNCT - N_{15-19} - TGANA -3' motif was found within the *sycE, yopO*, *yadA*, *yopK*, *sycH*, *yscH*, and *yscC* promoters. The transcriptional dependence of *yadA* on LcrF was previously demonstrated in a transcriptional reporter assay in *Y. pseudotuberculosis* (26). It is worth mentioning that we could not find LcrF binding sites upstream of two secreted

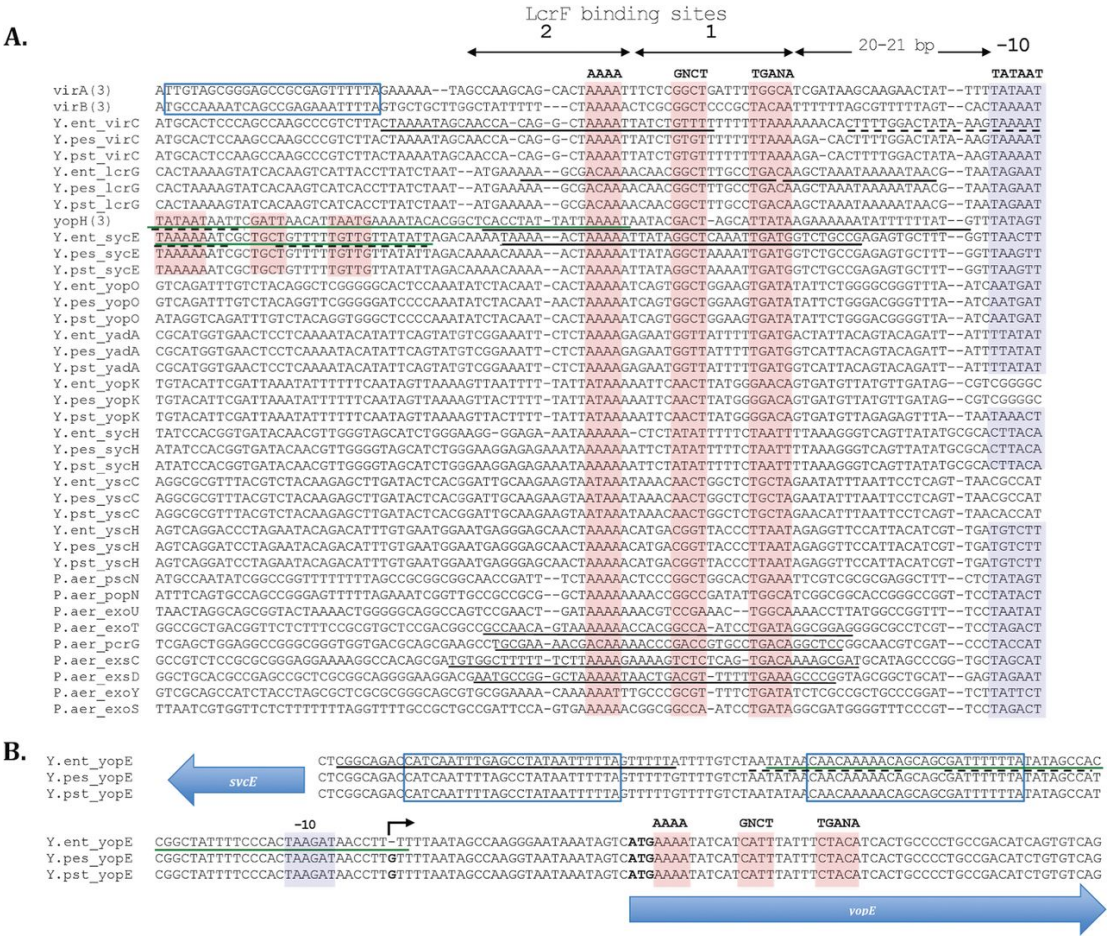

Figure 1: Alignment of verified and putative LcrF and ExsA binding sites within target gene promoters. **(A)** Promoter regions of *Yersinia* and *Pseudomonas* genes controlled by LcrF or ExsA, respectively, were aligned using Seaview (131). Sequences are from *Y. enterocolitica* 8081 (NC 008791), *Y. pestis* CO92 (NC 003131), *Y. pseudotuberculosis* IP 32953 (NC 006153), *P. aeruginosa* (NC 002516) and *P. aeruginosa* UCBPP PA14 (NC 008463). Predicted -10 regions are highlighted in blue. Identified 5'- AAAA - $N_{5\text{-}10}$ - GNCT - $N_{15\text{-}19}$ - TGANA -3' consensus sites containing three conserved regions are highlighted in red and the conserved nucleotides at each position of the motif are denoted in bold above the alignment,

with uppercase letter denoting highly conserved residues, and lowercase letters denoting more degenerate residues. The sequence of *virA*, *virB*, and *yopH* promoters from all three *Yersinia* species are identical, and thus a single sequence is shown (3). *VirA* and *virB* are proximal, but divergently encoded. Thus, we propose that what appears to be an inverted 5'- AAAA - N_{5-10} - GNCT - N_{15-19} - TGANA -3' motif upstream of the *virA* and *virB* promoters (blue solid-line box) actually belongs to the divergent *virB* or *virA* promoter, respectively. *YopH* and *sycE* have two tandem 5'- AAAA - N_{5-10} - GNCT - N_{15-19} - TGANA -3' motifs (both highlighted in red), which overlap with the protected regions identified by Wattiau and Cornelis (17). **(B)** Sequences upstream of *Yersinia yopE* were aligned using Seaview. Two regions containing inverted 5'- AAAA - N_{5-10} - GNCT - N_{15-19} - TGANA -3' motifs are outlined in blue boxes, which we propose belong to *sycE*. The putative translational *yopE* start site is denoted in bold. YtxR binding sites upstream of *yopH* (A) and *yopE* (B) are underlined in green (34). **(A, B)** Regions experimentally found to be strongly bound by LcrF/VirF or ExsA are underlined with solid lines and those found to be weakly bound are underlined with dashed lines (17). Identified LcrF binding site is highlighted in red and the conserved nucleotides are denoted in bold above the alignment, with uppercase letter denoting highly conserved residues, and lowercase letters denoting more degenerate residues.

effectors, *yopJ* and *yopM* unless the threshold for motif calling was much lower (data not shown). Note also that *yscC* and *yopK* (from *Y. enterocolitica* and *Y. pestis*) do not seem to have a consensus TATA box following the -35 region.

It appears that both LcrF/VirF- and ExsA-regulated genes have similar consensus binding motifs. The -35 box (TGANA) is conserved and thought to bind one of the two monomers of the activators (20). Notably, the distance between -10 and -35 regions of LcrF and ExsA-dependent genes is 4-5 bp longer than that seen in typical σ^{70}-dependent promoters. It was shown, however, that this spacer length is required for most, but not all, ExsA-dependent transcriptional activation (27).

Despite the resemblance in consensus binding sequence, the oligomeric state of the LcrF and ExsA during DNA binding as well as their binding properties are distinct, leading to differences in DNA-binding specificity and kinetics of transcriptional activation. King et al. (18) showed that ExsA is predominantly monomeric in solution and two molecules are sequentially recruited to target promoters and generate two higher-order DNA-protein complexes to activate T3SS genes, whereas LcrF is dimeric and results only in the formation of one large higher DNA-protein complex (28). In addition, LcrF-induced promoter bending is more pronounced and may account for its overall higher activator activity (2.5-20-fold) relative to ExsA (18, 22). Lower basal activity of ExsA could be compensated by the positive autoregulatory feedback loop, which leads to a rapid increase of ExsA under inducing conditions (29). While mutations in critical residues within the major groove disrupted both LcrF and ExsA DNA binding, LcrF, but not ExsA, was able to tolerate

certain mutations within the DNA binding motif, presumably because LcrF binds DNA as a preformed dimer and not in the sequential, ordered manner seen with ExsA monomers (18). Indeed, an LcrF mutant unable to dimerize was shown to bind to each half-site but, similar to ExsA, was more sensitive to mutations within the DNA (18). King et al. also suggested that due to its preformed dimeric state, LcrF could activate transcription of genes more rapidly than ExsA (18).

REGULATION OF LCRF TARGET GENES

To date, LcrF/VirF is the only characterized transcriptional activator of T3SS genes in pathogenic *Yersinia*, and all known LcrF targets genes are encoded on pCD1/pYV. Several groups have shown transcriptional activation or direct binding of LcrF to the promoter regions of *yopE, yopH, yadA*, and *ylpA* genes as well as the *yopBD-lcrGVH* and *virC* operons, which encode T3SS effector, regulatory, and structural proteins as well as the YadA adhesin and the YlpA lipoprotein (17, 20, 26, 30-33).

Several reports have suggested that regulation of T3SS genes can be mediated by proteins antagonizing LcrF (34, 35). Darwin and colleagues identified YtxR as a global transcriptional regulator that is conserved in all human pathogenic *Yersinia* species. Overexpression of YtxR rendered *Yersinia* defective in secretion of Yops into the bacterial culture supernatant (34). Using a DNase footprinting approach, the authors showed that YtxR protected specific regions in the *yopE/sycE* and *yopH* promoters that overlapped with known LcrF binding sites (denoted by green lines in Figure 1A), suggesting that YtxR competes with LcrF for binding to T3SS gene promoters (34). While YtxR may introduce an additional layer of regulation to T3SS

gene expression, the environmental conditions under which YtxR is expressed have yet to be elucidated (34).

Recently, Li et al. proposed another model in which the pYV-encoded regulatory protein LcrQ inhibits LcrF activity (35). *Y. pseudotuberculosis* LcrQ was first discovered as a gene required for calcium dependence at 37˚C and was shown to be secreted by the T3SS, relieving repression of Yop expression when the concentration of LcrQ in the bacterial cytoplasm decreased as a result of active secretion (36, 37). The *Y. enterocolitica* LcrQ orthologs YscM1 and YscM2 were subsequently suggested to control Yop expression dependent on pYV-encoded factors other than VirF (38). Indeed, the T3SS translocon protein YopD and its chaperone LcrH/SycD are thought to cooperate with LcrQ or YscM1/YscM2 to negatively control T3SS gene expression (39-43). LcrQ has no obvious DNA binding domain, and does not bind Yop promoter regions, as has been shown for LcrF and YtxR (35). In fact, it has been suggested that *Y. entercolitica* YscM1/YscM2, in cooperation with the YopD-LcrH complex, bind to the 5'-untranslated regions of Yop mRNAs to inhibit translation (42). However, Li et al proposed that *Y. pseudotuberculosis* LcrQ inhibits LcrF activity until the T3SS is assembled and LcrQ is secreted out of the cell. The authors showed that overexpression of LcrF mimicked the secretion profiles of a *DlcrQ* mutant. This suggested that the LcrF/LcrQ ratio may be important for activating T3SS gene transcription, but they could not detect a direct interaction of LcrF and LcrQ (35). Moreover, previous data indicated that *Y. enterocolitica* YscM1 was not capable of inhibiting VirF activity on the *yopH* promoter in the absence of

other pYV-encoded factors (38). Therefore, how LcrQ and YscM1/YscM2 repress T3SS gene expression in pathogenic *Yersinia* remains to be clarified.

TRANSCRIPTIONAL CONTROL OF LCRF

Thermoregulation and YmoA

There are several lines of evidence showing that transcription of *lcrF/virF* is strongly regulated by temperature. The first observations were made with *Y. enterocolitica*, in which an induction of a *virF-cat* fusion and a substantial increase in the abundance of the *virF* transcript was detected upon temperature upshift (15, 44). A comprehensive expression analysis revealed that the *lcrF* gene of *Y. pseudotuberculosis* is transcribed from a σ^{70}-dependent promoter located upstream of the *yscW* gene (named *virG* in *Y. enterocolitica*), which in turn is located 124 bp upstream of the *lcrF* coding sequence (Figure 2). Thermo-dependent *yscW-lcrF* transcription from this promoter is controlled by the nucleoid-associated protein YmoA with homology to the Hha protein of *E. coli* (45). YmoA, for '*Yersinia* modulator', was identified in a search for chromosomal insertion mutants of *Y. enterocolitica* transcribing *virF*, and hence VirF-dependent *yop* and *yadA* genes, at low temperatures (44). Mutations in *ymoA* led to increased *virF* and *yop* expression at 25˚C and decreased expression at 37˚C compared to the control strain, although *ymoA* mutants still induced expression of *virF* and *yop* upon temperature shift (44). Elevated expression of a *yscW-lacZ* fusion in a *ymoA* deficient *Y. pseudotuberculosis* strain further suggested that YmoA represses *yscW-lcrF* transcription from a promoter located 264 nt upstream of the start codon of *yscW* (45) (Figure 2). As YmoA dependency was lost when sequences

downstream of the *yscW* transcriptional start site were deleted, but maintained when the regulatory region upstream of the *yscW* promoter was removed, it is assumed that YmoA influences *lcrF* expression via sequences located downstream of the *yscW* promoter (45). However, even high concentrations of purified YmoA homodimers were unable to interact specifically with the *yscW* regulatory region, indicating that an additional factor contributes to YmoA-mediated repression of *yscW-lcrF* transcription at moderate temperatures (45).

The small size of YmoA, its unusual high number of charged amino acid residues, and its influence on the fragility of the chromosomal DNA suggested that YmoA is a histone-like protein involved in chromosome structure similar to H-NS, and controls *lcrF* expression through temperature-induced changes in DNA topology (44, 46, 47). Members of the Hha/YmoA protein family have a striking similarity to the oligomerization domain of the nucleoid-structuring protein H-NS and its paralogs, and were shown to interact specifically with different enterobacterial H-NS proteins (48, 49). Band shift analyses with *yscW* promoter fragments demonstrated that YmoA copurified with H-NS was able to interact specifically with the 5'-untranslated sequences of the *yscW* gene (Figure 2)(45). Therefore, heterocomplex formation of YmoA with H-NS seems responsible for the thermoregulation of the *yscW-lcrF* operon. Interestingly, H-NS alone is also able to interact with *yscW* promoter fragments (45). In this context it would be important to know how H-NS homo- and H-NS/YmoA heterodimers differ in their ability to interact with the *yscW* promoter region and how this influences expression of the *yscW-lcrF* operon in response to

temperature. Several independent attempts to construct an *hns*-deficient mutant in *Yersinia* to address this issue failed, indicating that H-NS is essential for the biological fitness of this genus (50, 51). However, DNA-binding assays comparing H-NS/H-NS and H-NS/YmoA complexes indicate that the binding affinity and specificity for the *yscW* promoter are slightly altered (Böhme & Dersch, unpublished results) (50).

It is also quite reasonable that the DNA binding ability of H-NS/H-NS and H-NS/YmoA complexes is differentially influenced by thermo-induced topological changes of the promoter and/or intrinsic conformational alterations of the regulatory proteins (52, 53). In fact, it has been reported that the DNA topology of the virulence plasmid undergoes a conformational change upon upshift to 37°C, leading to significant derepression of *virF/lcrF* expression (15, 31, 54, 55). Rohde et al. observed that *Y. entercolitica* mutants resistant to the DNA gyrase inhibitor novobiocin constitutively expressed Yops, similar to a *DymoA* mutant (55). Using a 2-D gel based assay, the authors identified several DNA intrinsic bends in the pYV plasmid. Interestingly, the presence of a DNA bend was identified within the intergenic region between the *yscW* and *virF* genes (Figure 2). This bend was shown to melt at 37˚C, suggesting that this intrinsic bend could potentially inhibit transcription of *virF* at non-inducing temperatures (55).

Lastly, YmoA of *Y. pestis* and *Y. pseudotuberculosis* is subject to proteolysis by the Lon and ClpP proteases at 37°C, but not at moderate temperatures (<30°C) (45, 53). As a result, YmoA-mediated repression of the *yscW-lcrF* operon is rapidly

eliminated at 37°C to induce the T3SS, but remains repressed at all temperatures in a *clpP/lon* deletion mutant (53). Nevertheless, LcrF synthesis is still significantly enhanced in a *ymoA* deficient strain at body temperature compared to 25°C. This demonstrates that the contribution of the thermo-labile modulator YmoA to thermal control of *lcrF* is quite small and mainly promoted by a YmoA-independent RNA thermometer (see below).

Cross-Regulation with Flagellar System

Many *Yersinia* flagellar genes, including the alternative flagellar-specific sigma factor s^{28} encoded by *fliA,* are strictly controlled by temperature. In contrast to T3SS genes, they are only upregulated at moderate temperatures and repressed at body temperature (56). *Yersinia* likely utilizes flagellar motility in the environment at temperatures under 37˚C and does not require the T3SS prior to transmission into a mammalian host. This suggests an inverse regulation of flagellar and T3SS genes and some evidence exists that s^{28}/FliA is crucial for this process (57). Through microarray analysis comparing *Y. enterocolitica* wildtype and a *DfliA* mutant, several pYV-encoded genes such as *virF* were found to be upregulated in the *DfliA* mutant at 25˚C (57). Furthermore, a putative binding site for FliA was identified in the *virF* promoter (57), suggesting that FliA binds to the *virF* promoter to repress transcription under temperatures that induce flagellar expression and assembly (57). However, we could not identify the putative FliA site described by Horne and Prüß within the *virF* upstream region either by scanning for the exact FliA binding site sequence suggested by the authors, or by using known FliA binding sites to make a motif model to search

against the *Y. enterocolitica* genome (unpublished observations). While a discernible FliA motif may not be present in the *virF* promoter region in the current *Y. enterocolitica* genome assembly, the discrepancy might be due to differences between the current genome assembly and the one used in Horne and Prüß. Interestingly, *Y. pseudotuberculosis* lacking the RNA chaperone Hfq is hypermotile but defective in type III secretion (58). Thus, further studies are needed to identify the mechanism(s) involved in maintaining this inverse relationship between flagellar motilify and T3SS expression.

IscR

It has been recently suggested that LcrF might be affected by environmental signals other than temperature. Through a forward genetic screen for modulators of the *Y. pseudotuberculosis* T3SS, the iron-sulfur cluster coordinating transcription regulator IscR was identified as important for type III secretion and *Yersinia* virulence (59). IscR is a global transcriptional regulator that has been extensively characterized in *E. coli* (60). The ability of IscR to modulate transcription of target genes depends on coordination of a [2Fe-2S] cluster and IscR is an active transcription factor in both the apo-IscR and holo-IscR forms (60-62). This is due to the ability of IscR to recognize two separate DNA binding motifs: type I motifs are bound by holo-IscR, while type II motifs are recognized by both apo-IscR and holo-IscR (60, 61, 63). In *Y. pseudotuberculosis*, it was shown that IscR binds to a type II motif within the *lcrF* promoter (Figure 2) (59), suggesting that IscR controls transcription of *Yersinia* type III secretion directly. Furthermore, this motif is 100% conserved within the *lcrF/virF*

promoter between *Y. pseudotubercolosis and Y. pestis* species and contains all nine residues found to be critical for IscR binding in *E. coli* (61). While the IscR binding site is not 100% conserved in *Y. enterocolitica*, the nine residues that were found to be critical for IscR binding are conserved (Figure 2, marked in bold). This indicates a possible conserved mechanism of T3SS gene regulation between the three pathogens. It has been suggested that oxidative stress and oxygen limitation (as a result of Fe-S cluster damage) as well as iron availability all influence the apo/holo IscR ratio, and these environmental signals may affect IscR expression and activity (64-67). Therefore, while it has not yet been demonstrated, oxidative stress, oxygen limitation, or iron availability may influence expression of LcrF and the T3SS.

RscB and CpxR in Response to Extra-cytoplasmic Stress

A recent study reported that T3SS/*yop* expression in *Yersinia* is regulated by the Rcs phosphorelay system – a complex signaling pathway used by *Enterobacteriaceae* to adapt their cellular physiology, biofilm and capsule formation, and motility in response to perturbations in external or surface-associated processes, i.e. overproduction of envelope components, osmotic shock or desiccation (68). Overexpression of the wildtype or a constitutive active variant of the response regulator RcsB enhanced mRNA levels of LcrF as well as Yop protein expression and secretion, suggesting that RcsB influences T3SS/Yop through LcrF (68). This was confirmed by the fact that activated/phosphorylated RcsB has the capacity to bind directly to a conserved RcsB box just upstream of the -35 promoter element of the *yscW-lcrF* operon (Figure 2). RcsB binding most likely enhances RNA polymerase

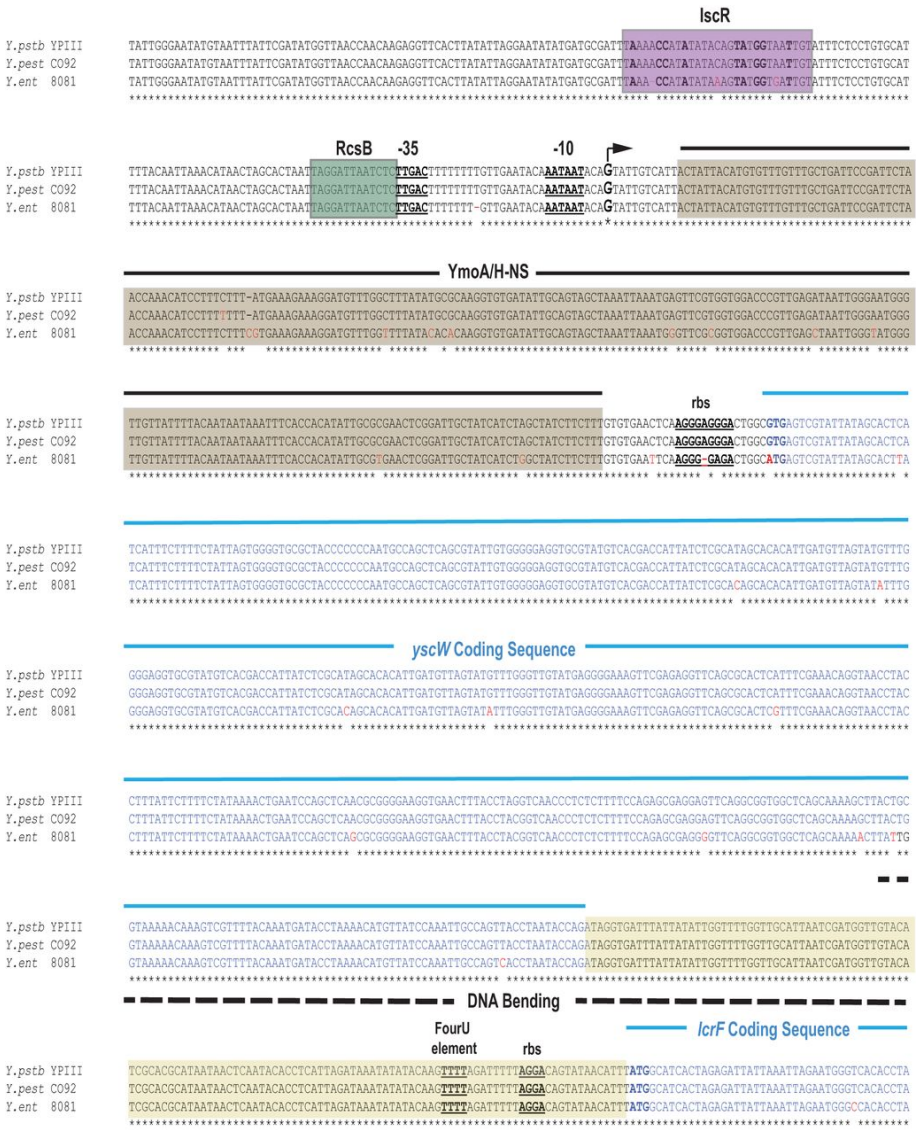

Figure 2: Regulatory elements encoded within the *yscW-lcrF* sequence. Nucleotide sequences of the *yscW* promoter regions for *Y. pestis* CO92, *Y. enterocolitica* and *Y. pseudotuberculosis* YPIII were aligned using ClustalW2. Nucleotides where the sequences are not identical are marked in red, while the nucleotides that are identical in sequence are indicated by dots. The identified binding sequence for IscR is marked in purple, and critical residues required for IscR binding

within this motif are in bold (59, 61). The binding site for RscB is marked in green (68). The region experimentally determined to be involved in YmoA/H-NS binding is marked in brown and is downstream of the transcriptional start site within the 5'-untranslated region (45). The sequence encoding the RNA thermosensor is marked in yellow and is encoded within the intergenic region between *yscW* and *lcrF* (45). The DNA bending region identified within the *yscW-lcrF* operon is denoted with a dotted line and is within the intergenic region between *yscW* and *lcrF* (55). The -10 and -35, transcriptional start site, ribosome binding sites (rbs) upstream of the *yscW* and *lcrF* coding sequence, and the fourU element in the intergenic region between the *yscW* and *lcrF* coding regions are marked in bold (45). All coding sequences are marked in blue.

binding and/or function (68). Activation of RcsB seems to be a prerequisite for *lcrF* induction, as no difference in T3SS/Yop expression was detectable between wildtype and *rcs* mutant strains of enteropathogenic *yersiniae* (68, 69).

In addition to RcsB, it has been established that a second response regulator, CpxR, of another prominent phosphorelay system that responses to extra-cytoplasmatic stress conditions targets the *yscW-lcrF* promoter region. However, in contrast to RcsB, CpxR represses transcription of the operon, suggesting that the two regulatory components are either part of a joint regulatory cascade or are separately induced during different infection stages or niches (68, 70).

Effects on *lcrF* Revealed by Global Expression Analyses

To gain insight into genes expressed by *Yersinia* during septicemia, global transcription patterns of bacteria grown in human plasma were compared with bacteria grown in Luria-Bertani broth, a standard laboratory medium (71, 72). *Y. pestis virG/yscW* and *Y. pseudotuberculosis lcrF* were specifically upregulated in human plasma at 37°C, indicating that induction of the *yscW-lcrF* operon is important for virulence during the septicaemic phase of the infection. A strong upregulation of *lcrF* gene expression was also observed at various time points after nasal infection of mice with *Y. pestis* in the lungs, spleen, and liver, supporting previous studies indicating that LcrF-controlled T3SS/*yop* genes are crucial in resisting immune and inflammatory defensive responses during the development of pneumonic plague (73).

A transcriptomic study directed to identify genes under the control of the recently recognized endonuclease YbeY demonstrated that deletion of the *ybeY* gene

led to an upregulation of *lcrF* and the T3SS/*yop* genes in *Y. enterocolitica* serotype O:3 under conditions in which these genes are usually repressed (i.e., at 22°C)(74). This derepression was not caused by lower YmoA levels, since the amount of *ymoA* transcript was increased in the *ybeY* mutant. Instead, the authors suggested that *lcrF* upregulation in the *ybeY* mutant was due to increased copy number of the virulence plasmid or an altered regulation of global regulators (e.g. Hfq, nucleoid-structuring proteins) affecting the non-coding RNA network and/or DNA supercoiling (74).

Transcriptional profiling further revealed that bacterial membrane permeability may affect expression of LcrF and the T3SS/Yops. Microarray analysis showed that LcrF was upregulated by ~2 fold in a *DrovA Y. pestis* mutant when grown under T3SS-inducing conditions (75). This result seems surprising as RovA is a transcriptional regulator that is upregulated at 25˚C and is best known for inducing expression of invasin, an important virulence factor in *Y. pseudotubercolosis* and *Y. enterocolitica* but is absent from *Y. pestis*. Through gel shift analysis, it was ruled out that RovA binds to the *lcrF* promoter to modulate transcription. However, small electron dense particles were found surrounding the Δ*rovA* mutant membrane upon transmission electron microscopy and membrane permeability of the mutant was decreased compared to wildtype (75). The authors suggested that membrane construction is altered in the absence of RovA and that this might impact assembly and regulation of the T3SS. However, the connection between membrane integrity and LcrF has not been further explored.

TRANSLATIONAL CONTROL OF LCRF IN RESPONSE TO TEMPERATURE

Several early studies on temperature sensing in *Yersinia* reported that LcrF-regulated genes such as *yopE* respond normally to thermal induction even under conditions in which *lcrF* transcription remains essentially constant/unchanged (33). Moreover, forced transcription of *lcrF* at low temperatures did not cause an induction of LcrF-dependent genes (20). This implied that post-transcriptional mechanisms modulate LcrF synthesis and/or its specific activity in response to temperature. Hoe *et al.* reported that *Y. pestis* LcrF is controlled at the translational level in response to temperature. This thermal control was maintained when *lcrF,* containing only 208 bp of the upstream 5'-untranslated region, was transcribed by the T7 polymerase in *E. coli* (76). Based on these data, a simple model of thermal regulation of *lcrF* translation was proposed in which the presence of a short predicted thermo-labile stem-loop structure, or RNA thermometer, sequesters the *lcrF* ribosome binding site (rbs) sequence and blocks translation initiation at moderate temperatures. The decreased stability/melting of this structure at higher temperatures liberates the rbs sequence and allows formation of a productive mRNA-complex and efficient translation (76).

A comprehensive secondary structure prediction of the 124 bp intergenic region of *yscW* and *lcrF* using algorithms such as mfold and RNA fold revealed that this untranslated region of the bicistronic operon folds into two hairpin structures with a free energy of -19.67 kcal/mol (Figure 2)(45). The second thermo-sensitive stem-loop

includes a stretch of four uridines base-paired with the AGGA sequence of the rbs (45). This short motif with its simple design is referred to as fourU element. It was first discovered in the heat shock gene *agsA* (aggregation suppression A) in *Salmonella enterica* serovar Typhimurium and bears resemblance to other potential fourU elements identified in the 5'-untranslated region of the heat shock genes *groES* and *dnaJ* of *Staphylococcus aureus* und *Brucella melitensis* (77). Presence of small loops and several non-canonical base pairs coupled with a network of weak hydrogen bonds, which facilitate liberation of the *lcrF* rbs, argued for a thermo-labile RNA structure prone to melting within a physiological temperature range (45).

Enzymatic structural probing experiments using RNases T1 and V1 confirmed *in silico* prediction and demonstrated thermo-induced partial, but not complete, opening of the second hairpin loop (45). Existence of a thermosensing RNA element (RNA thermometer) was further confirmed by (i) *lcrF-lacZ* translational fusions, which were thermally induced when the fusion was transcribed from a temperature-independent P_{BAD} promoter, (ii) toe printing assays demonstrating that binding of ribosomes to the *lcrF* translational start site is restricted to 37°C and does not occur at 25°C, and (iii) base substitutions within the second hairpin of the thermo-sensing RNA element designed to stabilize or destabilize the second stem-loop (45). These stabilizing point mutations led to a 'closed' conformation of the RNA element, resulting in full repression of LcrF synthesis at 37°C. In contrast, the destabilizing mutations allowed an opening of RNA structure ('open' conformation) and enhanced LcrF production at moderate and higher temperatures. Post-transcriptional control in

an RNA thermometer-like fashion was further confirmed with a deletion of a stretch of nucleotides implicated in the formation of hairpin II, which completely abolished the thermosensing function of the intergenic RNA element and provoked a constitutive increased synthesis of LcrF in a temperature range from 25°C to 37°C. In contrast, an RNA thermometer variant, which only consisted of the second hairpin, was more 'open' compared to the full RNA thermometer and was characterized by higher LcrF levels. Nevertheless, this shortened version was still thermo-inducible, indicating that the first stem-loop is not essential for thermo-sensing, but seems to promote proper folding, and/or supports the stability of the second hairpin (45).

In order to test the physiological relevance of the *lcrF* RNA thermometer and its role for *Yersinia* virulence, pathogenicity of a 'closed' and an 'open' RNA thermometer variant of *Y. pseudotuberculosis* was compared with the isogenic wildtype strain in an oral mouse infection model. Despite the fact that all mice were challenged with a normally lethal dose of *Y. pseudotuberculosis*, all animals infected with *Yersinia* mutants encoding the 'closed' RNA thermometer variant survived and showed no visible signs of infection, similar to an *lcrF* deficient strain, and displayed decreased colonization of the Peyer's patches, mesenteric lymph nodes, liver, and spleen (45). Intriguingly, overexpression of the T3SS/*yop* virulence program, as displayed by the 'open' variant, was not beneficial and did not cause greater host mortality. On the contrary, colonization of some host tissues was slightly reduced, and the average time to death remained unchanged or was even increased by several days, most likely due to biological fitness impediments (45). This clearly illustrated

that the *lcrF* RNA thermometer, which is 100% identical in all human pathogenic *Yersinia* species, is a decisive post-transcriptional control element evolved to produce just the right amount of LcrF to promote the most ideal infection efficiency.

Apparently, both, the YmoA- and RNA thermometer-mediated thermo-sensing mechanisms achieve a very rapid and efficient response. However, recent reports indicate that this control strategy seems to be complemented by additional regulatory modules adjusting LcrF synthesis according to host cell contact and T3SS-mediated effector translocation. In fact, the translocator protein YopD was recently found to bind to the 5'-untranslated sequences of multiple T3SS/*yop* genes including *lcrF* which facilitates their degradation, and reduces LcrF production in the absence of host cell contact (43)(Hoßmann & Dersch, unpublished results). The molecular mechanism of YopD-mediated repression of LcrF synthesis is still unknown, but it is possible that YopD binding to the *lcrF* transcript in the absence of host cells (i) promotes a more closed conformation of the RNA thermometer and/or (ii) accelerates the degradation of the *lcrF* transcript as a consequence of the blockage of ribosome binding and translation. Alternatively, it is possible that YopD may control expression of additional factors influencing *lcrF* transcript stability.

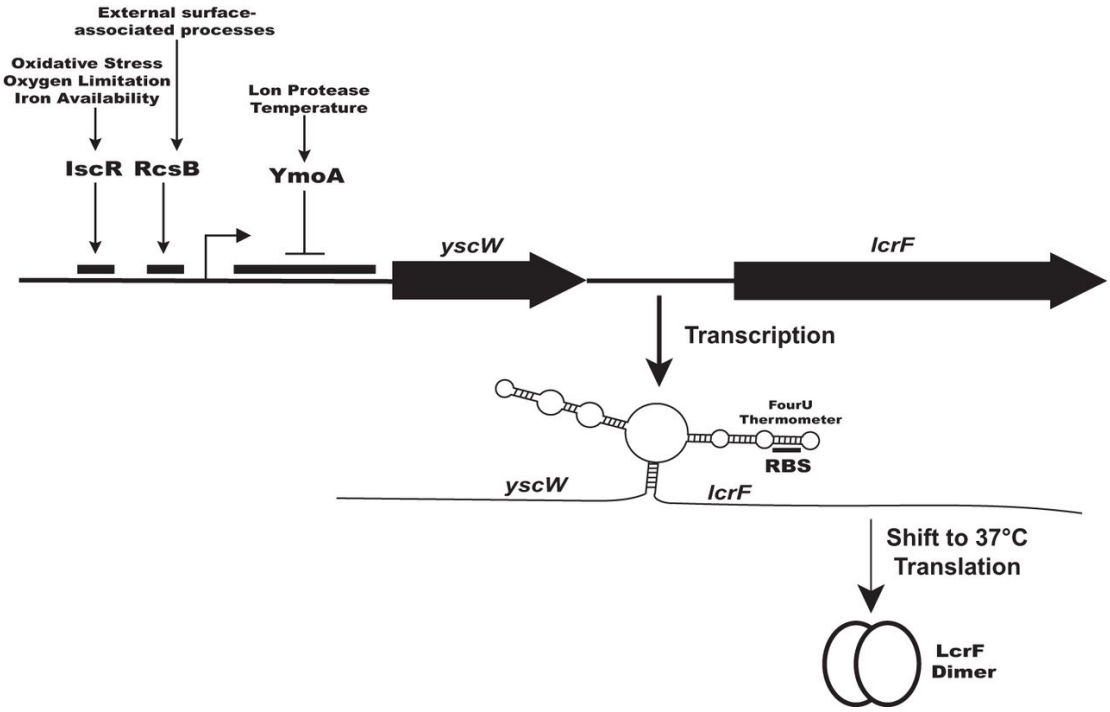

Figure 3. Multiple environmental signals control *lcrF* expression and, subsequently, T3SS expression through several distinct transcriptional and translational regulatory mechanisms. The data summarized in this review suggest that the YmoA, RcsB, and IscR regulators control transcription of *lcrF* in response to temperature, extracytoplasmic stress, iron bioavailability, oxygen tension, and reactive oxygen species. In addition, the RNA thermometer found upstream of *lcrF* allows LcrF translation only at the mammalian host body temperature, 37°C. As *Yersinia* transits from the environment or the flea vector to the mammalian host and then from localized to disseminated sites of infection, changes in temperature, iron availability, and stresses such as ROS may direct the regulatory network controlling LcrF, optimizing T3SS deployment and virulence.

CONNECTIONS TO OTHER T3SS REGULATORS

Gram-negative pathogens that utilize T3SSs do not require them continuously throughout their life cycle. Furthermore, active type III secretion is an energetically costly process that requires ATP and the proton motive force (78). Indeed, pathogenic *Yersinia* undergo growth restriction during active type III secretion (79, 80). In addition, the mammalian innate immune system has evolved several mechanisms to recognize deployment of a T3SS by a pathogen, leading to inflammation (81, 82). So it is not surprising that T3SS regulation by environmental cues through the action of LcrF and many other transcriptional regulators is a common theme in bacterial pathogenesis. As T3SSs are utilized during host cell contact to manipulate various eukaryotic processes, these T3SS regulators sense temperature, oxygen tension, iron bioavailability, and possibly other signals to optimize T3SS deployment. While the regulatory mechanisms used by different pathogens are distinct, a number of similarities exist.

Temperature

Enteric pathogens undergo a temperature shift upon entering the mammalian host, and it is not surprising that in several T3SS expressing pathogens, an increase in temperature allows for the expression of a T3SS regulator. In *Shigella flexneri*, the virulence regulator VirF binds directly to the promoter region of a gene called *virB* (83). VirB in turn activates T3SS components by relieving H-NS repression in T3SS gene promoters (84). Control of both regulators is temperature dependent (85). At non-inducing temperatures, H-NS binds to sites in the *virF* promoter to repress *virF*

transcription (86). However, upon shift to 37˚C, structural changes in the DNA prevent binding of H-NS, allowing for transcription of *virF* (86). Likewise, VirF activates expression of *virB* in a temperature-dependent manner; changes in DNA superhelicity upon shift to 37˚C allows for binding of VirF to the *virB* promoter, but not at 30˚C (87).

H-NS-mediated temperature control of the T3SS also occurs in enteropathogenic *E. coli* (EPEC). In EPEC, the T3SS and several other genes important for pathogenesis are encoded on the LEE pathogenicity island (88). This pathogenicity island encodes 5 major operons, LEE1, LEE2, LEE3, LEE4, and LEE5 (88, 89). The master regulator of the LEE in EPEC, Ler, is the first gene in the LEE1 operon (90, 91). Upon shift to 37˚C, it is thought that H-NS mediated repression of LEE1 is lifted, allowing for expression of Ler and other LEE1 genes (92). Ler then interacts with H-NS in the promoter regions of LEE2-LEE5 to relieve repression of these operons, leading to expression of T3SS components and other genes important for EPEC pathogenesis (92, 93).

H-NS also plays a role in the temperature-dependent regulation of a T3SS master regulator in *S. enterica* serovar *Typhimurium*. The *Salmonella* SPI-1 T3SS is used to invade and cross the intestinal barrier, and SPI-1 T3SS components are activated by the master regulator HilA (as reviewed in (94)). HilA is activated by three AraC-like transcriptional regulators: HilD, HilC, and RtsA, all of which can bind to the *hilA* promoter (94). These transcriptional regulators have been shown to directly or indirectly sense a variety of environmental factors to activate *hilA*, and in

turn, the SPI-1 T3SS (94). At non-inducing temperatures, H-NS silencing blocks transcription of *hilA* (95). Upon shift to 37˚C, H-NS mediated silencing of the *hilA* promoter is relieved in an integration host factor (IHF)-dependent mechanism (95). Once *hilA* silencing is alleviated, it is thought that regulatory factors such as HilD, HilC, and RtsA regulate *hilA* transcription (95).

There is also evidence that T3SS expression in *P. aeruginosa* is temperature dependent, but the mechanism has not been elucidated. Recent studies comparing the transcriptome of *Pseudomonas* at 28˚C versus 37˚C showed that T3SS regulators and components are upregulated at host body temperature (96, 97). Given that the T3SS has been shown to be important for *Pseudomonas* virulence not only in mammalian hosts, but also in cold blooded mammals, Wurtzel et al, 2012 proposed that temperature is just one of many signals that can activate the T3SS (96).

Oxygen Tension

Changes in oxygen tension influence expression of T3SS and T3SS master regulators in several bacterial pathogens, although the complete mechanisms in many cases remain unclear. In *P. aeruginosa*, T3SS expression is independent of calcium concentrations in anaerobic and microaerophillic conditions, suggesting that these conditions are important to activate the T3SS (98). O'Callaghan and colleagues have shown that the *Pseudomonas* oxygen sensing protein Anr, an Fnr homolog, activates synthesis of NarL, which downregulates expression of the small RNAs RsmY and RsmZ (98). Downregulation of these small RNAs allows for accumulation of RsmA, which in a post-transcriptional mechanism is thought to activate the *Pseudomonas*

T3SS master regulator ExsA, possibly through stabilization of *exsA* mRNA (98, 99). These findings may be important to understand *Pseudomonas* pathogenicity in the context of cystic fibrosis (CF), as the mucus-filled lungs of patients are hypoxic. However, it is also interesting to note that *Pseudomonas* isolated from CF patients often are defective in type III secretion due to mutation of regulatory proteins (100, 101). Therefore, it is not clear at what stage of *Pseudomonas* infection this regulation would be important (98).

There is evidence that anaerobic growth induces expression of the SPI-1 T3SS in *Salmonella* (102-104). The Hassan group compared the transcriptomes of wildtype *Salmonella* and an *fnr* mutant, and showed that T3SS gene expression is downregulated in the absence of Fnr (105). Fnr is a well-studied bacterial oxygen sensor. Under anaerobic conditions, Fnr contains a [4Fe-4S] cluster that promotes dimerization and binding to target gene promoters. However, exposure to oxygen converts the [4Fe-4S] cluster to a [2Fe-2S] cluster, inactivating Fnr (as reviewed in (106)). The Hassan group showed that transcription of the flagellar regulators *fliZ* and *fliA* as well as genes involved in accumulation of acetate and acetyl-phosphate were downregulated in an *fnr* mutant (105). Interestingly, FliZ influences expression of the T3SS master regulator HilA through HilD (107). Additionally, SirA can influence expression of HilA in response to accumulation of acetate and acetyl-P (108). The authors speculate that Fnr could activate HilA under anaerobic conditions in response to either or both of these pathways; however, the exact mechanism remains unknown.

In addition to regulation through T3SS master regulators, there is also work to suggest that regulation of the T3SS through oxygen sensing occurs downstream of the master regulator, and might actually fine-tune T3SS expression within the changing oxygen levels within the human gut. Due to the temperature-dependent mechanism discussed above, *Shigella* expresses T3SS components in the anaerobic gut lumen. However, at the same time, Fnr activates transcription of *spa32* and *spa33* (109). The consequence of this is that *Shigella* makes elongated T3SS needles, but secretion of effector proteins through the needle is blocked (109). Marteyn and colleagues propose a model where in the gut lumen, *Shigella* is in a 'primed' state, as T3SS needles are formed, but secretion is blocked. As *Shigella* approaches the intestinal epithelial cell barrier, the oxygen availability increases, and deactivates Fnr. This relieves the block on secretion of effector proteins, and active T3S allows for entry into intestinal epithelial cells (109). It has also been shown that microaerophillic conditions (1.5% oxygen) enhance T3SS expression in enterohaemorrhagic *E. coli* (EHEC) compared to aerobic conditions; however, a mechanism for this regulation has yet to be determined.

Iron

Iron-dependent regulation of T3SS master regulators can occur through the ferric uptake regulator, Fur. Fur senses iron availability through its requirement for a Fe^{2+} cofactor. When bound to Fe^{2+}, Fur represses transcription of target genes; upon loss of the Fe^{2+} cofactor, repression of Fur target genes is relieved (110, 111). Additionally, work in several bacterial species has shown that Fur represses

expression of the small noncoding regulatory RNA RyhB under high iron conditions (112, 113). Under low iron conditions, repression of *ryhB* by Fur is relieved and RyhB RNA is able to regulate target genes (112).

In *Shigella flexerni*, the master virulence regulator VirF not only activates expression of the T3SS activator VirB as discussed above, but also activates IscA, which is required for *Shigella* cell-to-cell spread via actin based motility (114, 115). Work done in the Murphy lab showed that overexpression of *Shigella* RyhB leads to decreased levels of *virB* mRNA (116). Further investigation suggested a mechanism in which the regulatory RNA RyhB binds to *virB* DNA to inhibit transcription (117). Importantly, RyhB did not influence VirF activity (117). Given that VirF is at the top of the regulatory cascade for both actin-based motility and T3SS expression, the Murphy lab proposed a model in which RyhB uncouples type III secretion and actin-based motility based on iron availability (117). Studies investigating the gene expression profiles of cells grown within cultured eukaryotic cells show increased expression of Fur-regulated genes, suggesting a low iron environment within the intracellular compartment of these cells (118, 119). Additionally, similar experiments have shown downregulation of genes in the VirB regulon during intracellular growth (118, 120). Consistent with this, the model suggests that RyhB responds to the low intracellular iron bioavailability within eukaryotic cells to upregulate cell-to-cell spread machinery over T3SS deployment through repression of *virB* (117).

The *Salmonella* SPI-1 T3SS is also influenced by Fur. Fur is required for HilD-mediated activation of the master regulator, HilA (121). Unlike *Shigella*, this

effect does not seem to be mediated by the RyhB homologs RfrA and RfrB, and a clear mechanism for how Fur affects HilD expression has yet to be elucidated (121). Fur also plays a role in the T3SS expression of the marine pathogen *Edwarsiella tarda*. T3SS expression decreases with increasing iron levels and a *fur* mutant did not display iron-dependent T3SS expression (122). Additional work suggested that Fur probably does not inhibit expression the T3SS master regulators EsrB and EsrC, but instead binds the promoter region of master regulator target genes to prevent transcription by these regulators under high iron conditions (122).

Host Cell Contact

The *P. aeruginosa* T3SS regulon, which is under control of the closely related LcrF/VirF homolog ExsA, is strongly induced upon host cell contact in a manner similar to what has been observed for LcrF/VirF-promoted Ysc T3SS gene expression in *Yersinia* (12, 21, 36, 123, 124). The molecular mechanisms responsible for host cell contact-mediated induction of *Yersinia* T3SS/Yops secretion are remain unknown (22, 36, 125), but a *Pseudomonas*-specific complex regulatory partner switching cascade has been identified and shown to promote contact induction in this species (22, 36, 125). In strong contrast to LcrF, ExsA activity is controlled through direct interaction with an anti-activator protein ExsD, which can interact with ExsC, a binding partner of ExsE encoded further upstream of the *exsCEBA* operon (29). Under non-inducing conditions, e.g. in the absence of host cell contact, ExsA-mediated activation of T3SS genes is inhibited, because binding affinities of all four Exs regulatory proteins favor heterocomplex formation of ExsA□ExsD (1:1) and

ExsC□ExsE (2:1), whereby interaction of ExsA with the anti-activator ExsD abrogates ExsA self-association and DNA-binding (126, 127). However, under inducing conditions, which trigger secretion and translocation of the ExsE protein, reduction of ExsE levels favors the formation of an ExsD□ExsC (2:2) complex, most likely by dissociation of existing ExsA□ExsD complexes (123, 124, 128-130). In contrast to *P. aeruginosa*, all human pathogenic *Yersinia* species lack the *exsB, exsC* and *exsE* genes, and dissimilar to ExsA the activity of the LcrF protein was not influenced by loss or overproduction of ExsD, suggesting that ExsD cannot act as an anti-activator of LcrF (18).

CONCLUSIONS

Yersinia and other T3SS-expressing pathogens have complex regulatory networks in place to control expression of T3SS genes. While the *Yersinia* T3SS master regulator LcrF was identified almost three decades ago, recent work has greatly expanded our understanding of how expression of LcrF is regulated and what environmental signals might contribute to its regulation. Future work focusing on expression of LcrF and T3SS genes in different host niches will enable a more complete understanding of how this T3SS master regulator facilitates optimization of T3SS expression to promote virulence.

ACKNOWLEDGEMENTS

The authors acknowledge the National Institutes of Health (R21AI099747 to V.A. and T32GM008646 to L.S.), the German Research Foundation (DE616/6 to P.D.), the

German Center for Infection Research (DZIF-TTU 06.801 to P.D.), and the Vietnam Education Foundation (to H.L.) for support.

REFERENCES

1. **Putzker M, Sauer H, Sobe D.** 2001. Plague and other human infections caused by *Yersinia* species. Clin Lab **47:**453-466.
2. **Khan FA, Fisher MA, Khakoo RA.** 2007. Association of hemochromatosis with infectious diseases: expanding spectrum. Int J Infect Dis **11:**482-487.
3. **Bottone EJ.** 1999. *Yersinia enterocolitica*: overview and epidemiologic correlates. Microbes Infect **1:**323-333.
4. **Smego RA, Frean J, Koornhof HJ.** 1999. Yersiniosis I: microbiological and clinicoepidemiological aspects of plague and non-plague *Yersinia* infections. Eur. J. Clin. Microbiol. Infect. Dis. **18:**1-15.
5. **Koornhof HJ, Smego RA, Jr., Nicol M.** 1999. Yersiniosis. II: The pathogenesis of *Yersinia* infections. Eur. J. Clin. Microbiol. Infect. Dis. **18:**87-112.
6. **Cornelis GR, Boland A, Boyd AP, Geuijen C, Iriarte M, Neyt C, Sory MP, Stainier I.** 1998. The virulence plasmid of *Yersinia*, an antihost genome. Microbiol. Mol. Biol. Rev. **62:**1315-1352.
7. **Bliska JB, Wang X, Viboud GI, Brodsky IE.** 2013. Modulation of innate immune responses by *Yersinia* type III secretion system translocators and effectors. Cell. Microbiol. **15:**1622-1631.

8. **Kupferberg LL, Higuchi K.** 1958. Role of calcium ions in the stimulation of growth of virulent strains of *Pasteurella pestis*. J. Bacteriol. **76:**120-121.

9. **Higuchi K, Kupferberg LL, Smith JL.** 1959. Studies on the nutrition and physiology of *Pasteurella pestis*. III. Effects of calcium ions on the growth of virulent and avirulent strains of Pasteurella pestis. J. Bacteriol. **77:**317-321.

10. **Yother J, Goguen JD.** 1985. Isolation and characterization of Ca2+-blind mutants of *Yersinia pestis*. J. Bacteriol. **164:**704-711.

11. **Perry RD, Harmon PA, Bowmer WS, Straley SC.** 1986. A low-Ca2+ response operon encodes the V antigen of *Yersinia pestis*. Infect. Immun. **54:**428-434.

12. **Yother J, Chamness TW, Goguen JD.** 1986. Temperature-controlled plasmid regulon associated with low calcium response in *Yersinia pestis*. J. Bacteriol. **165:**443-447.

13. **Cornelis G, Vanootegem JC, Sluiters C.** 1987. Transcription of the yop regulon from *Y. enterocolitica* requires trans acting pYV and chromosomal genes. Microb. Pathog. **2:**367-379.

14. **Bolin I, Forsberg A, Norlander L, Skurnik M, Wolf-Watz H.** 1988. Identification and mapping of the temperature-inducible, plasmid-encoded proteins of *Yersinia* spp. Infect. Immun. **56:**343-348.

15. **Cornelis G, Sluiters C, de Rouvroit CL, Michiels T.** 1989. Homology between VirF, the transcriptional activator of the *Yersinia* virulence regulon,

and AraC, the *Escherichia coli* arabinose operon regulator. J. Bacteriol. **171:**254-262.

16. **Schleif R.** 2010. AraC protein, regulation of the l-arabinose operon in *Escherichia coli*, and the light switch mechanism of AraC action. FEMS Microbiol. Rev. **34:**779-796.

17. **Wattiau P, Cornelis GR.** 1994. Identification of DNA sequences recognized by VirF, the transcriptional activator of the *Yersinia* yop regulon. J. Bacteriol. **176:**3878-3884.

18. **King JM, Schesser Bartra S, Plano G, Yahr TL.** 2013. ExsA and LcrF recognize similar consensus binding sites, but differences in their oligomeric state influence interactions with promoter DNA. J. Bacteriol. **195:**5639-5650.

19. **Rhee S, Martin RG, Rosner JL, Davies DR.** 1998. A novel DNA-binding motif in MarA: the first structure for an AraC family transcriptional activator. Proc Natl Acad Sci U S A **95:**10413-10418.

20. **Lambert de Rouvroit C, Sluiters C, Cornelis GR.** 1992. Role of the transcriptional activator, VirF, and temperature in the expression of the pYV plasmid genes of *Yersinia enterocolitica*. Mol. Microbiol. **6:**395-409.

21. **Diaz MR, King JM, Yahr TL.** 2011. Intrinsic and Extrinsic Regulation of Type III Secretion Gene Expression in *Pseudomonas Aeruginosa*. Front Microbiol **2:**89.

22. **Brutinel ED, Vakulskas CA, Brady KM, Yahr TL.** 2008. Characterization of ExsA and of ExsA-dependent promoters required for expression of the

Pseudomonas aeruginosa type III secretion system. Mol Microbiol **68:**657-671.

23. **Bailey TL, Boden M, Buske FA, Frith M, Grant CE, Clementi L, Ren J, Li WW, Noble WS.** 2009. MEME SUITE: tools for motif discovery and searching. Nucleic Acids Res. **37:**W202-208.

24. **Grant CE, Bailey TL, Noble WS.** 2011. FIMO: scanning for occurrences of a given motif. Bioinformatics **27:**1017-1018.

25. **Nuss AM, Heroven AK, Waldmann B, Reinkensmeier J, Jarek M, Beckstette M, Dersch P.** 2015. Transcriptomic profiling of *Yersinia pseudotuberculosis* reveals reprogramming of the Crp regulon by temperature and uncovers Crp as a master regulator of small RNAs. PLoS Genet. **11:**e1005087.

26. **China B, Michiels T, Cornelis GR.** 1990. The pYV plasmid of *Yersinia* encodes a lipoprotein, YlpA, related to TraT. Mol. Microbiol. **4:**1585-1593.

27. **Vakulskas CA, Brady KM, Yahr TL.** 2009. Mechanism of transcriptional activation by *Pseudomonas aeruginosa* ExsA. J Bacteriol **191:**6654-6664.

28. **Brutinel ED, Vakulskas CA, Yahr TL.** 2009. Functional domains of ExsA, the transcriptional activator of the *Pseudomonas aeruginosa* type III secretion system. J. Bacteriol. **191:**3811-3821.

29. **Yahr TL, Frank DW.** 1994. Transcriptional organization of the trans-regulatory locus which controls exoenzyme S synthesis in *Pseudomonas aeruginosa*. J Bacteriol **176:**3832-3838.

30. **Michiels T, Cornelis G.** 1988. Nucleotide sequence and transcription analysis of yop51 from *Yersinia enterocolitica* W22703. Microb. Pathog. **5:**449-459.

31. **Michiels T, Vanooteghem JC, Lambert de Rouvroit C, China B, Gustin A, Boudry P, Cornelis GR.** 1991. Analysis of *virC*, an operon involved in the secretion of Yop proteins by *Yersinia enterocolitica*. J. Bacteriol. **173:**4994-5009.

32. **Skurnik M, Toivanen P.** 1992. LcrF is the temperature-regulated activator of the *yadA* gene of *Yersinia enterocolitica* and *Yersinia pseudotuberculosis*. J. Bacteriol. **174:**2047-2051.

33. **Hoe NP, Minion FC, Goguen JD.** 1992. Temperature sensing in *Yersinia pestis*: regulation of *yopE* transcription by *lcrF*. J. Bacteriol. **174:**4275-4286.

34. **Axler-DiPerte GL, Hinchliffe SJ, Wren BW, Darwin AJ.** 2009. YtxR acts as an overriding transcriptional off switch for the *Yersinia enterocolitica* Ysc-Yop type 3 secretion system. J. Bacteriol. **191:**514-524.

35. **Li L, Yan H, Feng L, Li Y, Lu P, Hu Y, Chen S.** 2014. LcrQ blocks the role of LcrF in regulating the Ysc-Yop type III secretion genes in *Yersinia pseudotuberculosis*. PLoS One **9:**e92243.

36. **Pettersson J, Nordfelth R, Dubinina E, Bergman T, Gustafsson M, Magnusson KE, Wolf-Watz H.** 1996. Modulation of virulence factor expression by pathogen target cell contact. Science **273:**1231-1233.

37. **Rimpilainen M, Forsberg A, Wolf-Watz H.** 1992. A novel protein, LcrQ, involved in the low-calcium response of *Yersinia pseudotuberculosis* shows extensive homology to YopH. J. Bacteriol. **174:**3355-3363.

38. **Stainier I, Iriarte M, Cornelis GR.** 1997. YscM1 and YscM2, two *Yersinia enterocolitica* proteins causing downregulation of yop transcription. Mol. Microbiol. **26:**833-843.

39. **Kopaskie KS, Ligtenberg KG, Schneewind O.** 2013. Translational regulation of *Yersinia enterocolitica* mRNA encoding a type III secretion substrate. J. Biol. Chem. **288:**35478-35488.

40. **Williams AW, Straley SC.** 1998. YopD of *Yersinia pestis* plays a role in negative regulation of the low-calcium response in addition to its role in translocation of Yops. J. Bacteriol. **180:**350-358.

41. **Anderson DM, Ramamurthi KS, Tam C, Schneewind O.** 2002. YopD and LcrH regulate expression of *Yersinia enterocolitica* YopQ by a posttranscriptional mechanism and bind to *yopQ* RNA. J. Bacteriol. **184:**1287-1295.

42. **Cambronne ED, Schneewind O.** 2002. *Yersinia enterocolitica* type III secretion: yscM1 and yscM2 regulate yop gene expression by a posttranscriptional mechanism that targets the 5' untranslated region of *yop* mRNA. J. Bacteriol. **184:**5880-5893.

43. **Chen Y, Anderson DM.** 2011. Expression hierarchy in the *Yersinia* type III secretion system established through YopD recognition of RNA. Mol. Microbiol. **80:**966-980.

44. **Cornelis G, Sluiters C, Delor I, Geib D, Kaniga K, Lambert de Rouvroit C, Sory MP, Vanooteghem JC, Michiels T.** 1991. *ymoA*, a *Yersinia enterocolitica* chromosomal gene modulating the expression of virulence functions. Mol Microbiol **5:**1023-1034.

45. **Bohme K, Steinmann R, Kortmann J, Seekircher S, Heroven AK, Berger E, Pisano F, Thiermann T, Wolf-Watz H, Narberhaus F, Dersch P.** 2012. Concerted actions of a thermo-labile regulator and a unique intergenic RNA thermosensor control *Yersinia* virulence. PLoS Pathog **8:**e1002518.

46. **Cornelis GR.** 1993. Role of the transcription activator *virF* and the histone-like protein YmoA in the thermoregulation of virulence functions in Yersiniae. Zentralbl Bakteriol **278:**149-164.

47. **Mikulskis AV, Cornelis GR.** 1994. A new class of proteins regulating gene expression in enterobacteria. Mol Microbiol **11:**77-86.

48. **Madrid C, Nieto JM, Juarez A.** 2002. Role of the Hha/YmoA family of proteins in the thermoregulation of the expression of virulence factors. Int J Med Microbiol **291:**425-432.

49. **Nieto J, Madrid C, Miquelay E, Parra JL, Rodriguez S, Juarez A.** 2002. Evidence for direct protein-protein interaction between members of the

enterobacterial Hha/YmoA and H-NS families of proteins. J Bacteriol **184:**629-635.

50. **Heroven A, Nagel G, Tran HJ, Parr S, Dersch P.** 2004. RovA is autoregulated and antagonizes H-NS-mediated silencing of invasin and *rovA* expression in *Yersinia pseudotuberculosis*. Mol Microbiol **53:**871-888.

51. **Ellison DW, Miller VL.** 2006. H-NS represses inv transcription in *Yersinia enterocolitica* through competition with RovA and interaction with YmoA. J. Bacteriol. **188:**5101-5112.

52. **Ono S, Goldberg MD, Olsson T, Esposito D, Hinton JC, Ladbury JE.** 2005. H-NS is a part of a thermally controlled mechanism for bacterial gene regulation. Biochem J **391:**203-213.

53. **Jackson M, Silva-Herzog E, Plano GV.** 2004. The ATP-dependent ClpXP and Lon proteases regulate expression of the *Yersinia pestis* type III secretion system via regulated proteolysis of YmoA, a small histone-like protein. Mol Microbiol **54:**1364-1378.

54. **Rohde JR, Fox JM, Minnich SA.** 1994. Thermoregulation in *Yersinia enterocolitica* is coincident with changes in DNA supercoiling. Mol. Microbiol. **12:**187-199.

55. **Rohde JR, Luan XS, Rohde H, Fox JM, Minnich SA.** 1999. The *Yersinia enterocolitica* pYV virulence plasmid contains multiple intrinsic DNA bends which melt at 37 degrees C. J. Bacteriol. **181:**4198-4204.

56. **Kapatral V, Olson JW, Pepe JC, Miller VL, Minnich SA.** 1996. Temperature-dependent regulation of *Yersinia enterocolitica* Class III flagellar genes. Mol. Microbiol. **19:**1061-1071.

57. **Horne SM, Pruss BM.** 2006. Global gene regulation in *Yersinia enterocolitica*: effect of FliA on the expression levels of flagellar and plasmid-encoded virulence genes. Arch. Microbiol. **185:**115-126.

58. **Schiano CA, Bellows LE, Lathem WW.** 2010. The small RNA chaperone Hfq is required for the virulence of *Yersinia pseudotuberculosis*. Infect. Immun. **78:**2034-2044.

59. **Miller HK, Kwuan L, Schwiesow L, Bernick DL, Mettert E, Ramirez HA, Ragle JM, Chan PP, Kiley PJ, Lowe TM, Auerbuch V.** 2014. IscR is essential for *Yersinia pseudotuberculosis* type III secretion and virulence. PLoS Pathog **10:**e1004194.

60. **Schwartz CJ, Giel JL, Patschkowski T, Luther C, Ruzicka FJ, Beinert H, Kiley PJ.** 2001. IscR, an Fe-S cluster-containing transcription factor, represses expression of *Escherichia coli* genes encoding Fe-S cluster assembly proteins. Proc Natl Acad Sci U S A **98:**14895-14900.

61. **Nesbit AD, Giel JL, Rose JC, Kiley PJ.** 2009. Sequence-specific binding to a subset of IscR-regulated promoters does not require IscR Fe-S cluster ligation. J. Mol. Biol. **387:**28-41.

62. **Fleischhacker AS, Stubna A, Hsueh KL, Guo Y, Teter SJ, Rose JC, Brunold TC, Markley JL, Munck E, Kiley PJ.** 2012. Characterization of

the [2Fe-2S] cluster of *Escherichia coli* transcription factor IscR. Biochemistry **51:**4453-4462.

63. **Rajagopalan S, Teter SJ, Zwart PH, Brennan RG, Phillips KJ, Kiley PJ.** 2013. Studies of IscR reveal a unique mechanism for metal-dependent regulation of DNA binding specificity. Nat. Struct. Mol. Biol. **20:**740-747.

64. **Mettert EL, Kiley PJ.** 2014. Coordinate regulation of the Suf and Isc Fe-S cluster biogenesis pathways by IscR is essential for viability of *Escherichia coli*. J. Bacteriol. **196:**4315-4323.

65. **Giel JL, Rodionov D, Liu M, Blattner FR, Kiley PJ.** 2006. IscR-dependent gene expression links iron-sulphur cluster assembly to the control of O2-regulated genes in *Escherichia coli*. Mol. Microbiol. **60:**1058-1075.

66. **Yeo WS, Lee JH, Lee KC, Roe JH.** 2006. IscR acts as an activator in response to oxidative stress for the suf operon encoding Fe-S assembly proteins. Mol. Microbiol. **61:**206-218.

67. **Wu Y, Outten FW.** 2009. IscR controls iron-dependent biofilm formation in *Escherichia coli* by regulating type I fimbria expression. J. Bacteriol. **191:**1248-1257.

68. **Li Y, Hu Y, Francis MS, Chen S.** 2015. RcsB positively regulates the *Yersinia* Ysc-Yop type III secretion system by activating expression of the master transcriptional regulator LcrF. Environ. Microbiol. **17:**1219-1233.

69. **Venecia K, Young GM.** 2005. Environmental regulation and virulence attributes of the Ysa type III secretion system of *Yersinia enterocolitica* biovar 1B. Infect. Immun. **73:**5961-5977.

70. **Liu J, Thanikkal EJ, Obi IR, Francis MS.** 2012. Elevated CpxR~P levels repress the Ysc-Yop type III secretion system of *Yersinia pseudotuberculosis*. Res. Microbiol. **163:**518-530.

71. **Rosso ML, Chauvaux S, Dessein R, Laurans C, Frangeul L, Lacroix C, Schiavo A, Dillies MA, Foulon J, Coppee JY, Medigue C, Carniel E, Simonet M, Marceau M.** 2008. Growth of *Yersinia pseudotuberculosis* in human plasma: impacts on virulence and metabolic gene expression. BMC Microbiol. **8:**211.

72. **Chauvaux S, Rosso ML, Frangeul L, Lacroix C, Labarre L, Schiavo A, Marceau M, Dillies MA, Foulon J, Coppee JY, Medigue C, Simonet M, Carniel E.** 2007. Transcriptome analysis of *Yersinia pestis* in human plasma: an approach for discovering bacterial genes involved in septicaemic plague. Microbiology **153:**3112-3124.

73. **Liu H, Wang H, Qiu J, Wang X, Guo Z, Qiu Y, Zhou D, Han Y, Du Z, Li C, Song Y, Yang R.** 2009. Transcriptional profiling of a mice plague model: insights into interaction between *Yersinia pestis* and its host. J. Basic Microbiol. **49:**92-99.

74. **Leskinen K, Varjosalo M, Skurnik M.** 2015. Absence of YbeY RNase compromises the growth and enhances the virulence plasmid gene expression of *Yersinia enterocolitica* O:3. Microbiology **161:**285-299.

75. **Yang F, Ke Y, Tan Y, Bi Y, Shi Q, Yang H, Qiu J, Wang X, Guo Z, Ling H, Yang R, Du Z.** 2010. Cell membrane is impaired, accompanied by enhanced type III secretion system expression in *Yersinia pestis* deficient in RovA regulator. PLoS One **5**.

76. **Hoe NP, Goguen JD.** 1993. Temperature sensing in *Yersinia pestis*: translation of the LcrF activator protein is thermally regulated. J Bacteriol **175:**7901-7909.

77. **Waldminghaus T, Heidrich N, Brantl S, Narberhaus F.** 2007. FourU: a novel type of RNA thermometer in *Salmonella*. Mol Microbiol **65:**413-424.

78. **Galan JE.** 2008. Energizing type III secretion machines: what is the fuel? Nat. Struct. Mol. Biol. **15:**127-128.

79. **Brubaker RR.** 1972. The genus *Yersinia*: biochemistry and genetics of virulence. Curr. Top. Microbiol. Immunol. **57:**111-158.

80. **Portnoy DA, Moseley SL, Falkow S.** 1981. Characterization of plasmids and plasmid-associated determinants of *Yersinia enterocolitica* pathogenesis. Infect. Immun. **31:**775-782.

81. **Vance RE, Isberg RR, Portnoy DA.** 2009. Patterns of pathogenesis: discrimination of pathogenic and nonpathogenic microbes by the innate immune system. Cell Host Microbe **6:**10-21.

82. **Vance RE.** 2015. The NAIP/NLRC4 inflammasomes. Curr. Opin. Immunol. **32:**84-89.

83. **Tobe T, Yoshikawa M, Mizuno T, Sasakawa C.** 1993. Transcriptional control of the invasion regulatory gene *virB* of *Shigella flexneri*: activation by VirF and repression by H-NS. J. Bacteriol. **175:**6142-6149.

84. **Turner EC, Dorman CJ.** 2007. H-NS antagonism in *Shigella flexneri* by VirB, a virulence gene transcription regulator that is closely related to plasmid partition factors. J. Bacteriol. **189:**3403-3413.

85. **Tobe T, Nagai S, Okada N, Adler B, Yoshikawa M, Sasakawa C.** 1991. Temperature-regulated expression of invasion genes in *Shigella flexneri* is controlled through the transcriptional activation of the *virB* gene on the large plasmid. Mol. Microbiol. **5:**887-893.

86. **Falconi M, Colonna B, Prosseda G, Micheli G, Gualerzi CO.** 1998. Thermoregulation of *Shigella* and *Escherichia coli* EIEC pathogenicity. A temperature-dependent structural transition of DNA modulates accessibility of *virF* promoter to transcriptional repressor H-NS. EMBO J. **17:**7033-7043.

87. **Tobe T, Yoshikawa M, Sasakawa C.** 1995. Thermoregulation of *virB* transcription in *Shigella flexneri* by sensing of changes in local DNA superhelicity. J. Bacteriol. **177:**1094-1097.

88. **McDaniel TK, Kaper JB.** 1997. A cloned pathogenicity island from enteropathogenic *Escherichia coli* confers the attaching and effacing phenotype on *E. coli* K-12. Mol. Microbiol. **23:**399-407.

89. **Elliott SJ, Wainwright LA, McDaniel TK, Jarvis KG, Deng YK, Lai LC, McNamara BP, Donnenberg MS, Kaper JB.** 1998. The complete sequence of the locus of enterocyte effacement (LEE) from enteropathogenic *Escherichia coli* E2348/69. Mol. Microbiol. **28:**1-4.

90. **Friedberg D, Umanski T, Fang Y, Rosenshine I.** 1999. Hierarchy in the expression of the locus of enterocyte effacement genes of enteropathogenic *Escherichia coli*. Mol. Microbiol. **34:**941-952.

91. **Mellies JL, Elliott SJ, Sperandio V, Donnenberg MS, Kaper JB.** 1999. The Per regulon of enteropathogenic *Escherichia coli* : identification of a regulatory cascade and a novel transcriptional activator, the locus of enterocyte effacement (LEE)-encoded regulator (Ler). Mol. Microbiol. **33:**296-306.

92. **Umanski T, Rosenshine I, Friedberg D.** 2002. Thermoregulated expression of virulence genes in enteropathogenic *Escherichia coli*. Microbiology **148:**2735-2744.

93. **Winardhi RS, Gulvady R, Mellies JL, Yan J.** 2014. Locus of enterocyte effacement-encoded regulator (Ler) of pathogenic *Escherichia coli* competes off histone-like nucleoid-structuring protein (H-NS) through noncooperative DNA binding. J. Biol. Chem. **289:**13739-13750.

94. **Ellermeier JR, Slauch JM.** 2007. Adaptation to the host environment: regulation of the SPI1 type III secretion system in *Salmonella enterica* serovar Typhimurium. Curr. Opin. Microbiol. **10:**24-29.

95. **Queiroz MH, Madrid C, Paytubi S, Balsalobre C, Juarez A.** 2011. Integration host factor alleviates H-NS silencing of the *Salmonella enterica* serovar Typhimurium master regulator of SPI1, *hilA*. Microbiology **157:**2504-2514.

96. **Wurtzel O, Yoder-Himes DR, Han K, Dandekar AA, Edelheit S, Greenberg EP, Sorek R, Lory S.** 2012. The single-nucleotide resolution transcriptome of *Pseudomonas aeruginosa* grown in body temperature. PLoS Pathog **8:**e1002945.

97. **Barbier M, Damron FH, Bielecki P, Suarez-Diez M, Puchalka J, Alberti S, Dos Santos VM, Goldberg JB.** 2014. From the environment to the host: re-wiring of the transcriptome of *Pseudomonas aeruginosa* from 22°C to 37°C. PLoS One **9:**e89941.

98. **O'Callaghan J, Reen FJ, Adams C, O'Gara F.** 2011. Low oxygen induces the type III secretion system in *Pseudomonas aeruginosa* via modulation of the small RNAs *rsmZ* and *rsmY*. Microbiology **157:**3417-3428.

99. **Intile PJ, Diaz MR, Urbanowski ML, Wolfgang MC, Yahr TL.** 2014. The AlgZR two-component system recalibrates the RsmAYZ posttranscriptional regulatory system to inhibit expression of the *Pseudomonas aeruginosa* type III secretion system. J. Bacteriol. **196:**357-366.

100. **Mena A, Smith EE, Burns JL, Speert DP, Moskowitz SM, Perez JL, Oliver A.** 2008. Genetic adaptation of *Pseudomonas aeruginosa* to the

airways of cystic fibrosis patients is catalyzed by hypermutation. J. Bacteriol. **190:**7910-7917.

101. **Smith EE, Buckley DG, Wu Z, Saenphimmachak C, Hoffman LR, D'Argenio DA, Miller SI, Ramsey BW, Speert DP, Moskowitz SM, Burns JL, Kaul R, Olson MV.** 2006. Genetic adaptation by *Pseudomonas aeruginosa* to the airways of cystic fibrosis patients. Proc Natl Acad Sci U S A **103:**8487-8492.

102. **Bajaj V, Lucas RL, Hwang C, Lee CA.** 1996. Co-ordinate regulation of *Salmonella typhimurium* invasion genes by environmental and regulatory factors is mediated by control of *hilA* expression. Mol. Microbiol. **22:**703-714.

103. **Jones BD, Falkow S.** 1994. Identification and characterization of a *Salmonella typhimurium* oxygen-regulated gene required for bacterial internalization. Infect. Immun. **62:**3745-3752.

104. **Klein JR, Fahlen TF, Jones BD.** 2000. Transcriptional organization and function of invasion genes within *Salmonella enterica* serovar Typhimurium pathogenicity island 1, including the *prgH*, *prgI*, *prgJ*, *prgK*, *orgA*, *orgB*, and *orgC* genes. Infect. Immun. **68:**3368-3376.

105. **Fink RC, Evans MR, Porwollik S, Vazquez-Torres A, Jones-Carson J, Troxell B, Libby SJ, McClelland M, Hassan HM.** 2007. FNR is a global regulator of virulence and anaerobic metabolism in *Salmonella enterica* serovar Typhimurium (ATCC 14028s). J. Bacteriol. **189:**2262-2273.

106. **Miller HK, Auerbuch V.** 2015. Bacterial iron-sulfur cluster sensors in mammalian pathogens. Metallomics.

107. **Chubiz JE, Golubeva YA, Lin D, Miller LD, Slauch JM.** 2010. FliZ regulates expression of the *Salmonella* pathogenicity island 1 invasion locus by controlling HilD protein activity in *Salmonella enterica* serovar typhimurium. J. Bacteriol. **192:**6261-6270.

108. **Lawhon SD, Maurer R, Suyemoto M, Altier C.** 2002. Intestinal short-chain fatty acids alter *Salmonella typhimurium* invasion gene expression and virulence through BarA/SirA. Mol. Microbiol. **46:**1451-1464.

109. **Marteyn B, West NP, Browning DF, Cole JA, Shaw JG, Palm F, Mounier J, Prevost MC, Sansonetti P, Tang CM.** 2010. Modulation of *Shigella* virulence in response to available oxygen *in vivo*. Nature **465:**355-358.

110. **Troxell B, Hassan HM.** 2013. Transcriptional regulation by Ferric Uptake Regulator (Fur) in pathogenic bacteria. Front Cell Infect Microbiol **3:**59.

111. **Porcheron G, Dozois CM.** 2015. Interplay between iron homeostasis and virulence: Fur and RyhB as major regulators of bacterial pathogenicity. Vet. Microbiol.

112. **Oglesby-Sherrouse AG, Murphy ER.** 2013. Iron-responsive bacterial small RNAs: variations on a theme. Metallomics **5:**276-286.

113. **Salvail H, Masse E.** 2012. Regulating iron storage and metabolism with RNA: an overview of posttranscriptional controls of intracellular iron homeostasis. Wiley Interdiscip Rev RNA **3:**26-36.

114. **Goldberg MB, Theriot JA, Sansonetti PJ.** 1994. Regulation of surface presentation of IcsA, a *Shigella* protein essential to intracellular movement and spread, is growth phase dependent. Infect. Immun. **62:**5664-5668.

115. **Adler B, Sasakawa C, Tobe T, Makino S, Komatsu K, Yoshikawa M.** 1989. A dual transcriptional activation system for the 230 kb plasmid genes coding for virulence-associated antigens of *Shigella flexneri*. Mol. Microbiol. **3:**627-635.

116. **Murphy ER, Payne SM.** 2007. RyhB, an iron-responsive small RNA molecule, regulates *Shigella dysenteriae* virulence. Infect. Immun. **75:**3470-3477.

117. **Broach WH, Egan N, Wing HJ, Payne SM, Murphy ER.** 2012. VirF-independent regulation of *Shigella virB* transcription is mediated by the small RNA RyhB. PLoS One **7:**e38592.

118. **Lucchini S, Liu H, Jin Q, Hinton JC, Yu J.** 2005. Transcriptional adaptation of *Shigella flexneri* during infection of macrophages and epithelial cells: insights into the strategies of a cytosolic bacterial pathogen. Infect. Immun. **73:**88-102.

119. **Runyen-Janecky LJ, Payne SM.** 2002. Identification of chromosomal *Shigella flexneri* genes induced by the eukaryotic intracellular environment. Infect. Immun. **70:**4379-4388.

120. **Headley VL, Payne SM.** 1990. Differential protein expression by *Shigella flexneri* in intracellular and extracellular environments. Proc Natl Acad Sci U S A **87:**4179-4183.

121. **Ellermeier JR, Slauch JM.** 2008. Fur regulates expression of the *Salmonella* pathogenicity island 1 type III secretion system through HilD. J. Bacteriol. **190:**476-486.

122. **Chakraborty S, Sivaraman J, Leung KY, Mok YK.** 2011. Two-component PhoB-PhoR regulatory system and ferric uptake regulator sense phosphate and iron to control virulence genes in type III and VI secretion systems of *Edwardsiella tarda*. J. Biol. Chem. **286:**39417-39430.

123. **Urbanowski ML, Lykken GL, Yahr TL.** 2005. A secreted regulatory protein couples transcription to the secretory activity of the *Pseudomonas aeruginosa* type III secretion system. Proc Natl Acad Sci U S A **102:**9930-9935.

124. **Urbanowski ML, Brutinel ED, Yahr TL.** 2007. Translocation of ExsE into Chinese hamster ovary cells is required for transcriptional induction of the *Pseudomonas aeruginosa* type III secretion system. Infect Immun **75:**4432-4439.

125. **Tengel T, Sethson I, Francis MS.** 2002. Conformational analysis by CD and NMR spectroscopy of a peptide encompassing the amphipathic domain of YopD from *Yersinia*. Eur. J. Biochem. **269:**3659-3668.

126. **Brutinel ED, Vakulskas CA, Yahr TL.** 2010. ExsD inhibits expression of the *Pseudomonas aeruginosa* type III secretion system by disrupting ExsA self-association and DNA binding activity. J Bacteriol **192:**1479-1486.

127. **Thibault J, Faudry E, Ebel C, Attree I, Elsen S.** 2009. Anti-activator ExsD forms a 1:1 complex with ExsA to inhibit transcription of type III secretion operons. J Biol Chem **284:**15762-15770.

128. **Zheng Z, Chen G, Joshi S, Brutinel ED, Yahr TL, Chen L.** 2007. Biochemical characterization of a regulatory cascade controlling transcription of the *Pseudomonas aeruginosa* type III secretion system. J Biol Chem **282:**6136-6142.

129. **Dasgupta N, Lykken GL, Wolfgang MC, Yahr TL.** 2004. A novel anti-anti-activator mechanism regulates expression of the *Pseudomonas aeruginosa* type III secretion system. Mol Microbiol **53:**297-308.

130. **Lykken GL, Chen G, Brutinel ED, Chen L, Yahr TL.** 2006. Characterization of ExsC and ExsD self-association and heterocomplex formation. J Bacteriol **188:**6832-6840.

131. **Gouy M, Guindon S, Gascuel O.** 2010. SeaView version 4: A multiplatform graphical user interface for sequence alignment and phylogenetic tree building. Mol. Biol. Evol. **27:**221-224.

CHAPTER 2

Hereditary Hemochromatosis Predisposes Mice to *Yersinia pseudotuberculosis* Infection Even in the Absence of the Type III Secretion System

By Halie K Miller*, Leah Schwiesow*, Winnie Au-Yeung and Victoria Auerbuch

*Authors contributed equally to this work

ABSTRACT

The iron overload disorder hereditary hemochromatosis (HH) predisposes humans to serious disseminated infection with pathogenic *Yersinia* as well as several other pathogens. Recently, we showed that the iron-sulfur cluster coordinating transcription factor IscR is required for type III secretion in *Y. pseudotuberculosis* by direct control of the T3SS master regulator LcrF. In *E. coli* and *Yersinia*, IscR levels are predicted to be regulated by iron bioavailability, oxygen tension, and oxidative stress, such that iron depletion should lead to increased IscR levels. To investigate how host iron overload influences *Y. pseudotuberculosis* virulence and the requirement for the Ysc type III secretion system (T3SS), we utilized two distinct murine models of HH: hemojuvelin knockout mice that mimic severe, early-onset HH as well as mice with the $Hfe^{C282Y/C282Y}$ mutation carried by 10% of people of Northern European descent, associated with adult-onset HH. $Hjv^{-/-}$ and $Hfe^{C282Y/C282Y}$ transgenic mice displayed enhanced colonization of deep tissues by *Y. pseudotuberculosis* following oral inoculation, recapitulating enhanced susceptibility of humans with HH to disseminated infection with enteropathogenic *Yersinia*. Importantly, HH mice orally infected with *Y. pseudotuberculosis* lacking the T3SS-encoding virulence plasmid, pYV, displayed increased deep tissue colonization relative to wildtype mice. Consistent with previous reports using monocytes from HH versus healthy donors, macrophages isolated from $Hfe^{C282Y/C282Y}$ mice were defective in *Yersinia* uptake compared to wildtype macrophages, indicating that the anti-phagocytic property of the *Yersinia* T3SS plays a less important role in HH animals. These data suggest that

Yersinia may rely on distinct virulence factors to cause disease in healthy versus HH hosts.

INTRODUCTION

Iron is an essential element for almost all microorganisms, with the exception of some examples including *Lactobacillus plantarum* and *Borrelia burgdorferi* (Archibald, 1983;Posey and Gherardini, 2000). Most bacteria require anywhere from 10^{-6} to 10^{-7} M free iron to support growth. However, pathogenic bacteria often encounter iron-limiting conditions, particularly during growth within mammalian hosts due to the success of host iron sequestration systems (Weinberg, 1978;Cassat and Skaar, 2013). These systems include binding of iron to the storage protein ferritin, complexing iron with heme, and the tight association of serum iron to transferrin (Cassat and Skaar, 2013). Free iron in humans is further sequestered during infection via inflammation-induced hypoferremia, which includes host production of increased amounts of lactoferrin in an attempt to restrict bacterial growth (Jurado, 1997). To compensate, pathogens employ a number of iron acquisition mechanisms to acquire iron from the host, including siderophores, transferrin/lactoferrin receptors, heme acquisition systems, and other types of iron uptake systems (Cassat and Skaar, 2013).

The ability to sense the iron limiting environment of mammalian hosts not only allows for induction of bacterial iron acquisition systems, but serves as a signal for many pathogens to regulate virulence determinant expression (Skaar, 2010). An important virulence determinant for many Gram-negative pathogens that can be

regulated by iron is the type III secretion system (T3SS) (Murphy and Payne, 2007;Ellermeier and Slauch, 2008;Gode-Potratz et al., 2010;Chakraborty et al., 2011;Kurushima et al., 2012). This system utilizes a needle-like apparatus to deliver a series of effector proteins directly into host cells leading to modulation of normal host cell processes (Cornelis, 2006). *Shigella dysenteriae*, *Salmonella enterica*, *Vibrio parahaemolyticus*, *Bordetella bronchiseptica*, and *Edwardsiella tarda* are a few of the Gram-negative pathogens that regulate their T3SS in response to iron bioavailability within the host (Murphy and Payne, 2007;Ellermeier and Slauch, 2008;Gode-Potratz et al., 2010;Chakraborty et al., 2011;Kurushima et al., 2012). The *Yersinia* Ysc T3SS, which is encoded on the 70 kb virulence plasmid termed pYV, is modulated in response to temperature, calcium concentration, and host cell contact. Iron has never been demonstrated to modulate expression or function of the *Yersinia* Ysc T3SS and studies are typically performed under iron replete conditions (Cornelis et al., 1998). Recently, our group identified the iron-sulfur cluster coordinating transcription factor IscR as a novel component of the *Yersinia* T3SS regulatory cascade; deletion of IscR leads to a dramatic decrease in secretion of T3SS effector proteins (Miller et al., 2014). In that study, we demonstrated that IscR is essential for T3SS expression through direct regulation of *lcrF*, which encodes an AraC-type DNA binding protein responsible for expression of the majority of T3SS genes (Cornelis et al., 1998). It remains unclear exactly which environmental stimuli influence IscR target gene expression; however, the closely related *E. coli* IscR has been shown to respond to

oxidative stress and oxygen limitation as well as iron starvation (Giel et al., 2006;Yeo et al., 2006;Wu and Outten, 2009).

The fact that IscR regulates the *Y. pseudotuberculosis* Ysc T3SS suggests that iron may play an important role in modulating expression of *Yersinia* virulence factors. Indeed, enteropathogenic *Yersinia* transit from the intestinal lumen, where they may be able to successfully compete for dietary iron, to severely iron restricted distal tissues. It is in these deeper tissue sites where the *Yersinia* Ysc T3SS has been shown to translocate effector proteins called Yops into cells such as macrophages and neutrophils (Marketon et al., 2005;Koberle et al., 2009;Durand et al., 2010). These Yops act to inhibit phagocytosis and to dampen inflammatory properties of innate immune cells (McCance and Widdowson, 1938;Martin et al., 1987;Miret et al., 2003;Heesemann et al., 2006;Matsumoto and Young, 2009). How host iron availability impacts T3SS utilization and virulence in *Yersinia* is unclear.

Iron overload disorders such as hereditary hemochromatosis (HH) predispose individuals to *Yersinia* infection (Jacquenod et al., 1984;Mennecier et al., 2001a;Harris and Paraskevakis, 2012;Quenee et al., 2012). Hereditary hemochromatosis (HH) is a genetic iron overload disorder and is one of the most common genetic disorders in Caucasians (Bahram et al., 1999). Individuals with HH absorb excess dietary iron, which then accumulates in tissues such as the liver. If left untreated, this iron accumulation can lead to organ failure as a result of iron-induced oxidative stress (MacKenzie et al., 2008). Mutations within several different genes, including the high iron Fe (*Hfe*) and the hemojuvelin (*Hjv*) genes, have been linked to

HH. Both *Hfe* and *Hjv* act to control expression of the iron-regulating hormone hepcidin, which regulates iron uptake in the gut and the recycling of senescent red blood cells by macrophages (Feder et al., 1996;Bahram et al., 1999;Huang et al., 2005). The *Hfe* C282Y mutation is associated with adult-onset HH, while *Hjv* mutations are rare and associated with more severe, early onset iron overload (Brandhagen et al., 2002;Lanzara et al., 2004). The $Hfe^{C282Y/C282Y}$ and $Hjv^{-/-}$ mouse models have been developed for the study of HH and mimic a number of the symptoms seen in the human disease, including excess liver iron (Levy et al., 1999;Huang et al., 2005).

Quenee et al. previously showed that an *Hjv* mutation predisposes mice to infection with a *Y. pestis* vaccine strain lacking the *pgm* locus, which encodes the yersiniabactin siderophore iron uptake system. However, the authors observed no difference in the ability of fully virulent *Y. pestis* to cause disease in wildtype and $Hjv^{-/-}$ mice (Quenee et al., 2012). While humans with HH are at higher risk for contracting disseminated enteropathogenic *Yersinia* infection (Piroth et al., 1997;Bergmann et al., 2001;Hopfner et al., 2001;Mennecier et al., 2001b), whether $Hfe^{C282Y/C282Y}$ and $Hjv^{-/-}$ mice are more susceptible to *Y. pseudotuberculosis* is unknown. Additionally, based on the knowledge that IscR directly regulates T3SS expression, it is unclear to what extent the Ysc T3SS contributes to *Y. pseudotuberculosis* pathogenesis in an HH host. This work provides the first evidence for enhanced susceptibility of $Hfe^{C282Y/C282Y}$ and $Hjv^{-/-}$ mice to *Y. pseudotuberculosis*.

Furthermore, we demonstrate that there is a decreased requirement for the *Yersinia* Ysc T3SS for disease causation in hosts with hereditary hemochromatosis.

MATERIALS AND METHODS

All animal use procedures were in strict accordance with the NIH Guide for the Care and Use of Laboratory Animals and were approved by the UCSC Institutional Animal Care and Use Committee.

Bacterial strains and growth conditions. *Y. pseudotuberculosis* strains used in this study are included in Table 1. Unless specified, *Y. pseudotuberculosis* strains were grown overnight in LB at 26°C with shaking at 250 rpm for animal infections. For macrophage infections, bacteria were grown overnight in 2xYT at 26˚C at 250 rpm, back-diluted to OD_{600} of 0.2 into low calcium medium (2xYT with 20 mM sodium oxalate and 20 mM $MgCl_2$), grown for 1.5 hours at 26˚C at 250 rpm, and then for 1.5 hours at 37˚C at 250 rpm to induce the T3SS (Auerbuch et al., 2009).

Table 1. *Y. pseudotuberculosis* strains used in this study.

Strain	Background	Mutation(s)	Reference
WT	IP2666	pYV+, Naturally lacks full-length YopT	(Bliska et al., 1991)
Δyop6	IP2666	Δ*yopHEMOJ*	(Auerbuch et al., 2009)
pYV-	IP2666	Δ*yscBL* pYV cured	(Auerbuch et al., 2009)
Δyop6/Δ*yopB*	IP2666	Δ*yopHEMOJ* Δ*yopB*	(Auerbuch et al., 2009)

Mouse infections. *Hfe*$^{C282Y/C282Y}$ mice were rederived in the UC Santa Cruz vivarium and *Hjv*$^{-/-}$ breeding pairs were obtained from Dr. Nancy Andrews (Duke University). Colonies were maintained through a combination of mating pairs including

homozygous knockout/homozygous knockout, heterozygous mutant/heterozygous mutant as well as homozygous knockout/heterozygous mutant. Age matched wildtype mice were obtained through wildtype/wildtype as well as the above mentioned heterozygous mutant/heterozygous mutant matings. Genotypes were determined from tail biopsies processed using the DNeasy Blood & Tissue Kit (Qiagen) per the manufacture's protocol. Wildtype or knockout female and male, eleven to twelve-week-old *Hfe*$^{C282Y/C282Y}$ mice and five to twelve-week-old *Hjv*$^{-/-}$ mice in the 129S6/SvEvTac background from our breeding facilities were used for oral infections as previously described (Auerbuch and Isberg, 2007). Mice were orogastrically inoculated with $2x10^8$ colony forming units (CFU) for *Hfe*$^{C282Y/C282Y}$ infections or $2x10^7$ CFU for *Hjv*$^{-/-}$ infections in a 200 µl volume of PBS using a feeding needle. Mice were given food containing a standard amount of iron (200 ppm) and water *ad libitum* and were euthanized at either 3 or 5 days post-inoculation. Peyer's patches, mesenteric lymph nodes, spleens, and livers were isolated and homogenized for 30 s in PBS followed by serial dilution and plating on LB supplemented with 1 µg mL^{-1} irgasan for CFU determination.

Tissue iron content. Total hepatic iron content was measured in tissue homogenates (tissue homogenized in PBS containing 0.2% NP-40, 1:4 w/v tissue:buffer) processed for analyses by aliquoting into acid-cleaned polyethylene tubes, evaporating to dryness, and digesting in 16N quartz-distilled HNO_3 (Optima, Fisher Scientific) at 80°C in a heat block. Following complete digestion, samples were diluted with Milli-Q water (18 Mohm/cm^2) for analyses; rhodium was added as an internal standard.

Iron levels were measured by high resolution inductively coupled plasma–mass spectrometry (Thermo Scientific Element XR ICP-MS), measuring masses ^{54}Fe, ^{56}Fe, ^{57}Fe, and ^{103}Rh. The analytical detection limit and measurement precision was 5.68 ng/mL 1.04% RSD, respectively.

Peritoneal Macrophages. Peritoneal macrophages were isolated from 129S6/SvEvTac wildtype, *Hfe*$^{C282Y/C282Y}$, and *Hjv*$^{-/-}$ mice as described in (Layoun et al., 2015). Briefly, mice were injected with 1 mL of 3.8% Brewer's thioglycollate media (BD Biosciences). Four days post-injection, mice were euthanized and peritoneal macrophages isolated. Macrophages were seeded at 5x10^5 cells/well into a 24 well plate and allowed to adhere to the plate for two hours. Macrophages were then treated with 100 ng ml^{-1} of lipopolysaccharide (LPS) from *Salmonella minnesota* (UltraPure), or exposed to either a *Y. pseudotuberculosis* mutant lacking Yop effectors but otherwise expressing a functional T3SS (T3SS+, Δyop6; (Auerbuch et al., 2009)) or with T3SS translocon deficient *Y. pseudotuberculosis* (T3SS-, Δ*yopB*; (Adams et al., 2015)) at an MOI of 10. Macrophages were treated for 3 hrs, at which time supernatants were collected and analyzed for cytokine levels as described below.

Inside/Outside Staining. Peritoneal macrophages were isolated as described above. After being allowed to adhere to coverslips for two hours, macrophages were infected with pYV- *Y. pseudotuberculosis* at an MOI of 10. After 0.5 hours, infected cell monolayers were fixed for 10 minutes with 4% paraformaldehyde. Infected macrophages were treated with rabbit anti-*Yersinia* antibody (1:500), generously provided by Dr. Ralph Isberg (Tufts University), for 40 minutes at 37°C followed

treatment with goat anti-rabbit AlexaFlour 594 antibody (1:100, Life Technologies) for 40 minutes at 37°C. Macrophages were washed and then treated with ice cold methanol for 10 seconds to permeabilize. After permeabilizaton, macrophages were treated with rabbit anti-*Yersinia* antibody (1:500) for 40 minutes at 37°C followed by treatment with goat anti-rabbit FITC antibody (1:100, Santa Cruz Biotech) and Hoescht stain (1:10,000) for 40 minutes at 37°C. Coverslips were then mounted onto slides with Prolong Gold Antifade Reagent (Life Technologies). Slides were visualized on a Leica SP5 confocal microscope using Leica Application Suite Advanced Fluorescence software. Nine frames were obtained for each condition, and for each frame, the number of red bacteria and the number of green bacteria were counted using FIJI ImageJ software.

ELISA Cytokine Measurement. Cytokine measurements were performed as previously described (Auerbuch and Isberg, 2007). Briefly, liver homogenates from *Hfe*$^{C282Y/C282Y}$ and wildtype mice, either uninfected or orogastrically inoculated with $2x10^8$ CFU of wildtype *Y. pseudotuberculosis*, were thawed on ice and centrifuged at 13,000 rpm for 1 min. The mouse inflammatory cytometric bead array kit (BD Biosciences) was used to detect IL-12p70, TNF-α, IFN-γ, MCP-1, IL-10, and IL-6 according to the manufacturer's protocol with the following exceptions. The amount of antibody-conjugated beads was decreased to 4 µl each with 20 µl of sample/standard and 20 µl of detection reagent per reaction. Data were acquired and analyzed using a BD FACS LSRII flow cytometer and BD analysis software, respectively. Cytokine levels detected in the livers of uninfected mice (3

Hfe$^{C282Y/C282Y}$ and 3 wildtype) were averaged and the standard deviations calculated for each cytokine tested (Excel). Standard deviations were added to the averages to determine the baseline cytokine level for uninfected livers. Individual cytokine concentrations in pg per ml^{-1} from infected samples were plotted against CFU per gram of liver tissue determined at the time of organ harvest.

Statistical Methods. All statistical methods in this study were analyzed using Kaleidagraph v4.1.1 for Windows (Synergy Software). Oral gavage infection studies were analyzed using the unpaired Wilcoxon-Mann-Whitney rank sum test. Measurement of hepatic iron load from tissues and measurement of cytokine levels from liver homogenates and peritoneal macrophages were analyzed using a Student's *t*-test. The correlation between bacterial burden and cytokine production was analyzed using Pearson's coefficient. Lastly, Student *t* test was used for analysis of the uptake assay. Statistical significance for all analyses in this study was defined as $p \leq 0.05$.

RESULTS

Host mutations associated with iron overload, *Hfe*$^{C282Y/C282Y}$ and *Hjv*$^{-/-}$, lead to enhanced systemic colonization of *Y. pseudotuberculosis*. In order to better understand the biological significance of the influence of iron on *Y. pseudotuberculosis* pathogenesis, we studied susceptibility of murine models of hereditary hemochromatosis (HH) to *Y. pseudotuberculosis* infection. We began by evaluating the susceptibility of two distinct mouse models of HH, *Hfe*$^{C282Y/C282Y}$ and *Hjv*$^{-/-}$, to *Y. pseudotuberculosis* oral infection. While all wildtype mice survived for

five days (when the experiment was terminated) following an oral inoculation dose of $2x10^8$ *Y. pseudotuberculosis*, 100% of *Hjv*$^{-/-}$ mice receiving the same dose had to be euthanized prior to day five because of symptoms indicative of more severe disease including hunched appearance and ruffled fur (unpublished observations), in accordance with institutional guidelines. This indicates that *Hjv*$^{-/-}$ mice may be more susceptible to oral infection with *Y. pseudotuberculosis* than normal mice. Using a lower oral inoculation dose of $2x10^7$ *Y. pseudotuberculosis* allowed both wildtype and *Hjv*$^{-/-}$ mice to survive five days of infection. We observed some differences in *Y. pseudotuberculosis* colonization of wildtype and *Hjv*$^{-/-}$ Peyer's patches and mesenteric lymph nodes (MLN) three and five days post-inoculation (Figure 1AB). However, more strikingly, while bacterial loads were below the limit of detection from the spleens and livers of all wildtype mice three days post-inoculation, the majority of *Hjv*$^{-/-}$ mouse spleens and livers contained greater numbers of bacteria relative to wild type (Figure 1A). Furthermore, by five days post-inoculation, *Hjv*$^{-/-}$ mice had 215-fold and 380-fold more CFU per gram tissue, on average, in the spleen and liver compared to wildtype mice (Figure 1B). Collectively, these data suggest that *Y. pseudotuberculosis* colonize deep tissues earlier in *Hjv*$^{-/-}$ mice compared to normal mice following the natural oral route of infection.

Analysis of the *Hfe*$^{C282Y/C282Y}$ mice, which display less severe iron overload relative to the *Hjv*$^{-/-}$ background (Huang et al., 2005), showed no significant differences in bacterial colonization three days post-inoculation compared to wildtype mice (data not shown) and comparable levels of colonization in the Peyer's patches,

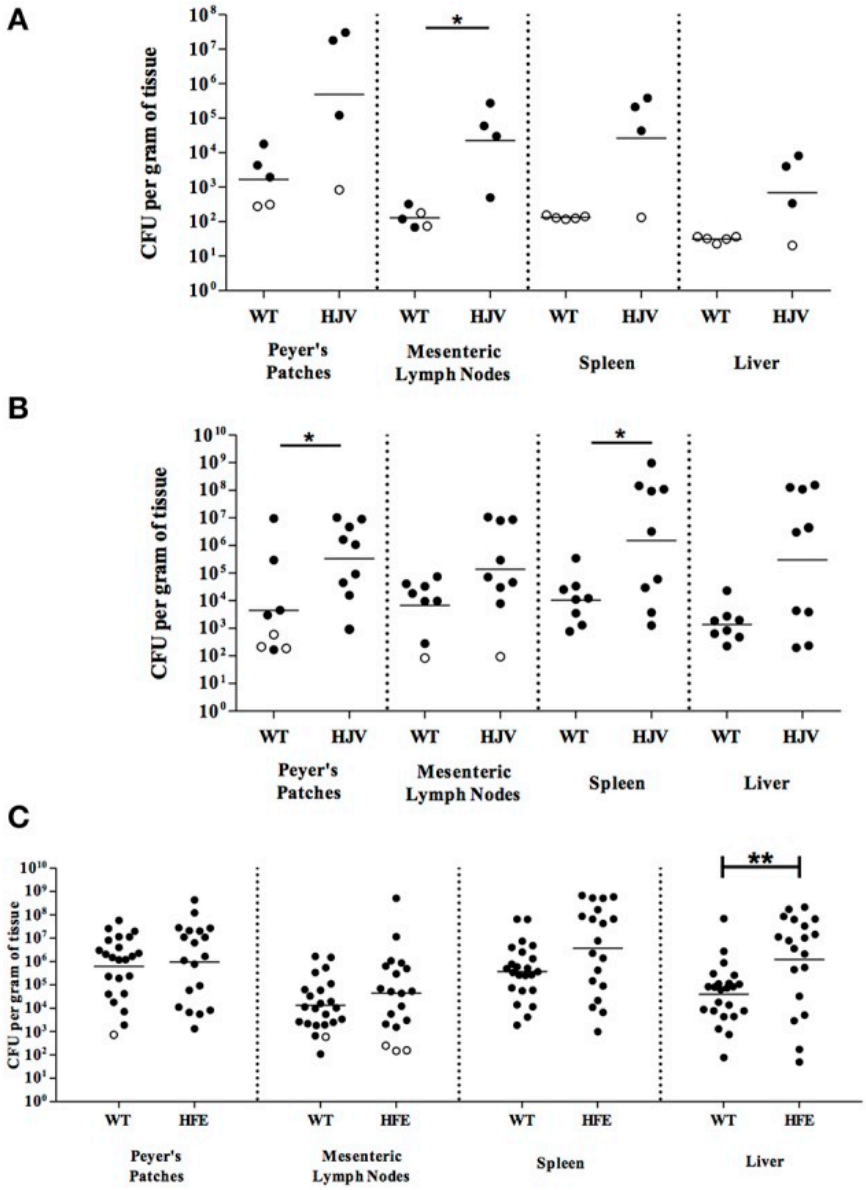

Figure 1. Iron overload leads to enhanced colonization of mice orally infected with *Y. pseudotuberculosis*. Wildtype (WT) and *Hjv*$^{-/-}$ (HJV) mice were infected with 2x10^{7} WT *Y. pseudotuberculosis* via orogastric gavage. At **(A)** 3 days and **(B)** 5 days post-inoculation, the Peyer's patches, mesenteric lymph nodes, spleens and livers were collected, homogenized, and CFU determined. **(C)** WT and *Hfe*$^{C282Y/C282Y}$ (HFE) mice were infected with 2x10^{8} WT *Y. pseudotuberculosis* via orogastric gavage and

tissues harvested 5 days post-inoculation. Each symbol represents data from one organ. Open symbols are set at the limit of detection for each individual organ based on weight and represent CFU that were below this limit. Dashes represent the geometric mean. Shown are data from (A) two, (B) four, and (C) seven independent experiments. * $p<0.05$, ** $p<0.01$ as determined by an unpaired Wilcoxon-Mann-Whitney rank sum test. Dashes represent the geometric mean

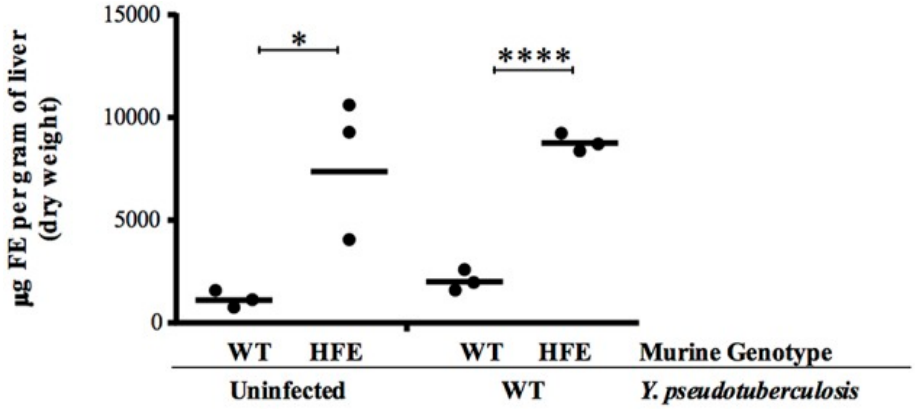

Figure 2. *Hfe*$^{C282Y/C282Y}$ mice harbor increased hepatic iron. Hepatic iron load was measured from tissues isolated from WT and *Hfe*$^{C282Y/C282Y}$ (HFE) mice that were left uninfected or were infected 5 days earlier with $2x10^8$ WT *Y. pseudotuberculosis* via orogastric gavage. Each symbol represents data from one organ. * $p<0.05$ and **** $p<0.0001$ as determined by a Student *t* test.

MLN, and spleens relative to wildtype mice five days post-inoculation with $2x10^8$ *Y. pseudotuberculosis* (Figure 1C). However, colonization of the liver five days post-inoculation was increased in *Hfe*$^{C282Y/C282Y}$ mice by 30-fold ($p<0.01$). This increased liver colonization of *Hfe*$^{C282Y/C282Y}$ mice correlated with four-fold more iron in *Hfe*$^{C282Y/C282Y}$ livers relative to wildtype livers during *Yersinia* infection (Figure 2).

Collectively, these data suggest that both the *Hfe*$^{C282Y/C282Y}$ and *Hjv*$^{-/-}$ mice are effective models for the study of *Y. pseudotuberculosis* infection in iron overloaded hosts. Based on the knowledge that the *Hfe*$^{C282Y/C282Y}$ mutation is far more common in humans than mutations in the *Hjv* gene, and that the *Hjv*$^{-/-}$ animals were significantly more challenging to breed, we focused the remainder of our studies on the *Hfe*$^{C282Y/C282Y}$ mouse model (Brandhagen et al., 2002;Lanzara et al., 2004).

***Y. pseudotuberculosis* lacking the T3SS encoding virulence plasmid pYV display enhanced virulence in *Hfe*$^{C282Y/C282Y}$ mice.** Excess iron should lead to decreased IscR levels, and therefore decreased expression of the T3SS (Miller et al., 2014). Yet while the Ysc T3SS is required for *Yersinia* virulence in normal mice (Cornelis, 2002), we observed increased susceptibility of iron overloaded mice to *Y. pseudotuberculosis* (Figures 1). Thus, we evaluated the susceptibility of *Hfe*$^{C282Y/C282Y}$ mice to *Y. pseudotuberculosis* lacking the T3SS-encoding virulence plasmid, pYV. The pYV$^-$ strain was better able to colonize livers of *Hfe*$^{C282Y/C282Y}$ mice compared to wildtype mice; pYV$^-$ colonization of *Hfe*$^{C282Y/C282Y}$ livers was increased 8-fold ($p<0.0001$) compared to pYV$^-$ infection of wildtype tissues (Figure 3). In fact, while the pYV$^-$ strain was able to colonize the liver to levels above the

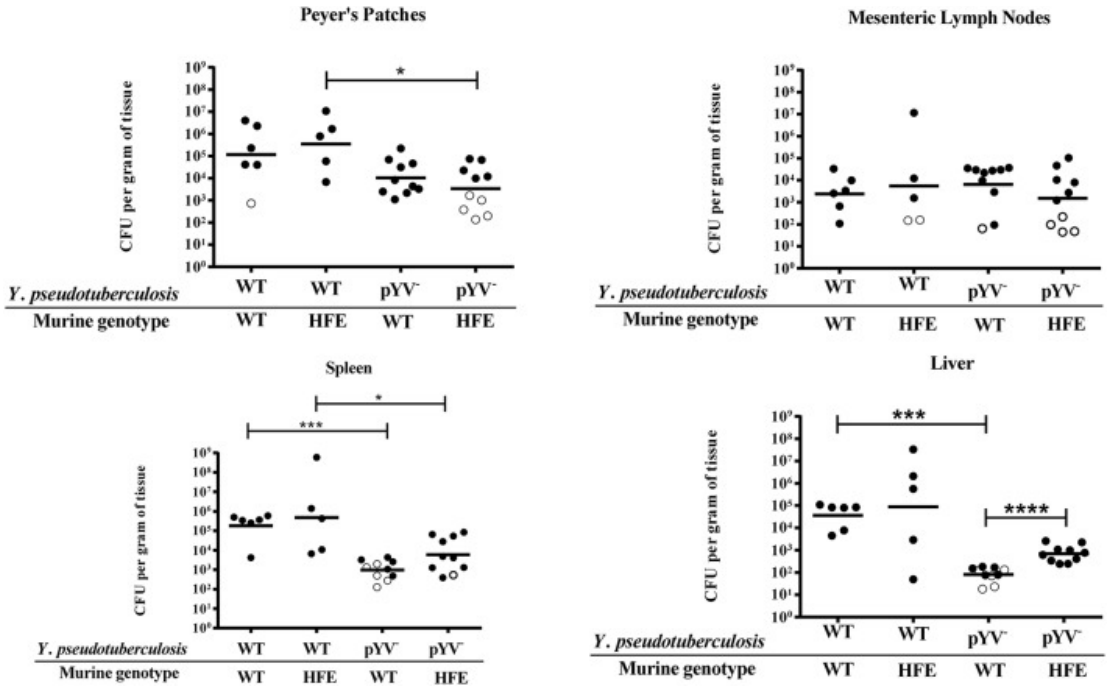

Figure 3. *Y. pseudotuberculosis* lacking the T3SS encoding virulence plasmid, pYV, are able to better colonize the spleens and livers of *Hfe*$^{C282Y/C282Y}$ mice relative to wildtype mice. WT and *Hfe*$^{C282Y/C282Y}$ (HFE) mice were infected with $2x10^8$ CFU of either WT *Y. pseudotuberculosis* or the pYV$^-$ strain via orogastric gavage. At 5 days post-inoculation, the Peyer's patches, mesenteric lymph nodes, spleens and livers were collected, homogenized, and CFU determined. Each symbol represents data from one organ. Open symbols are set at the limit of detection for each individual organ based on weight and represent CFU that were below this limit. Dashes represent the geometric mean. Shown are data from three independent experiments. The wildtype data presented here is also included in Figure 1C. * $p<0.05$, ***$p<0.001$, and **** $p<0.0001$ as determined by an unpaired Wilcoxon-Mann-Whitney rank sum test. Dashes represent the geometric mean.

limit of detection in only 50% of the wildtype animals by day 5, this T3SS-deficient strain was able to colonize deep tissues to levels above the limit of detection in 95% of *Hfe*$^{C282Y/C282Y}$ mice. These findings suggest that there may be a decreased requirement for the *Y. pseudotuberculosis* Ysc T3SS in iron overloaded animals.

Peritoneal macrophages from HH mice are not attenuated in their cytokine and chemokine response to *Yersinia*. Previous work by Wang et al., demonstrated that peritoneal macrophages isolated from *Hfe*$^{-/-}$ mice were defective in their cytokine response to *Salmonella* through Toll-like receptor 4, as a result of decreased cytokine mRNA translation (Wang et al., 2009). Several *Yersinia* T3SS effector proteins are known to inhibit production of several cytokines (Pha and Navarro, 2016). Therefore, we sought to examine whether cytokine production was decreased in HH mice during *Yersinia* infection, as diminished cytokine production may account for both the increased bacterial burden as well as the decreased requirement for the T3SS observed for these mice. We measured the levels of the six different cytokines, TNF-α, IFN-γ, IL-6, IL-10, IL-12p70, and MCP-1, in *Yersinia*-infected mouse tissues. We found levels of IL-10 and IL-12p70 for both wildtype and *Hfe*$^{C282Y/C282Y}$ mice to be comparable to those of our uninfected controls (data not shown). These findings are not surprising as previous reports demonstrate these cytokines to be present at low levels until very late stages of infection (Auerbuch and Isberg, 2007). Liver TNF-α, IFN-γ, MCP-1, and IL-6 levels were above background in both *Hfe*$^{C282Y/C282Y}$ and wildtype mice and TNF-α, MCP-1, and IL-6 levels correlated with bacterial burden (Figure 4AB; Pearson correlation). When WT and *Hfe*$^{C282Y/C282Y}$ liver cytokine levels

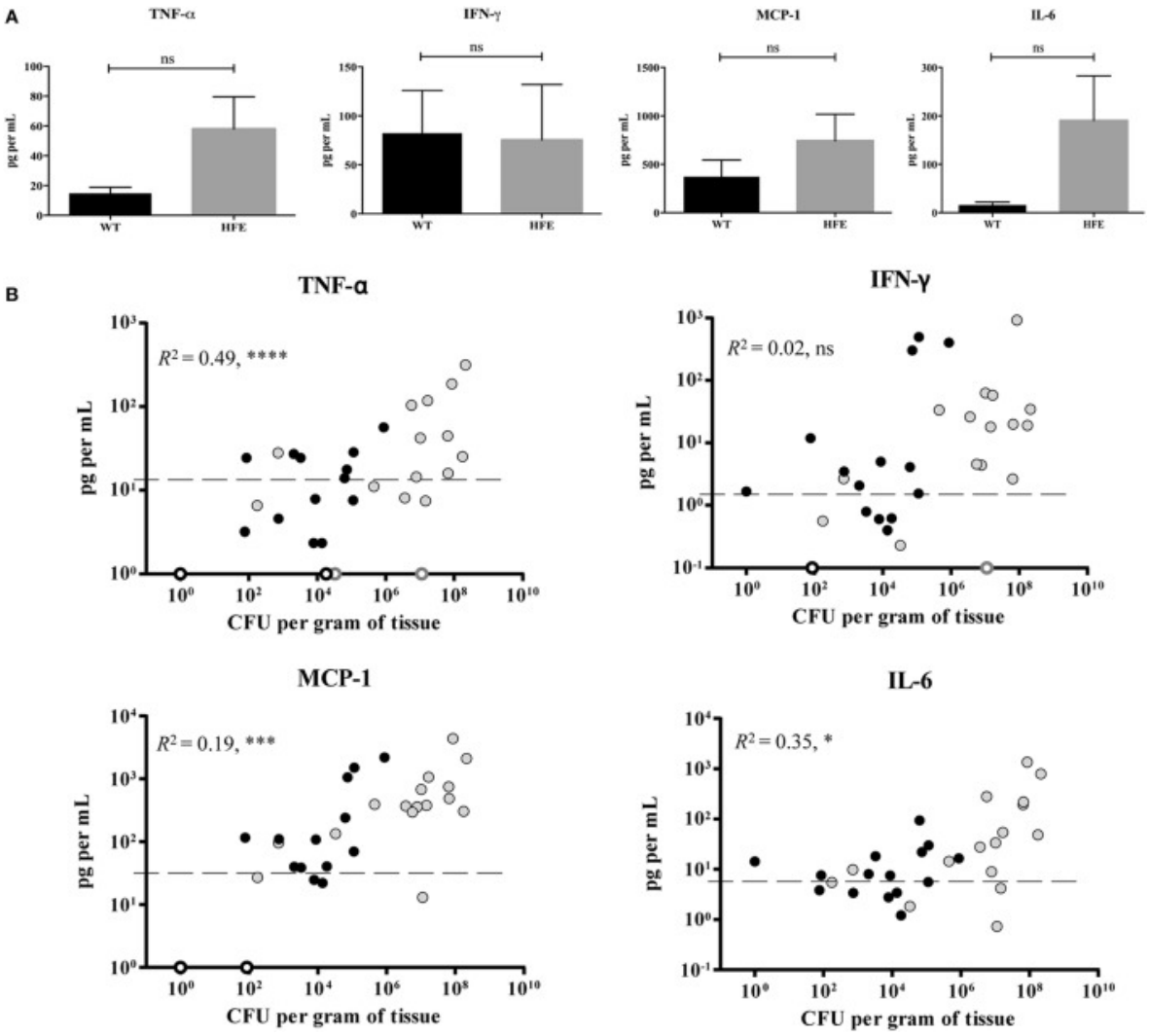

Figure 4. *Hfe*$^{C282Y/C282Y}$ mice display robust hepatic cytokine production during *Y. pseudotuberculosis* infection. WT (black) and *Hfe*$^{C282Y/C282Y}$ (HFE; grey) mice were infected with 2x10^8 WT *Y. pseudotuberculosis* via orogastric gavage and tissues harvested 5 days post-inoculation. Flow cytometry-based ELISA was used to measure levels of the cytokines IFN-γ, IL-6, and TNF-α and the chemokine MCP-1 from liver homogenates. **(A)** IFN-γ, IL-6, TNF-α, and MCP-1 levels are displayed as mean pg per ml liver homogenate ± standard error of the mean; ns = no significance as

determined by a Student *t* test. **(B)** Individual cytokine concentrations in pg/ml are plotted against CFU per gram of liver tissue determined at the time of organ harvest. Open circles represent samples where CFU were below the limit of detection. Average uninfected cytokine concentrations are displayed as a dashed line and represent the average plus the standard deviation for uninfected liver samples. R^2 values were determined based on Pearson's correlation coefficient using combined WT and HFE data; ns = no significance, *p<0.05, ***p<0.001, and **** p<0.0001.

were average together, no significant differences could be detected (Figure 4A). In fact, consistent with many HH livers having higher average CFU burdens than wildtype mice, cytokine levels for a number of the HH livers were actually higher than for wildtype livers (Figure 4B).

Because CFU burden differences between wildtype and HH mice complicated our cytokine analysis, we isolated thioglycollate-elicited peritoneal macrophages (which serve as a model for tissue macrophages) from wildtype, *Hfe*$^{C282Y/C282Y}$, and *Hjv*$^{-/-}$ mice, and infected them with *Y. pseudotuberculosis* either expressing a functional T3SS translocon but lacking the known T3SS effector proteins (Δyop6) or lacking a functional T3SS translocon (Δyop6/Δ*yopB*). These strains were used because several T3SS effector proteins have been shown to modulate cytokine production upon translocation inside host cells (Bliska et al., 2013). Surprisingly, the amount of IL-6, MCP-1, and TNFα secreted by *Hfe*$^{C282Y/C282Y}$ or *Hjv*$^{-/-}$ macrophages after three hours was significantly higher than that secreted by wildtype macrophages in response to the Δyop6 or Δyop6/Δ*yopB Y. pseudotuberculosis* strains or to LPS (Figure 5A & B). Similar results were seen for the cytokine response to the WT and pYV- *Yersinia* strains (data not shown). Furthermore, incubating peritoneal macrophages for only two hours following isolation and prior to inoculation, rather than overnight, did not alter these findings (data not shown). These data are in contrast to results from *Hfe*$^{-/-}$ C57Bl/6 mouse peritoneal macrophages treated with LPS or *Salmonella* (Wang et al., 2009), for reasons that remain unclear. However, these data suggest that an attenuated HH cytokine response is not responsible for the

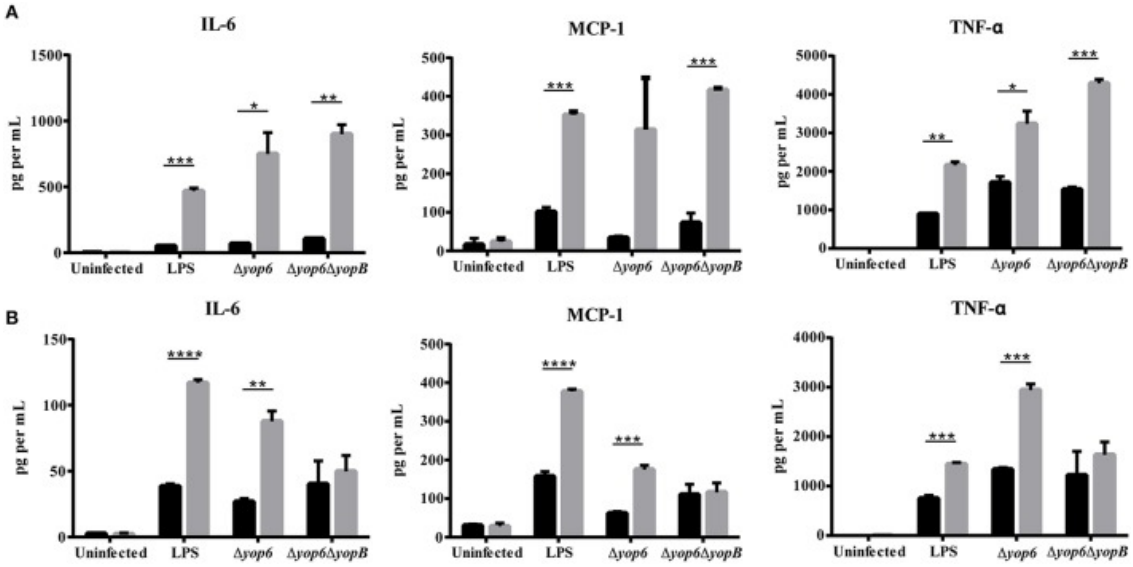

Figure 5. Peritoneal macrophages isolated from hemochromatosis mice produce elevated levels of IL-6, MCP-1, and TNF-α in response to *Y. pseudotuberculosis* compared to macrophages from wildtype mice. Elicited peritoneal macrophages from naïve WT (black bars), **(A)** *Hfe*$^{C282Y/C282Y}$ (grey bars), and **(B)** *Hjv*$^{-/-}$ (grey bars) mice were either left untreated, treated with 100 ng ml^{-1} of lipopolysaccharide (LPS) from *Salmonella minnesota* (UltraPure), or exposed to either Δyop6, a *Y. pseudotuberculosis* mutant lacking Yop effectors but expressing a functional T3SS translocon, or with Δyop6/Δ*yopB*, a T3SS translocon-deficient *Y. pseudotuberculosis* at an MOI of 10. Flow cytometry-based ELISA was used to measure levels of the cytokines IL-6 and TNF-α and the chemokine MCP-1 in the supernatant after 3 hours. Data is displayed as the average cytokine concentration from the macrophages of two mice that had been pooled and analyzed in triplicate. * $p<0.05$, ** $p<0.01$, *** $p<0.001$, **** $p<0.0001$ as determined by a Student *t* test.

increased bacterial burden or decreased requirement for the T3SS during *Yersinia* infection of HH mice.

Peritoneal macrophages from HH mice are defective in their ability to take up *Yersinia*. Previous studies indicated that phagocytic cells isolated from human HH patients were defective in phagocytosis (van Asbeck et al., 1984;Moura et al., 1998). As the *Yersinia* T3SS has potent anti-phagocytic activity (Pha and Navarro, 2016), we examined the ability of peritoneal macrophages to take up pYV^{-} *Y. pseudotuberculosis*. Consistent with previous studies, *Hfe*$^{C282Y/C282Y}$ macrophages contained two-fold fewer intracellular bacteria than wildtype macrophages (Figure 6). These data indicate that the effector function defect of HH mouse phagocytes partly negates the virulence requirement of the *Yersinia* T3SS.

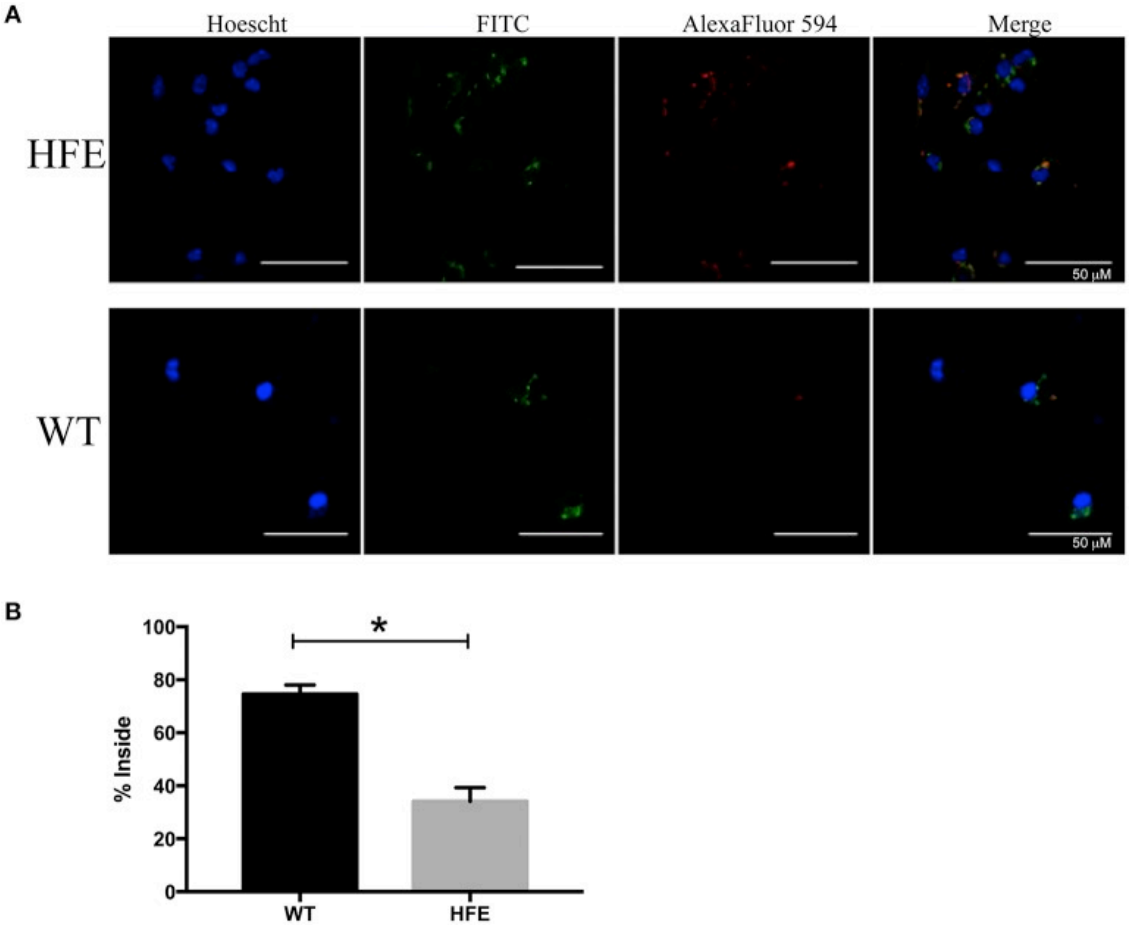

Figure 6. Peritoneal macrophages isolated from hemochromatosis mice are defective in *Yersinia* uptake compared to wildtype macrophages. Elicited peritoneal macrophages from naïve WT and *Hfe*$^{C282Y/C282Y}$ mice were infected with pYV^{-} *Y. pseudotuberculosis* and percent of bacterial uptake quantitated after 30 minutes by immunofluorescence microscopy. Extracellular bacteria were stained both red and green, while internalized bacteria were only stained green. **(A)** Representative images are shown in addition to the **(B)** average % internalized bacteria ± standard deviation of 17-20 frames from two biological replicates. * $p<0.02$ as determined by a Student *t* test.

DISCUSSION

In this study, we demonstrate that two HH mouse models are more susceptible to disseminated infection with fully virulent *Y. pseudotuberculosis* than are wildtype mice, consistent with clinical data on humans with HH. Furthermore, *Y. pseudotuberculosis* lacking the T3SS-encoding virulence plasmid pYV are able to colonize a higher percentage of HH hosts and disseminate into deeper tissues. As peritoneal macrophages isolated from HH mice were less phagocytic towards pYV$^-$ *Yersinia* than their wildtype counterparts, we propose that the requirement for the *Yersinia* T3SS, which is strongly anti-phagocytic, is diminished in HH hosts compared to healthy hosts.

Hereditary hemochromatosis is characterized by an increase in intestinal absorption of iron (Hanson et al., 2001). As there is no physiological process to rid the body of this excess iron, it accumulates in organs throughout the body such as the heart, pancreas, and liver, leading to tissue damage and decreased immune response (Hanson et al., 2001;Wang et al., 2008;Hentze et al., 2010;Pietrangelo, 2010;Ekanayake et al., 2015;Rishi et al., 2015). This condition causes an increased susceptibility to serious infection with specific bacterial pathogens including enteropathogenic *Yersinia*. However, it is unclear whether this increase in susceptibility of HH hosts is due to increased virulence of the pathogen, enhanced bacterial fitness due to increased iron availability, or a combination of these factors (Sinkovics et al., 1980;Christopher, 1985;Abbott et al., 1986;Bullen et al., 1991;Mennecier et al., 2001a;Harris and Paraskevakis, 2012). In this study, we

demonstrate that two murine models of HH, carrying *Hfe*$^{C282Y/C282Y}$ or *Hjv*$^{-/-}$ mutations, display increased susceptibility to *Y. pseudotuberculosis* infection. The more severely iron overloaded *Hjv*$^{-/-}$ mice were significantly more susceptible to *Yersinia* infection than the *Hfe*$^{C282Y/C282Y}$ mice with milder iron overload, as *Hjv*$^{-/-}$ but not *Hfe*$^{C282Y/C282Y}$ mice or wildtype mice showed overt signs of disease 5 days post-inoculation with $2x10^8$ *Y. pseudotuberculosis*, while *Hfe*$^{C282Y/C282Y}$ mice had higher liver CFU than wildtype mice. This defect in resistance of *Hjv*$^{-/-}$ mice to *Y. pseudotuberculosis* is consistent with the enhanced susceptibility of these mice to a *pgm*$^{-}$ vaccine strain of *Y. pestis* (Quenee et al., 2012).

Perhaps most intriguing is the finding that the increased bacterial burden observed for HH mice can occur in the absence of the Ysc T3SS, which is required for disseminated *Yersinia* infection of wildtype mice (Cornelis, 2002). Wang et al. described an attenuated inflammatory response of macrophages isolated from HH mice to *Salmonella* (Wang et al., 2008). In addition, macrophages and polymorphonuclear leukocytes from HH humans have been previously shown to have decreased phagocytic and microbicidal properties (van Asbeck et al., 1984;Weiss et al., 1994;Moura et al., 1998;Walker and Walker, 2000). As these host defenses are also targeted by *Yersinia* T3SS effector proteins, it is possible that in HH mice, several host defense pathways that must normally be inactivated by the Ysc T3SS to enable *Yersinia* growth are already compromised as a result of the downstream consequences of iron overload. However, we could not detect any statistically significant differences in production of TNF-α, MCP-1, IFN-γ, or IL-6 in the livers of

wildtype and HH mice infected with *Y. pseudotuberculosis*, although the elevated colonization of HH mice compared to wildtype mice complicated this analysis, as cytokine/chemokine level correlated with CFU load. Furthermore, elicited peritoneal macrophages from naïve HH mice actually produced increased levels of TNF-α, MCP-1, or IL-6 in response to *Yersinia* compared to wildtype macrophages. However, we did observe a defect in the ability of HH peritoneal macrophages to take up *Yersinia* compared to wildtype macrophages. Therefore, it is possible that the phagocytic properties of tissue macrophages in the HH mice are compromised, rendering the anti-phagocytic activity of the Ysc T3SS less important in these tissues. Interestingly, there was no decrease in $Ly6G^+$ cell infiltration in infected $Hjv^{-/-}$ mouse livers compared to infected WT livers (data not shown). Collectively, these data suggest that phagocytes are recruited to sites of infection in HH animals and produce cytokines in response to microbial PAMPS, yet are ineffective in microbial uptake.

Our data support the proposed model that an increase in iron availability might dampen T3SS expression through IscR control of the T3SS master regulator LcrF (Miller et al., 2014), as loss of the T3SS in iron overloaded mice would not be as detrimental to *Y. pseudotuberculosis* virulence as it is in wildtype mice. Furthermore, with increased emphasis on identification of novel antimicrobial strategies and research on chemical inhibitors of the T3SS as virulence blockers, our data suggests that, while T3SS inhibitors may one day be used to prevent or treat *Yersinia* infection, they may not be effective in the context of host iron overload. Recently there was a case of lethal laboratory-acquired plague in a researcher with

undiagnosed HH who became infected while working with pgm$^-$ *Y. pestis*, a strain with diminished virulence (Quenee et al., 2012). *Yersinia* strains lacking the T3SS are also considered to have decreased pathogenic potential; however, based on the data presented here, HH hosts may be more susceptible to these strains as well.

Huang et al. showed that *Hjv*$^{-/-}$ mice contained less splenic non-heme iron compared to wildtype mice, in contrast to the elevated non-heme iron observed in *Hjv*$^{-/-}$ livers (Huang et al., 2005). Quenee et al. also found iron deposits in the livers, but not the spleens, of *Hjv*$^{-/-}$ mice. Macrophages play an important role in the recycling of iron from senescent red blood cells, and Huang et al. demonstrated that the increased iron recycling in *Hjv*$^{-/-}$ mice leads to higher extracellular iron and lower macrophage intracellular iron (Huang et al., 2005). As the spleen contains numerous macrophages (Cesta, 2006), it is possible that decreased macrophage iron in *Hjv*$^{-/-}$ mice contributes to the lower overall splenic iron level (Hentze et al., 2010). Interestingly, we observed an increase in bacterial burden in both the liver and spleen of *Hjv*$^{-/-}$ mice compared to wildtype mice. As we did not perform perfusion prior to organ harvesting, as per standard practice in the field, it is possible that enhanced bacterial colonization of *Hjv*$^{-/-}$ spleens reflects enhanced *Y. pseudotuberculosis* growth in *Hjv*$^{-/-}$ blood. Unlike *Hfe*$^{C282Y/C282Y}$ mice, which have been shown to have comparable serum iron concentrations relative to wild type mice, *Hjv*$^{-/-}$ mice have elevated iron levels in the blood relative to wild type (Zhou et al., 1998;Gkouvatsos et al., 2014). Indeed, *Hjv*$^{-/-}$ mice displayed enhanced *Yersinia* spleen colonization but *Hfe*$^{C282Y/C282Y}$ mice did not.

Interestingly, Quenee et al. showed that a recombinant protein vaccine that targets the T3SS needle tip protein LcrV protects *Hjv*$^{-/-}$ mice against fully virulent plague or against a live, attenuated vaccine strain of *Y. pestis* (Quenee et al., 2012). The rV10 vaccine was previously shown to elicit antibodies to LcrV, and anti-LcrV antibodies are known to inhibit translocation of Yop effectors into host cells (DeBord et al., 2006;Quenee et al., 2010). These data suggest that anti-LcrV antibody targeting of *Y. pestis* protects HH mice against otherwise lethal plague either by inactivation of the T3SS and/or through opsonization of *Yersinia* (Quenee et al., 2010). Given our data showing that the *Y. pseudotuberculosis* T3SS is dispensable for disseminated infection, it is possible that the increased bacterial load that we observed also occurs in the model of survival utilized by Quenee et al., but that the HH mice are able to clear the infection.

Our findings as well as those of Quenee et al (Quenee et al., 2012) suggest that the increased susceptibility of HH hosts to *Yersinia* infection is likely a result of excess iron available to promote bacterial growth. Indeed, *Y. pestis* strains lacking the ability to synthesize yersiniabactin, an iron scavenging siderophore, are fully virulent in HH hosts (Quenee et al., 2012). Additionally, mice infected with *Y. enterocolitica* or *Y. pestis* that were given either iron-dextran or the siderophore Desferal, which can be used by *Yersinia* as an iron source, displayed reduced lethal doses as well as a more severe yersiniosis (Burrows and Jackson, 1956;Robins-Browne and Prpic, 1985;Galvan et al., 2010;Quenee et al., 2012). Collectively, these results and the data shown here suggest that the progression and pathology of yersiniosis may differ

greatly in iron overloaded versus non-iron overloaded hosts because of excess bioavailable iron, deficiency in the phagocytic properties of immune cells, and differences in bacterial virulence factors required to cause disease.

ACKNOWLEDGEMENTS

We thank Martha Zuniga for critical review of the manuscript, Donald Smith and Rob Franks for technical support with the tissue iron measurement, Nancy Andrews for the *Hjv*$^{-/-}$ mice, Armen Shamamian in the UCSC vivarium for rederivation of the HFE$^{C282Y/C282Y}$ mice, Bari Holm Nazario in the UCSC Flow Cytometry Facility for technical support with the flow-cytometry assay, Ben Abrams in the UCSC Life Sciences Microscopy Center for technical support with microscopy, Richard Frothingham for useful discussion on HH mouse infection, Ralph Isberg for the anti-*Yersinia* antibody, and the UCSC vivarium staff for their assistance with animal care and maintenance. Research reported in this publication was supported by the National Institute of Allergy and Infectious Diseases of the National Institutes of Health under Award Number R21AI099747 (to V.A.). L.S. was supported by the National Institutes of Health training grant T32GM008646.

REFERENCES

Abbott, M., Galloway, A., and Cunningham, J.L. (1986). Hemochromatosis Presenting with a Double *Yersinia* Infection. *Journal of Infection* 13**,** 143-145. doi: Doi 10.1016/S0163-4453(86)92869-0.

Archibald, F. (1983). *Lactobacillus plantarum*, an Organism Not Requiring Iron. *FEMS Microbiol Lett* 19**,** 29-32. doi: DOI 10.1111/j.1574-6968.1983.tb00504.x.

Auerbuch, V., Golenbock, D.T., and Isberg, R.R. (2009). Innate immune recognition of *Yersinia pseudotuberculosis* type III secretion. *PLoS Pathog* 5**,** e1000686. doi: 10.1371/journal.ppat.1000686.

Auerbuch, V., and Isberg, R.R. (2007). Growth of *Yersinia pseudotuberculosis* in mice occurs independently of Toll-like receptor 2 expression and induction of interleukin-10. *Infect Immun* 75**,** 3561-3570. doi: 10.1128/IAI.01497-06.

Bahram, S., Gilfillan, S., Kuhn, L.C., Moret, R., Schulze, J.B., Lebeau, A., and Schumann, K. (1999). Experimental hemochromatosis due to MHC class I HFE deficiency: immune status and iron metabolism. *Proc Natl Acad Sci U S A* 96**,** 13312-13317.

Bergmann, T.K., Vinding, K., and Hey, H. (2001). Multiple hepatic abscesses due to *Yersinia enterocolitica* infection secondary to primary haemochromatosis. *Scand J Gastroenterol* 36**,** 891-895.

Bliska, J.B., Guan, K.L., Dixon, J.E., and Falkow, S. (1991). Tyrosine phosphate hydrolysis of host proteins by an essential *Yersinia* virulence determinant. *Proc Natl Acad Sci U S A* 88**,** 1187-1191.

Bliska, J.B., Wang, X., Viboud, G.I., and Brodsky, I.E. (2013). Modulation of innate immune responses by *Yersinia* type III secretion system translocators and effectors. *Cell Microbiol* 15**,** 1622-1631. doi: 10.1111/cmi.12164.

Brandhagen, D.J., Fairbanks, V.F., and Baldus, W. (2002). Recognition and management of hereditary hemochromatosis. *Am Fam Physician* 65**,** 853-860.

Bullen, J.J., Spalding, P.B., Ward, C.G., and Gutteridge, J.M.C. (1991). Hemochromatosis, Iron, and Septicemia Caused by *Vibrio vulnificus*. *Arch Intern Med* 151**,** 1606-1609. doi: DOI 10.1001/archinte.151.8.1606.

Burrows, T.W., and Jackson, S. (1956). The virulence-enhancing effect of iron on nonpigmented mutants of virulent strains of *Pasteurella pestis*. *Br J Exp Pathol* 37**,** 577-583.

Cassat, J.E., and Skaar, E.P. (2013). Iron in Infection and Immunity. *Cell Host & Microbe* 13**,** 510-520. doi: DOI 10.1016/j.chom.2013.04.010.

Cesta, M.F. (2006). Normal structure, function, and histology of the spleen. *Toxicol Pathol* 34**,** 455-465. doi: 10.1080/01926230600867743.

Chakraborty, S., Sivaraman, J., Leung, K.Y., and Mok, Y.K. (2011). Two-component PhoB-PhoR regulatory system and ferric uptake regulator sense phosphate and iron to control virulence genes in type III and VI secretion systems of *Edwardsiella tarda*. *J Biol Chem* 286**,** 39417-39430. doi: 10.1074/jbc.M111.295188.

Christopher, G.W. (1985). *Escherichia coli* Bacteremia, Meningitis, and Hemochromatosis. *Arch Intern Med* 145**,** 1908-1908.

Cornelis, G.R. (2002). The *Yersinia* Ysc-Yop 'type III' weaponry. *Nat Rev Mol Cell Biol* 3**,** 742-752. doi: 10.1038/nrm932.

Cornelis, G.R. (2006). The type III secretion injectisome. *Nat Rev Microbiol* 4**,** 811-825. doi: 10.1038/nrmicro1526.

Cornelis, G.R., Boland, A., Boyd, A.P., Geuijen, C., Iriarte, M., Neyt, C., Sory, M.P., and Stainier, I. (1998). The virulence plasmid of *Yersinia*, an antihost genome. *Microbiol Mol Biol Rev* 62**,** 1315-1352.

DeBord, K.L., Anderson, D.M., Marketon, M.M., Overheim, K.A., DePaolo, R.W., Ciletti, N.A., Jabri, B., and Schneewind, O. (2006). Immunogenicity and protective immunity against bubonic plague and pneumonic plague by immunization of mice with the recombinant V10 antigen, a variant of LcrV. *Infect Immun* 74**,** 4910-4914. doi: 10.1128/IAI.01860-05.

Durand, E.A., Maldonado-Arocho, F.J., Castillo, C., Walsh, R.L., and Mecsas, J. (2010). The presence of professional phagocytes dictates the number of host cells targeted for Yop translocation during infection. *Cell Microbiol* 12**,** 1064-1082. doi: 10.1111/j.1462-5822.2010.01451.x.

Ekanayake, D., Roddick, C., and Powell, L.W. (2015). Recent advances in hemochromatosis: a 2015 update : A summary of proceedings of the 2014 conference held under the auspices of Hemochromatosis Australia. *Hepatol Int* 9**,** 174-182. doi: 10.1007/s12072-015-9608-2.

Ellermeier, J.R., and Slauch, J.M. (2008). Fur regulates expression of the *Salmonella* pathogenicity island 1 type III secretion system through HilD. *J Bacteriol* 190**,** 476-486. doi: 10.1128/JB.00926-07.

Feder, J.N., Gnirke, A., Thomas, W., Tsuchihashi, Z., Ruddy, D.A., Basava, A., Dormishian, F., Domingo, R., Jr., Ellis, M.C., Fullan, A., Hinton, L.M., Jones, N.L., Kimmel, B.E., Kronmal, G.S., Lauer, P., Lee, V.K., Loeb, D.B., Mapa, F.A., McClelland, E., Meyer, N.C., Mintier, G.A., Moeller, N., Moore, T., Morikang, E., Prass, C.E., Quintana, L., Starnes, S.M., Schatzman, R.C., Brunke, K.J., Drayna, D.T., Risch, N.J., Bacon, B.R., and Wolff, R.K. (1996). A novel MHC class I-like gene is mutated in patients with hereditary haemochromatosis. *Nature Genetics* 13**,** 399-408. doi: 10.1038/ng0896-399.

Galvan, E.M., Nair, M.K., Chen, H., Del Piero, F., and Schifferli, D.M. (2010). Biosafety level 2 model of pneumonic plague and protection studies with F1 and Psa. *Infect Immun* 78**,** 3443-3453. doi: 10.1128/IAI.00382-10.

Giel, J.L., Rodionov, D., Liu, M., Blattner, F.R., and Kiley, P.J. (2006). IscR-dependent gene expression links iron-sulphur cluster assembly to the control of O2-regulated genes in *Escherichia coli*. *Mol Microbiol* 60**,** 1058-1075. doi: 10.1111/j.1365-2958.2006.05160.x.

Gkouvatsos, K., Fillebeen, C., Daba, A., Wagner, J., Sebastiani, G., and Pantopoulos, K. (2014). Iron-Dependent Regulation of Hepcidin in Hjv-/- Mice: Evidence That Hemojuvelin Is Dispensable for Sensing Body Iron Levels. *PLoS One* 9. doi: ARTN e85530DOI 10.1371/journal.pone.0085530.

Gode-Potratz, C.J., Chodur, D.M., and McCarter, L.L. (2010). Calcium and iron regulate swarming and type III secretion in *Vibrio parahaemolyticus*. *J Bacteriol* 192**,** 6025-6038. doi: 10.1128/JB.00654-10.

Hanson, E.H., Imperatore, G., and Burke, W. (2001). HFE gene and hereditary hemochromatosis: A HuGE review. *Am J Epidemiol* 154**,** 193-206. doi: DOI 10.1093/aje/154.3.193.

Harris, S., and Paraskevakis, I. (2012). Multiple Liver Abscesses Due to *Yersinia enterocolitica* Uncovering Hemochromatosis. *Journal of Investigative Medicine* 60**,** 364-364.

Heesemann, J., Sing, A., and Trulzsch, K. (2006). *Yersinia*'s stratagem: targeting innate and adaptive immune defense. *Curr Opin Microbiol* 9**,** 55-61. doi: DOI 10.1016/j.mib.2005.10.018.

Hentze, M.W., Muckenthaler, M.U., Galy, B., and Camaschella, C. (2010). Two to tango: regulation of Mammalian iron metabolism. *Cell* 142**,** 24-38. doi: 10.1016/j.cell.2010.06.028.

Hopfner, M., Nitsche, R., Rohr, A., Harms, D., Schubert, S., and Folsch, U.R. (2001). *Yersinia enterocolitica* infection with multiple liver abscesses uncovering a primary hemochromatosis. *Scand J Gastroenterol* 36**,** 220-224.

Huang, F.W., Pinkus, J.L., Pinkus, G.S., Fleming, M.D., and Andrews, N.C. (2005). A mouse model of juvenile hemochromatosis. *Journal of Clinical Investigation* 115**,** 2187-2191. doi: Doi 10.1172/Jci25049.

Jacquenod, P., Poitrine, A., Loiseau, D., and Naveau, S. (1984). *Yersinia enterocolitica* Septicemia and Idiopathic Hemochromatosis - Role of Iron Overload. *Gastroenterol Clin Biol* 8**,** 293-294.

Jurado, R.L. (1997). Iron, infections, and anemia of inflammation. *Clinical Infectious Diseases* 25**,** 888-895. doi: Doi 10.1086/515549.

Koberle, M., Klein-Gunther, A., Schutz, M., Fritz, M., Berchtold, S., Tolosa, E., Autenrieth, I.B., and Bohn, E. (2009). *Yersinia enterocolitica* targets cells of the innate and adaptive immune system by injection of Yops in a mouse infection model. *PLoS Pathog* 5**,** e1000551. doi: 10.1371/journal.ppat.1000551.

Kurushima, J., Kuwae, A., and Abe, A. (2012). Iron starvation regulates the type III secretion system in *Bordetella bronchiseptica*. *Microbiol Immunol* 56**,** 356-362. doi: 10.1111/j.1348-0421.2012.00442.x.

Lanzara, C., Roetto, A., Daraio, F., Rivard, S., Ficarella, R., Simard, H., Cox, T.M., Cazzola, M., Piperno, A., Gimenez-Roqueplo, A.P., Grammatico, P., Volinia, S., Gasparini, P., and Camaschella, C. (2004). Spectrum of hemojuvelin gene mutations in 1q-linked juvenile hemochromatosis. *Blood* 103**,** 4317-4321. doi: 10.1182/blood-2004-01-0192.

Layoun, A., Samba, M., and Santos, M.M. (2015). Isolation of murine peritoneal macrophages to carry out gene expression analysis upon Toll-like receptors stimulation. *J Vis Exp***,** e52749. doi: 10.3791/52749.

Levy, J.E., Montross, L.K., Cohen, D.E., Fleming, M.D., and Andrews, N.C. (1999). The C282Y mutation causing hereditary hemochromatosis does not produce a null allele. *Blood* 94**,** 9-11.

MacKenzie, E.L., Iwasaki, K., and Tsuji, Y. (2008). Intracellular iron transport and storage: from molecular mechanisms to health implications. *Antioxid Redox Signal* 10**,** 997-1030. doi: 10.1089/ars.2007.1893.

Marketon, M.M., DePaolo, R.W., DeBord, K.L., Jabri, B., and Schneewind, O. (2005). Plague bacteria target immune cells during infection. *Science* 309**,** 1739-1741. doi: 10.1126/science.1114580.

Martin, R.B., Savory, J., Brown, S., Bertholf, R.L., and Wills, M.R. (1987). Transferrin binding of Al3+ and Fe3+. *Clin Chem* 33**,** 405-407.

Matsumoto, H., and Young, G.M. (2009). Translocated effectors of *Yersinia*. *Curr Opin Microbiol* 12**,** 94-100. doi: DOI 10.1016/j.mib.2008.12.005.

McCance, R.A., and Widdowson, E.M. (1938). The absorption and excretion of iron following oral and intravenous administration. *J Physiol* 94**,** 148-154.

Mennecier, D., Lapprand, M., Hernandez, E., Minvielle, F., Bredin, C., Potier, V., Thiolet, C., and Farret, O. (2001a). Liver abscess caused by *Yersinia pseudotuberculosis* revealing genetic hemochromatosis. *Gastroenterol Clin Biol* 25**,** 1113-1115.

Mennecier, D., Lapprand, M., Hernandez, E., Minvielle, F., Bredin, C., Potier, V., Thiolet, C., and Farret, O. (2001b). [Liver abscesses due to *Yersinia pseudotuberculosis* discloses a genetic hemochromatosis]. *Gastroenterol Clin Biol* 25**,** 1113-1115.

Miller, H.K., Kwuan, L., Schwiesow, L., Bernick, D.L., Mettert, E., Ramirez, H.A., Ragle, J.M., Chan, P.P., Kiley, P.J., Lowe, T.M., and Auerbuch, V. (2014).

IscR Is Essential for *Yersinia pseudotuberculosis* Type III Secretion and Virulence. *PLoS Pathog* 10. doi: ARTN e1004194.

Miret, S., Simpson, R.J., and McKie, A.T. (2003). Physiology and molecular biology of dietary iron absorption. *Annu Rev Nutr* 23**,** 283-301. doi: 10.1146/annurev.nutr.23.011702.073139.

Moura, E., Verheul, A.F., and Marx, J.J. (1998). A functional defect in hereditary haemochromatosis monocytes and monocyte-derived macrophages. *European Journal of Clinical Investigation* 28**,** 164-173.

Murphy, E.R., and Payne, S.M. (2007). RyhB, an iron-responsive small RNA molecule, regulates *Shigella dysenteriae* virulence. *Infect Immun* 75**,** 3470-3477. doi: 10.1128/IAI.00112-07.

Pha, K., and Navarro, L. (2016). *Yersinia* type III effectors perturb host innate immune responses. *World J Biol Chem* 7**,** 1-13. doi: 10.4331/wjbc.v7.i1.1.

Pietrangelo, A. (2010). Hereditary hemochromatosis: pathogenesis, diagnosis, and treatment. *Gastroenterology* 139**,** 393-408, 408 e391-392. doi: 10.1053/j.gastro.2010.06.013.

Piroth, L., Meyer, P., Bielefeld, P., and Besancenot, J.F. (1997). [*Yersinia* bacteremia and iron overload]. *Revue De Medecine Interne* 18**,** 932-938.

Posey, J.E., and Gherardini, F.C. (2000). Lack of a role for iron in the Lyme disease pathogen. *Science* 288**,** 1651-1653. doi: DOI 10.1126/science.288.5471.1651.

Quenee, L.E., Berube, B.J., Segal, J., Elli, D., Ciletti, N.A., Anderson, D., and Schneewind, O. (2010). Amino acid residues 196-225 of LcrV represent a

plague protective epitope. *Vaccine* 28**,** 1870-1876. doi: 10.1016/j.vaccine.2009.11.076.

Quenee, L.E., Hermanas, T.M., Ciletti, N., Louvel, H., Miller, N.C., Elli, D., Blaylock, B., Mitchell, A., Schroeder, J., Krausz, T., Kanabrocki, J., and Schneewind, O. (2012). Hereditary hemochromatosis restores the virulence of plague vaccine strains. *J Infect Dis* 206**,** 1050-1058. doi: 10.1093/infdis/jis433.

Rishi, G., Wallace, D.F., and Subramaniam, V.N. (2015). Hepcidin: Regulation of the master iron regulator. *Biosci Rep*. doi: 10.1042/BSR20150014.

Robins-Browne, R.M., and Prpic, J.K. (1985). Effects of iron and desferrioxamine on infections with *Yersinia enterocolitica*. *Infect Immun* 47**,** 774-779.

Sinkovics, J.G., Cormia, F., and Plager, C. (1980). Hemochromatosis and *Listeria* Infection. *Arch Intern Med* 140**,** 284-284.

Skaar, E.P. (2010). The battle for iron between bacterial pathogens and their vertebrate hosts. *PLoS Pathog* 6**,** e1000949. doi: 10.1371/journal.ppat.1000949.

van Asbeck, B.S., Marx, J.J., Struyvenberg, A., and Verhoef, J. (1984). Functional defects in phagocytic cells from patients with iron overload. *J Infect* 8**,** 232-240.

Walker, E.M., Jr., and Walker, S.M. (2000). Effects of iron overload on the immune system. *Ann Clin Lab Sci* 30**,** 354-365.

Wang, L., Harrington, L., Trebicka, E., Shi, H.N., Kagan, J.C., Hong, C.C., Lin, H.Y., Babitt, J.L., and Cherayil, B.J. (2009). Selective modulation of TLR4-activated inflammatory responses by altered iron homeostasis in mice. *J Clin Invest* 119**,** 3322-3328. doi: 10.1172/JCI39939.

Wang, L.J., Johnson, E.E., Shi, H.N., Walker, W.A., Wessling-Resnick, M., and Cherayil, B.J. (2008). Attenuated inflammatory responses in hemochromatosis reveal a role for iron in the regulation of macrophage cytokine translation. *Journal of Immunology* 181**,** 2723-2731.

Weinberg, E.D. (1978). Iron and Infection. *Microbiol Rev* 42**,** 45-66.

Weiss, G., Werner-Felmayer, G., Werner, E.R., Grunewald, K., Wachter, H., and Hentze, M.W. (1994). Iron regulates nitric oxide synthase activity by controlling nuclear transcription. *J Exp Med* 180**,** 969-976.

Wu, Y., and Outten, F.W. (2009). IscR controls iron-dependent biofilm formation in *Escherichia coli* by regulating type I fimbria expression. *J Bacteriol* 191**,** 1248-1257. doi: 10.1128/JB.01086-08.

Yeo, W.S., Lee, J.H., Lee, K.C., and Roe, J.H. (2006). IscR acts as an activator in response to oxidative stress for the suf operon encoding Fe-S assembly proteins. *Mol Microbiol* 61**,** 206-218. doi: 10.1111/j.1365-2958.2006.05220.x.

Zhou, X.Y., Tomatsu, S., Fleming, R.E., Parkkila, S., Waheed, A., Jiang, J., Fei, Y., Brunt, E.M., Ruddy, D.A., Prass, C.E., Schatzman, R.C., O'Neill, R., Britton, R.S., Bacon, B.R., and Sly, W.S. (1998). HFE gene knockout produces mouse

model of hereditary hemochromatosis. *Proc Natl Acad Sci U S A* 95, 2492-2497.

Chapter 3

A Role for IscR in *Yersinia pseudotuberculosis* Heme Uptake and Survival in Blood

By Leah Schwiesow, Halie K Miller, Natalia Herrera, Erin Mettert, Patricia J Kiley and Victoria Auerbuch

INTRODUCTION

Iron is an essential element for almost all microorganisms except for some unique examples such as *Borrelia burgdorferi* (1). Most bacteria require anywhere from 10^{-6} to 10^{-7} M free iron to support growth (2). However, pathogenic bacteria often encounter iron-limiting conditions, particularly during growth within mammalian hosts due to the success of host iron sequestration systems (3). These systems include binding of iron to the storage protein, ferritin, complexing iron with heme, and the tight association of serum iron to transferrin (3). Free iron in humans is further sequestered during infection via inflammation-associated hypoferremia in an attempt to restrict bacterial growth (3). To compensate, pathogens employ a number of iron acquisition mechanisms to obtain host iron including siderophores, transferrin/lactoferrin receptors, iron transporters, and heme acquisition systems (3).

The importance of iron acquisition during infection is underscored by evidence suggesting that a correlation exists between high-pathogenicity *Yersinia* and their ability to successfully acquire iron *in vivo* (4, 5). Indeed, there are at least seven different functional iron acquisition systems (Ybt, Yfe, Yfu, Yiu, Feo, Fet, and Hmu) utilized by human pathogenic *Yersinia* (6). These pathogens include *Yersinia pestis*, the causative agent of bubonic plague, and the foodborne enteropathogens, *Yersinia pseudotuberculosis* and *Yersinia enterocolitica*. The most well characterized *Yersinia* iron acquisition system is the siderophore yersiniabactin, which is required for full virulence in a mouse model of bubonic plague (7). The Yfu and Yiu systems are ABC transporters that play a role in ferric iron uptake under aerobic conditions, while

the Feo and Fet systems can uptake ferrous iron under microaerophilic conditions (6). The Yfe system has been shown to play a role in both ferric and ferrous iron transport under aerobic and microaerophillic conditions, respectively (6).

Hemin and hemoproteins provide the largest source of iron for bacterial pathogens within the host (8). The HmuRSTUV (HemRSTUV in *Yersinia enterocolitica*) hemin uptake system has been characterized in *Yersinia pestis* and *Yersinia enterocolitica* (9-12). HmuR is a TonB-dependent outer membrane transporter that is required for the utilization of hemin, hemoglobin, hemoglobin-haptoglobin, myoglobin, hemopexin, and heme albumin in *Y. pestis* (10). HmuTUV make up an inner membrane ABC transporter required for the uptake of heme and all hemoproteins except hemopexin and haptoglobin-hemoglobin into the cytoplasm (10). The cytoplasmic protein HmuS was thought to play a role in the detoxification and degradation of heme as deletion of the HmuS homolog in *Yersinia enterocolitica*, HemS, is lethal (12). Very recently, studies in *Yersinia pseudotuberculosis* have demonstrated that HmuS releases iron via degradation of heme to biliverdin in the presence of molecular oxygen, an electron donor such as NADPH, and ferrodoxin-$NADP^+$ reductase (13).

Sensing of low iron environments to regulate virulence programs within the host is a hallmark of bacterial pathogenesis (14). Accordingly, heme uptake pathways in several bacterial pathogens, including *Staphylococcus aureus*, *Neisseria meningitides,* and *Yersinia pestis,* are regulated by the ferric uptake regulator (Fur) (8, 10). Under iron replete conditions, Fur is bound by ferrous iron (Fe^{2+}), thereby

allowing it to bind target operator sequences (Fur boxes) to repress transcription (15). Conversely, as iron becomes limiting, Fur is no longer bound by iron leading to derepression of iron uptake systems (15). *Yersinia pestis hmuR* contains a Fur box in its promoter region and its transcription is responsive to iron (10). Jacobi et al demonstrated that *hemR* of *Yersinia enterocolitica* was upregulated in the peritoneal cavity, Peyer's patches, and spleen during infection of mice, suggesting a role for low-iron responsive heme uptake in these tissues (16). Recently, our group demonstrated that the iron-sulfur coordinating transcription factor, IscR, is a global regulator of transcription in *Yersinia pseudotuberculosis* and demonstrated that the genes *hmuSTUV* were downregulated in a Δ*iscR* mutant (17). In *E. coli*, IscR has been shown to respond to oxidative stress and oxygen limitation as well as iron limitation, suggesting that oxygen, as well as iron, may be important in the regulation of heme uptake in *Yersinia* species (18-20). In this study, we demonstrate that Apo-IscR binds to an intergenic region between *hmuR* and *hmuSTUV* and show that IscR is important for survival in sheep's whole blood, perhaps due to a heme-dependent mechanism. This work provides evidence that a transcriptional regulator other than Fur plays a role in bacterial heme uptake and increases our understanding of the role of IscR in *Yersinia pseudotuberculosis* survival in host environments.

MATERIALS AND METHODS

Bacterial Strains, Plasmids, and Growth Conditions. All strains used in this study are listed in Table 1. *Y. pseudotuberculosis* strains were grown in either 2xYT or M9

minimal media supplemented with casamino acids referred to here as M9, at 26°C with shaking at 250 rpm, unless otherwise indicated (21).

Table 1. *Y. pseudotuberculosis* strains used in this study

Strain	Background	Mutation(s)	Reference
WT	IP2666	Naturally lacks full length YopT	(22)
Δ*iscR*	IP2666	Δ*iscR*	(17)
Δ*yscNU*	IP2666	Δ*yscNU*	(24)
Δ*hmuRSTUV*/pYV-	IP2666	Δ*hmuRSTUV* plasmid cured	This study
Δ*hmuSTUV*/pYV-	IP2666	Δ*hmuSTUV* plasmid cured	This study
pYV-	IP2666	Δ*yscBL* pYV cured	(25)
Δ*phoP*	IP2666	Δ*phoP*	(26)
WT/pFU99::p1	IP2666	WT+pFU99 containing promoter upstream of *hmuR*	This study
Δ*iscR*/pFU99::p1	IP2666	Δ*iscR*+pFU99 containing promoter upstream of *hmuR*	This study
Apo-IscR/pFU99::p1	IP2666	IscR-C92A/C98A/C104 + pFU99 containing promoter upstream of *hmuR*	This study
WT/pFU99::p2	IP2666	WT+pFU99 containing intergenic region between *hmuR* and *hmuSTUV*	This study
Δ*iscR*/pFU99::p2	IP2666	Δ*iscR*+ pFU99 containing intergenic region between *hmuR* and *hmuSTUV*	This study
Apo-IscR/pFU99::p2	IP2666	IscR-C92A/C98A/C104 + pFU99 containing	This study

		intergenic region between *hmuR* and *hmuSTUV*	
Δ*iscR*/pYV-	IP2666	Δ*iscR* plasmid cured	(17)

Construction of *Y. pseudotuberculosis* Mutant Strains. The Δ*hmuRSTUV* and Δ*hmuSTUV* mutants were generated via splicing by overlap extension (27). Primer pairs F5/R5Δ*hmuRSTUV* and F5/R5Δ*hmuSTUV* (Table 2) were used to amplify ~1000 bp 5' of *hmuRSTUV* and *hmuSTUV*, respectively. Primer pair F3/R3Δ*hmuRSTUV* were used to amplify ~1000 bp 3' of Δ*hmuRSTUV* (Table 2). Amplified PCR fragments served as templates in an overlap extension PCR using the outside primers F5/R3Δ*hmuRSTUV* and F5Δ*hmuSTUV*/R3Δ*hmuRSTUV* for Δ*hmuRSTUV* and Δ*hmuSTUV*, respectively The resulting ~2 kb fragments were cloned into the TOPO TA cloning vector (Invitrogen) and further subcloned into a BamHI- and NotI-digested pSR47s suicide plasmid (λpir-dependent replicon, kanamycin^R (Kan^R), *sacB* gene conferring sucrose sensitivity) (28, 29). Recombinant plasmids were transformed into *E. coli* S17-1 λpir competent cells and later introduced into *Y. pseudotuberculosis* IP2666 via conjugation. The resulting Kan^R, irgansan^R (*Yersinia* selective antibiotic) integrants were grown in the absence of antibiotics and plated on sucrose-containing media to select for clones that had lost *sacB* (and by inference, the linked plasmid DNA). Kan^S, sucrose^R, congo red-positive colonies were screened by PCR and sequencing.

The plasmids pFU99::p1 and pFU99::p2 were generated using NEB Hifi Assembly Master Mix. Briefly, primers FhmuR and RhmuR were used to amplify ~100 bp fragment containing the promoter upstream of *hmuR* and primers FhmuS and RhmuS were used to amplify the 123 bp intergenic region between *hmuR* and *hmuSTUV*. Plasmid pFU99a (30) was digested with BamHI/SalI and PCR fragments were introduced into the plasmid using Hifi Assembly Master Mix (NEB) according to the manufacturer's protocol to make plasmids pFU99::p1 and pFU99::p2. These plasmids were then eletroporated into WT, Δ*iscR*, or Apo-locked IscR strains as previously described (17). Clones were selected by plating on chloramphenicol and their sequences were confirmed by PCR analysis.

Table 2. *Y. pseudotuberculosis* primers used in this study

Name	Primer Sequence (5'-3')	Reference
F5Δ*hmuSTUV*	ATGATGGGATCCCCGATGTCGATGCCGATAAA	This Study
R5Δ*hmuSTUV*	GATAAATCTGTGGCAGGATGCGTTCATAATGGCTTCCTAA	This Study
F5Δ*hmuRSTUV*	ATGATGGGATCCCAATGCGAACTATCAGGGTAATC	This Study
R5Δ*hmuRSTUV*	GATAAATCTGTGGCAGCATGTCGGCAATTCTCCATATT	This Study
F3Δ*hmuRSTUV*	CTGCCACAGATTTATCTGCGGCAATA	This Study
R3Δ*hmuRSTUV*	ATGATGGCGGCCGCGTTGATGCCAGATAGTGTGTATA	This Study
FhmuS	CCTTTCGTCTTCACCTCGAGCTAATGAAAAAAAGTTAGTCT GAAAT	This Study
RhmuS	TTCATTTTTAATTCCTCCTGAATGGCTTCCTAATTAATTG	This Study
FhmuR	CCTTTCGTCTTCACCTCGAGATAAAGGCCAGGAAGCATTC	This Study
RhmuR	TTCATTTTTAATTCCTCCTGCTGCTTCTGAAATCCCCATC	This Study

Whole Sheep's Blood Assay. Strains were grown overnight in 2xYT at 26°C and subsequently standardized to an OD_{600} of 0.2. Standardized cultures were centrifuged at 3,500 rpm for 3 min and the supernatants discarded. Bacterial pellets were resuspended in 2 mL of whole sheep's blood in sodium heparin (Hemostat, Inc.) and CFU determined via serial dilution and plating at hour 0. Samples were then placed in a rollerdrum at 37°C and CFU were determined at hours 2, 4, 6 and 8. Data is representative of three independent experiments.

EMSA. Electrophoretic mobility shift assays were performed as in (31)

DNAse I Footprinting. DNAse footprinting was performed as in (18).

***In Vitro* Transcription Assay.** Plasmid DNA containing the intergenic promoter region between *hmuR* and *hmuSTUV* was purified with the QIAfilter Maxi kit (Qiagen). The effect of IscR on σ^{70}-dependent promoter activity from the candidate control regions was determined as previously described (32); 2 nM supercoiled plasmid DNA was incubated with IscR, [α-^{32}P]-UTP and NTPs for 30 min at 37°C. Eσ^{70} RNA polymerase (50 nM) (Epicentre) was added and the reaction was terminated after 5 min. Assays were performed under aerobic conditions with anaerobically purified IscR that was diluted immediately before the start of the incubation of IscR with DNA.

RNAseq Analysis. Strains were grown overnight in 2XYT. Bacterial culture corresponding to OD 0.2 was pelleted and resuspended in 2 mL Sheep's Whole Blood (Hemostat). After a 45 minute incubation at 37°C on a rollerdrum, cultures were treated with 5X EL buffer (Qiagen) to lyse erthyocytes. After a 10-minute incubation

on ice, cultures were pelleted by centrifugation for 5 minutes at 4,000 rpm. The supernatant was removed and pellets were resuspended in 500 mL PBS and treated with 1 mL Bacterial RNA Protect Reagent (Qiagen) according to the manufacturer's protocol. Total RNA was isolated using the RNAeasy Mini Kit (Qiagen) per the manufacturer's protocol. Contaminating DNA was removed using the TURBO DNA-free Kit (Life Technologies/Thermo Fischer). rRNA was removed using the RiboZero Magnetic Kit for Gram Negative Bacteria (Illumina). The cDNA library was prepared using the NEB Ultra Directional RNA Library Prep Kit for Illumina. Quality of total RNA, mRNA after rRNA depletion and cDNA libraries were assessed using a Agilent 2000 Bioanalyzer. These studies were performed with three biological replicates per condition. Six indexed samples were sequenced per single lane using the HiSeq4000 Illumina sequencing platform for 50 bp single reads (UC Davis Genome Center) and subsequently were analyzed and visualized via the CLC Genomics Workbench version 9.5.3 (CLC bio). Reads were mapped to the *Yersinia pseudotuberculosis* genome (IP32953). Differentially regulated genes were identified as those displaying a fold change with an absolute value of 2 or greater. Statistical significance was determined using an EdgeR-like analysis within the RNAseq plugin in CLC workbench with a corrected false discovery rate (FDR)-post hoc test where $p \geq 0.01$ was deemed significant.

β-galactosidase Assays. *Y. pseudotuberculosis* strains containing the β-galactosidase reporter construct pFU99::p1 or pFU99::p2 were grown overnight at 26°C in 2 mL M9 media containing 15 μg/mL chloramphenicol. Cultures were diluted to OD 0.1 in

fresh M9 and allowed to grow at 26°C or 37°C for 3 hrs at which time cultures were pelleted at 4,000 rpm for 10 minutes and resuspended in 100 µL Tropix lysis solution. Lysis was allowed to proceed at room temperature for 10 minutes. Cell debris was pelleted for 5 minutes at 13,200 rpm. Cell lysates were used in the Galacton-Light Plus β-Galactosidase Reporter Gene Assay System per the manufacturer's protocol (Thermo Fischer Scientific). Data is representative of three independent experiments.

Hemin Growth Curves. Hemin growth curves were performed similar to Thompson et al. (10). *Y. pseudotuberculosis* was grown in 5 mL of M9 minimal media overnight. In the morning, cultures were back-diluted to OD 0.1 in 20 mL of chelex treated M9 media without iron and allowed to grow for 8 hrs. The cultures were then back-diluted to OD_{600} 0.1 into 20 mL fresh M9 media without iron and chelex treated overnight. Cultures were back-diluted iOD_{600} 0.1 into 20 mL chelex treated M9 media with no iron, in which 10µM hemin had been added or 1 mg/L $FeSO_4$ had been added. Before addition, 10 mM stock hemin solution was chelex treated overnight. OD_{600} was measured every hour for 9 hours. Data is representative of three independent experiments.

RESULTS

IscR plays a role in regulation of the *hmuRSTUV* genetic locus. Previous work from our group suggested that IscR may play a role in the regulation of the *hmuRSTUV* hemin uptake system (17). The genetic structure of the *hmuRSTUV* hemin uptake locus has been previously characterized in *Yersinia pestis* (10). This characterization showed that this locus contains two promoter regions- one upstream

of *hmuSTUV*, and one in the intergenic region between *hmuR* and *hmuSTUV* (10). To better understand the control of IscR on this locus, we performed β-galactosidase assays using constructs in which *lacZ* was fused to the promoter upstream of *hmuR* or the intergenic region between *hmuR* and *hmuSTUV* (Figure 1A) in a WT, Δ*iscR* or Apo-locked IscR background. The Apo-locked IscR mutant contains alanine mutations in the three cysteine residues, which are essential to coordinate the iron-sulfur cluster (17). In *E. coli*, mutations in these three residues leave IscR unable to coordinate an iron-sulfur cluster, but still able to bind motif II transcription sites and to regulate gene transcription (18-20, 33). Transcription from the promoter upstream of *hmuR* was significantly upregulated in the Δ*iscR* mutant compared to the WT and Apo-locked IscR strains (Figure 1B). Additionally, transcription from the intergenic region between *hmuR* and *hmuSTUV* was significantly upregulated in an Apo-locked IscR mutant compared to the WT and Δ*iscR* strains (Figure 1C). Collectively, these data demonstrate that IscR plays a role in regulation of both *hmuR* and *hmuSTUV*.

Fur directly binds to the promoter upstream of *hmuR*, but not to the intergenic region between *hmuR* and *hmuS*. Previous work in *Yersinia pestis* suggested that Fur may bind to both the promoter upstream of *hmuR* and to the intergenic region between *hmuR* and *hmuSTUV* (10). However, Fur binding to either promoter region has never been tested biochemically (10). To determine if Fur impacts regulation of the *hmuR* promoter and/or the intergenic promoter between *hmuR* and *hmuSTUV,* we performed gel shift assays using purified *E. coli* Fur protein. When incubated with

increasing amounts of Fur protein, a shift was observed for the promoter region upstream of *hmuR* at 31.25 nm protein, while a shift for the intergenic region between *hmuR* and *hmuSTUV* was not observed until 250 nm protein (Figure 2). These data suggest that Fur directly regulates the *hmuRSTUV* heme uptake locus through direct binding to the promoter upstream of *hmuR*, and not through binding the intergenic region between *hmuR* and *hmuSTUV*. This is consistent with the findings of the previous *Y. pestis* study (10). Furthermore, it suggests that the increased expression of *hmuR* promoter-*lacZ* fusion that is seen in a Δ*iscR* mutant may be due to derepression of Fur in this background.

Apo-IscR directly binds to the intergenic region between *hmuR* and *hmuS*. Given that expression of the intergenic promoter-*lacZ* fusion was increased in an Apo-IscR background, we next asked if Apo-IscR could directly bind to the intergenic region between *hmuR* and *hmuSTUV* (Figures 1 and 2). *E. coli* IscR has been shown to complement *Y. pseudotuberculosis* IscR (17). Using purified *E. coli* IscR-C92A protein, which has one Fe-S cluster coordinating cysteine mutated and is also in an apo-locked conformation, we performed gel shift assays using the intergenic region between *hmuR* and *hmuSTUV* and a control region within the 3' end of the *hmuR* coding region. When incubated with increasing concentrations of IscR-C92A protein, a shift was observed for the intergenic region DNA at 62.5 nM protein, while a

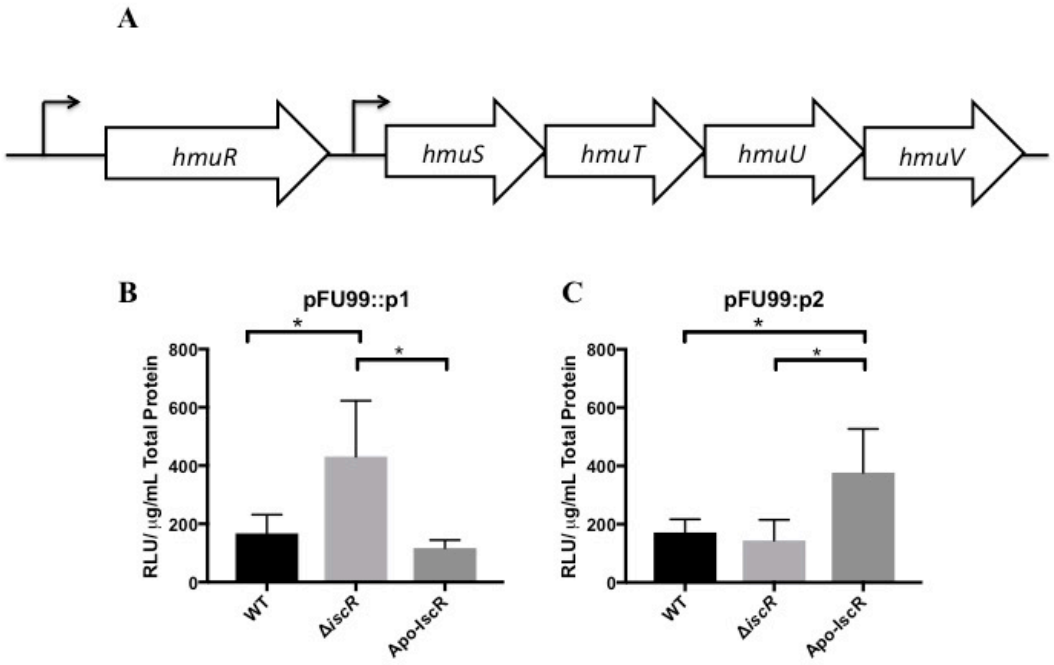

Figure 1. Activity of promoters associated with the *hmuRSTUV* heme uptake locus are altered in a Δ*iscR* and Apo-IscR mutant. **(A)** The genetic structure of the *hmuRSTUV* heme uptake locus in *Yersinia*. Thin black arrows represent promoters. Activity of **(B)** *hmuR* (p1)–*lacZ* fusion and **(C)** intergenic (p2)-lacZ fusion on the plasmid pFU99 as measured via β-galactosidase assays in WT, Δ*iscR*, and Apo-IscR strains grown under aerobic conditions in M9 media at 37°. Relative light units (RLU) were normalized to total protein concentration in the cell lysate as determined by a Bradford assay. Data is from three independent experiments. *p≤0.05, One-way ANOVA.

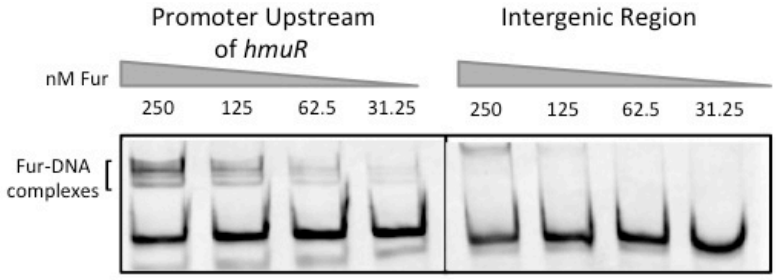

Figure 2. *E. coli* Fur binds to the *Y. pseudotuberculosis* promoter upstream of *hmuR*. Electrophoretic mobility shift assays using radiolabeled DNA from the promoter upstream of *hmuR* or the intergenic region between *hmuR* and *hmuSTUV* (Intergenic Region). Concentrations of Fur protein used in the gel shift assays are denoted above the gel lanes.

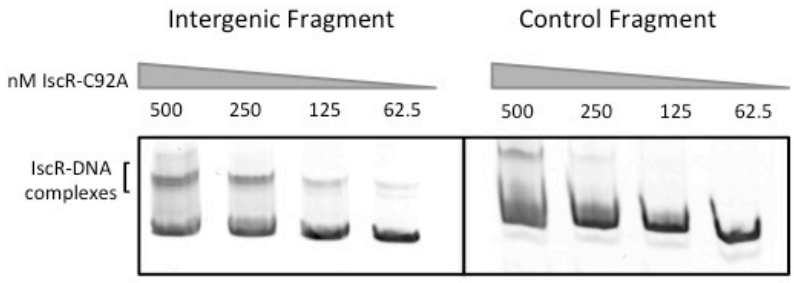

Figure 3. *E. coli* IscR-C92A binds to the intergenic region between *Y. pseudotuberculosis hmuR* and *hmuSTUV*. Electrophoretic mobility shift assays using radiolabeled DNA from the intergenic region between *hmuR* and *hmuSTUV* (Intergenic Fragment) or control DNA within the *hmuR* coding region (Control Fragment). Concentrations of Apo-locked IscR-C92A protein used in the gel shift assays are denoted above the gel lanes.

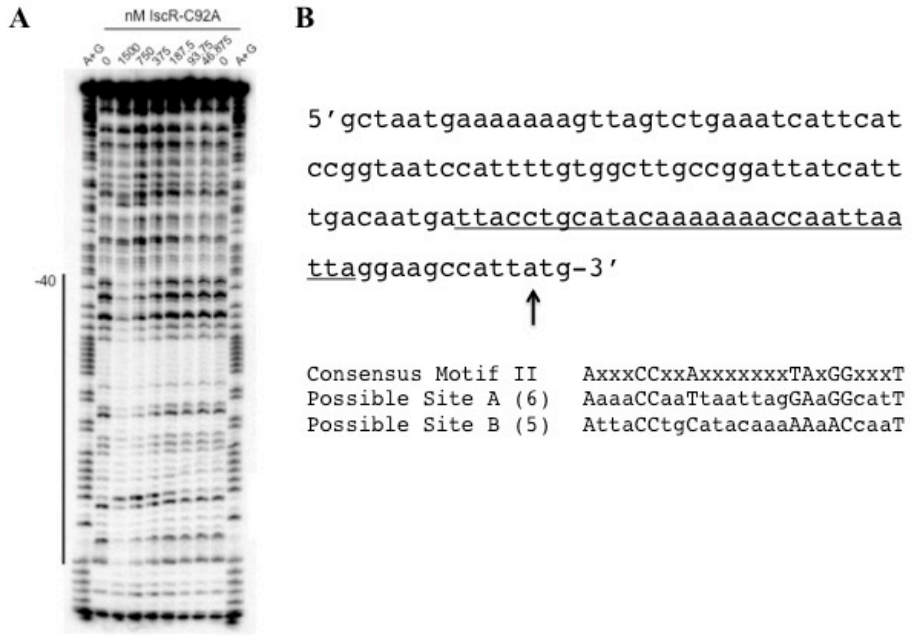

Figure 4. *E. coli* IscR-C92A DNAse I footprinting reveals possible IscR Motif II binding sites in the intergenic region between *hmuR* and *hmuSTUV*. (A) DNase I footprinting of IscR-C92A binding to the intergenic region between *hmuR* and *hmuSTUV*. The labeled DNA is the top strand from −123 to +0 relative to the *hmuS* translational start site. The region protected by IscR-C92A is marked by a black line. **(B)** Sequence of the intergenic region between *hmuR* and *hmuSTUV*. The region of protection by IscR-C92A is underlined. Possible Motif II Sites are marked below the sequence and the number of nucleotides contained in each sequence shown to be important for IscR binding are denoted.

shift for the control DNA fragment was not observed until 250 nM protein was used (Figure 3). To better characterize IscR binding to the intergenic region between *hmuR* and *hmuSTUV*, we performed DNAse footprinting assays with *E. coli* IscR-C92A to determine the binding site (Figure 4A). A region of protection was observed from -40 to 0 nucleotides upstream of the translational start site of *hmuS* (Figure 4A). From this area of protection, we identified two potential IscR Motif II binding sites, termed site 1 and site 2 (Figure 4B). Comparison of these binding sites with the consensus Motif II binding site shows that they contain six and five of the nine bases in the consensus motif binding motif, respectively (Figure 4B) (18). These data suggest that IscR directly binds to the intergenic region between *hmuR* and *hmuSTUV* through a Motif II site.

IscR is important for *Y. pseudotuberculosis* growth in the presence of hemin as the sole iron source, but is dispendable for growth on non-heme iron. Both *hmuR* and *hmuSTUV* have been shown to be necessary for the utilization of hemin under iron-deplete conditions in *Y. pestis* (9, 10). We have observed robust transcription from the intergenic promoter between *hmuR* and *hmuSTUV* in an Apo-locked IscR mutant, and we have shown that *E. coli* IscR-C92A binds to this region. Given these data, we hypothesized that IscR would be important in utilization of hemin in iron deplete conditions through control of *hmuSTUV*. We assessed the ability of a pYV-, Δ*iscR*/pYV-, Δ*hmuRSTUV*/pYV-, and Δ*hmuSTUV*/pYV- mutant strains to utilize hemin as an iron source under iron-replete conditions. We chose to use the pYV-

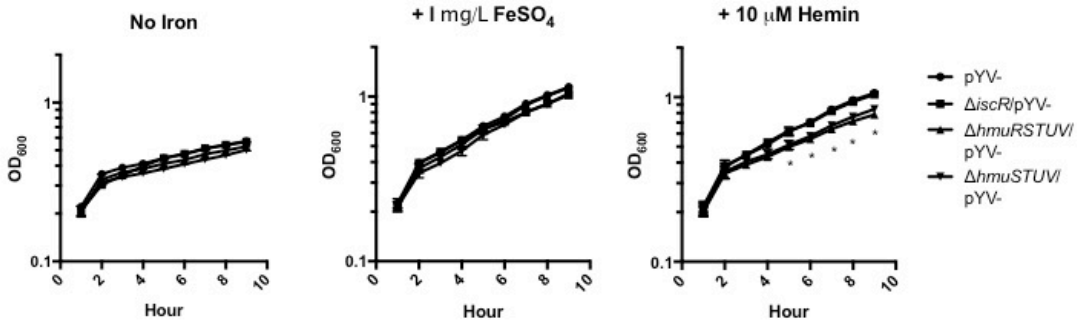

Figure 5. A Δ*iscR*/pYV- mutant is not defective in growing in media in which hemin is the sole iron source. Iron starved cells, as described in Materials and Methods, were transferred to Chelex treated M9-Fe media alone or supplemented with 1 mg/L $FeSO_4$ or 10 μM Hemin. Cultures were grown at 37°C for 9 hours and optical density at 600 nm was taken every hour. Data are representative of three independent experiments. *p≤0.05 for Δ*hmuSTUV*/pYV- and Δ*hmuRSTUV*/pYV-, One-way ANOVA.

background because WT *Y. pseudotuberculosis* undergoes growth restriction at 37°C, while a strain lacking pYV does not. While all strains could utilize $FeSO_4$ as an iron source (Figure 5), Δ*hmuRSTUV*/pYV- and Δ*hmuSTUV*/pYV-, but not Δ*iscR*/pYV-, were defective in utilizing hemin as an iron source compared to the pYV- parental strain. These data suggest that IscR is not important for growth when hemin is the sole iron source. Alternatively, deletion of *iscR* may cause pleiotrophic effects on growth under these conditions, masking any defects resulting from IscR regulation of *hmuSTUV*.

IscR is not sufficient to activate transcription from the intergenic promoter between *hmuR* and *hmuSTUV*. Since IscR was not essential for growth on hemin following iron-depletion, we asked Apo-IscR binding to the intergenic region between *hmuR* and *hmuSTUV* directly affected transcription. We performed *in vitro* transcription assays to determine if IscR was affecting transcription from the intergenic promoter (Figure 6). We observed no change in transcriptional activation from the intergenic promoter between *hmuR* and *hmuSTUV* in the presence or absence of locked IscR-C92A (Figure 6). Given these data and the fact that IscR directly binds to this intergenic promoter, we hypothesize that IscR blocks binding of another transcriptional regulator to the *hmu* intergenic promoter in order to affect transcription of *hmuSTUV*.

IscR is required for survival in whole sheep's blood. To begin to address the importance of IscR in a heme-rich environment, we measured the ability of *Y. pseudotuberculosis* to survive in whole sheep's blood to mimic septic infection. Analysis of survival in blood by colony forming units (CFU) showed that a Δ*iscR* mutant was decreased by 1-2-logs compared to the WT strain at 4 and 8 hours (Figure 7A). This suggests that IscR plays a role in the survival of *Y. pseudotuberculosis* in blood.

We previously characterized IscR as important for expression of the type III secretion system (T3SS) though the master regulator LcrF in *Y. pseudotuberculosis* (17). The *Yersinia* T3SS is important for the evasion of phagocytic cells, which may be present in our *ex vivo* blood model (34). Additionally, the pYV-encoded protein YadA, which is controlled by LcrF, has been shown to be important in the evasion of complement in *Yersinia enterocolitica* through exploitation of C3 and iC3b to sequester large amounts of Factor H (35, 36). We assessed the requirement for IscR-mediated T3SS control in the survival of Y. pseudotuberculosis in blood (Figure 7B). We observed that a pYV- strain of *Y. pseudotuberculosis* that does not contain the T3SS-encoding virulence plasmid, nor a Δ*yscNU* mutant that lacks expression of the T3SS basal body machinery, do not display survival defects in whole blood compared to WT (Figure 6B). These data suggest that the IscR-mediated T3SS regulation is not important for survival of *Y. pseudotuberculosis* in blood. The response regulator PhoP is required for *Y. pseudotuberculosis* to replicate in macrophages (37). We found that a Δ*phoP* mutant survives in blood (Figure 7B).

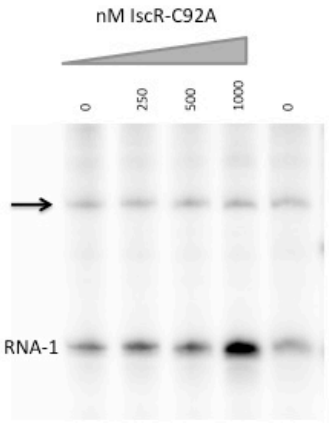

Figure 6. *E. coli* IscR-C92A cannot activate transcription from the intergenic promoter between *hmuR* and *hmuSTUV*. *In vitro* transcription reactions contain plasmids harboring the intergenic promoter between *hmuR* and *hmuSTUV,* $E\sigma^{70}$ RNA polymerase, and increasing concentrations of IscR-C92A protein. Transcripts from the intergenic promoter are marked with an arrow and transcripts from the control RNA-1 promoter are indicated.

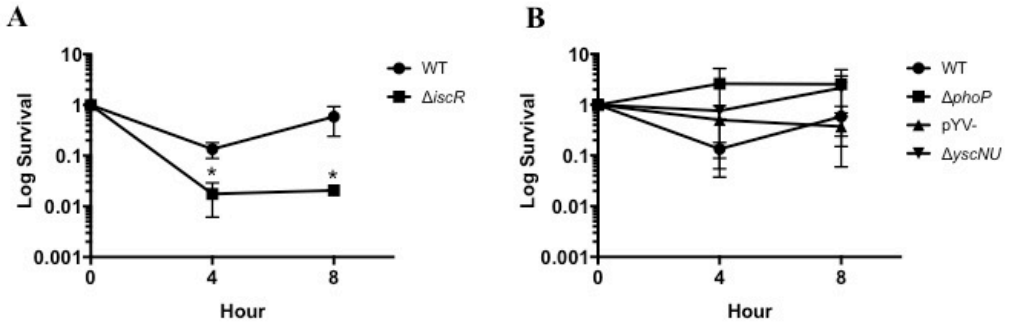

Figure 7. A Δ*iscR* mutant has a survival defect in sheep's whole blood. **(A)** WT and Δ*iscR* log survival in sheep's whole blood after 4 and 8 hours of incubation. **(B)** WT, Δ*phoP*, pYV-, and Δ*yscNU* log survival in sheep's whole blood after 4 and 8 hours of incubation. Log survival is calculated as the CFU/mL bacteria at 4 or 8 hours divided by the CFU/mL bacteria at hour 0 as enumerated by plating for CFU. Data are from three biological replicates.*$p \leq 0.05$, upaired student t test compared to WT.

This result suggests that the inability of the Δ*iscR* mutant to survive in blood is not due to an inability to replicate in macrophages.

Transcriptional response of WT and *ΔiscR Y. pseudotuberculosis* grown in whole blood. To investigate the cause of the survival defect observed for the Δ*iscR* mutant in blood, we performed high throughput transcriptome sequencing (RNAseq) to compare the transcriptomes of a Δ*iscR* mutant and a WT strain grown in sheep's whole blood. In addition, we compared our whole blood transcriptome data to our previous transcriptome data comparing a Δ*iscR* mutant and a WT strain grown in M9 minimal media (17). Comparing the two data sets showed that 19 genes that were differentially regulated (FDR-corrected p value ≤ 0.1 and a fold change ≥ 2) between the Δ*iscR* mutant and WT strain in blood were also differentially regulated in M9 (Figure 7). Genes upregulated in both data sets included those required for Fe-S cluster biogenesis, including genes in the *iscRSUA* operon, and genes downregulated in both data sets, including T3SS genes (Table 3). These processes are directly regulated by IscR in *Y. pseudotuberculosis* (17).

A total of 100 genes were differentially expressed between the Δ*iscR* mutant and the WT strain grown in whole blood compared to the M9 minimal media dataset. Of these genes, 46 were upregulated in the Δ*iscR* mutant (Table 4), while 54 genes were downregulated in the Δ*iscR* mutant (Table 5). Several genes upregulated in the Δ*iscR* mutant in blood are iron uptake genes, including *hmuR*, the putative ferric siderophore receptor YPTB0792, and *bdf*. In *Yersinia pestis*, all of these genes have

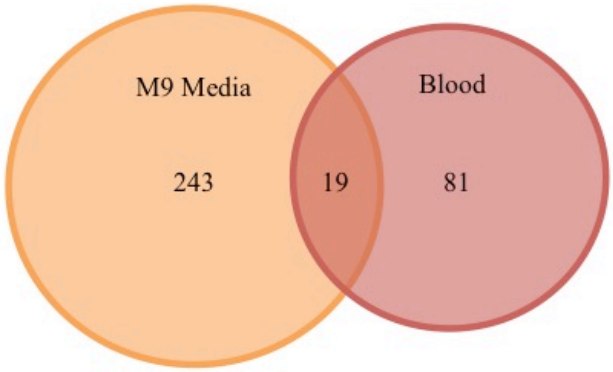

Figure 7. Differentially regulated genes between Δ*iscR* and WT in M9 media and sheep's whole blood. A Venn diagram showing the number different and overlapping genes differentially expressed between a Δ*iscR* mutant and WT in M9 media and sheep's whole blood. RNAseq data was analyzed using an EdgeR-like analysis in CLC Workbench. The cutoff for significantly regulated genes was an FDR-corrected p value ≤ 0.1 and a fold change ≥ 2.

been shown to be part of the Fur (ferric uptake regulator) regulon, suggesting derepression of Fur in the Δ*iscR* mutant grown in whole sheep's blood (38). Many genes upregulated in the Δ*iscR* mutant are involved in the cellular stress response, including *terY*, putative oxidoredutases, *emrR* and *katA*, indicating that the Δ*iscR* mutant is under more stress than a WT strain in whole blood. Genes downregulated in the Δ*iscR* mutant compared to the WT strain included the methionine synthesis gene *metE* and genes of the *nuo* operon, which encode NADH dehydrogenase, among others.

Table 3. Differentially regulated genes found in both M9 media and sheep's whole blood

***Y.pstb* Locus Tag**	**Fold Change Blood**	**Fold Change M9**	**Gene**
YPTB2858	6.598490741	30.27362768	*nifU/IscU*
YPTB2856	6.30987557	10.01574064	*hscB*
YPTB2857	6.275819347	17.39430553	*iscA*
YPTB2859	5.892213877	25.76213208	*iscS*
YPTB2853	5.354509121	13.19859578	*iscX*
YPTB2854	5.303063191	12.67459525	*fdx*
YPTB2299	4.138308115	7.556794132	*sodB*
YPTB2855	4.107728817	9.424493875	*hscA*
YPTB2852	3.958923665	11.35048893	*pepB*
YPTB2851	3.497297958	7.684218552	*sseB*
---	3.490368442	2.896440235	*hypothetical protein*
YPTB2103	2.025554555	2.145367933	*adhE*
pYV0078	-2.227268727	-2.782431754	T3SS Protein
pYV0025	-2.479310178	-2.980244468	*yopE*
pYV0076	-2.486080736	-2.479010983	*lcrF*
pYV0083	-2.509145826	-2.505959816	*yscG*
YPTB3577	-2.52822991	2.317068097	*fis*
pYV0082	-2.585411115	-2.353281842	*yscF*
YPTB2860	-126.2279104	-42.4870724	*iscR*

Table 4. Genes significantly upregulated in the Δ*iscR* mutant unique to sheep's whole blood

Y.pstb Locus Tag	Fold Change Blood	Fold Change M9	Gene
YPTB0396	6.181799862	0.534477198	*putative oxidoreductase*
YPTB3462	6.079496084	0.56793568	*terY*
YPTB3463	5.147457815	0.662890869	*terX*
YPTB3464	4.654908895	-0.010316466	*terY like protein*
YPTB1723	3.986564164	0.060600155	*putA*
YPTB0397	3.962495656	0.109842112	*hydN*
YPTB1583	3.763670323	-0.3265317	*hypothetical protein*
YPTB3740	3.371616489	-0.658965322	*nirB*
YPTB0790	3.273146319	0.702144477	*yhjA cytochrome c peroxidase*
YPTB1246	3.153591884	0.959087106	*katA*
YPTB2903	3.120771743	0.51283134	*grcA*
YPTB0160	2.851424103	-0.392987694	*fimbrial protein*
YPTB2229	2.798364888	0.432523114	*hypothetical protein*
YPTB0857	2.757995016	0.243138379	*emrR*
YPTB3465	2.741258842	-0.2397224	*hypothetical protein*
YPTB1921	2.683126488	-0.4638635	*fimbrial protein*
YPTB2374	2.609774855	-0.125709168	*fimbrial protein*
YPTB0792	2.562748737	-0.215011912	*Iha*
YPTB0398	2.521605877	0.473955148	*fdhF*
YPTB1988	2.441106888	0.742342425	*hypothetical protein*
YPTB3963	2.435281106	0.369729231	*pstS*
YPTB0343	2.372212989	-0.268355488	*heme utilization carrier protein*
YPTB1940	2.36562801	0.476325453	*putative iron transporter*
YPTB0844	2.355707529	0.159247193	*yfiA*
YPTB0344	2.343143695	-0.415877107	*hutW*
YPTB0340	2.303821612	-0.44689154	*hmuR*
---	2.253105459	-0.708945571	*hypothetical protein*
---	2.215625055	-0.25833166	*hypothetical protein*
YPTB3263	2.176697142	-0.838981773	*rhbC*
YPTB1987	2.171648014	0.668442252	*hypothetical protein*
YPTB1939	2.162502547	-0.230664932	*iron permease*
YPTB1540	2.135004188	-0.179158786	*fhuF*
YPTB3962	2.085690738	-0.216911777	*ptsC*
YPTB3701	2.01271519	0.746245854	*bfd*

Table 5. Genes significantly downregulated in the Δ*iscR* mutant unique to sheep's whole blood

Y.pstb Locus Tag	Fold Change Blood	Fold Change M9	Gene
---	-5.150875891	1.883187412	*hypothetical protein*
YPTB0248	-4.605418406	-1.372063133	*metE*
YPTB2311	-3.934924944	1.108559144	*sufD*
pYV0075	-3.873291608	-1.981587884	*yscW*
YPTB2312	-3.83304456	-1.071652467	*sufC*
YPTB2314	-3.770881341	-1.046984032	*sufA*
YPTB2313	-3.493708313	-1.091814077	*sufB*
pYV0080	-3.174735649	-1.773905017	*yscD*

YPTB2310	-3.121674061	1.063577789	*sufS*
YPTB3576	-3.095438154	1.594733664	*dusB*
YPTB0836	-3.07337322	1.962279749	*trmD*
YPTB2862	-3.025505608	1.004593668	*suhB*
pYV0081	-2.79868433	-1.591765731	*yscE*
YPTB0467	-2.674752958	1.38433871	*obgE*
YPTB2166	-2.55249968	-1.255035974	*rsxB*
YPTB1630	-2.50429935	-1.185698206	*mntP*
pYV0079	-2.504298622	-1.772463777	*yscC*
pYV0067	-2.434491505	-1.496489221	*fliI_1*
YPTB3697	-2.424284011	1.631197474	*rplD*
YPTB1568	-2.399270255	1.160604836	*yeeF*
YPTB3698	-2.377151941	1.590343015	*rplC*
YPTB2165	-2.338188551	1.106385356	*rnfC*
pYV0068	-2.313160365	-1.785993603	*yscO*
YPTB0835	-2.288519585	1.886470321	*rimM*
YPTB2583	-2.287442619	1.642895092	*nuoF*
YPTB2587	-2.285713946	-1.05190457	*nuoA*
pYV0088	-2.260150975	-1.858681997	*T3SS protein*
YPTB2167	-2.259666751	-1.260601135	*electron transport complex subunit A*
---	-2.255990414	-1.372783599	*hypothetical protein*
YPTB0478	-2.253288254	1.277037844	*rimP*
YPTB2011	-2.213752898	-1.657626798	*sodium-independent anion transporter*
YPTB0479	-2.18525486	1.651516013	*nusA*
YPTB2161	-2.14367402	1.059413709	*electron transport complex subunit E*
YPTB0834	-2.136886544	1.879592755	*rpsP*
YPTB2584	-2.111417859	1.558090325	*nuoE*
YPTB3417	-2.107138474	1.597027964	*dnaG*
YPTB2318	-2.10668317	1.984599069	*ppsA*
YPTB3737	-2.099915415	1.212719829	*putative iron receptor*
YPTB2585	-2.071421396	1.277136982	*nuoD*
YPTB2474	-2.057433815	1.279972034	*plsX*
YPTB1410	-2.052687773	-1.196516605	*hypothetical protein*
pYV0084	-2.045084128	-1.853744385	*yscH*
YPTB2309	-2.013678941	-1.093644899	*sufE*
pYV0085	-2.010361321	-1.435356749	*yscL*

DISCUSSION

In this study, we present evidence that IscR plays a role in regulating heme uptake and survival in blood in the bacterial pathogen *Yersinia pseudotuberculosis*. DNA binding analysis revealed an IscR binding site within the intergenic region between *hmuR* and *hmuSTUV*. We also observed that a Δ*iscR* mutant has a survival

defect growing in whole blood. Transcriptome analysis revealed that a Δ*iscR* mutant displays large expression changes in genes involved in oxidative stress, iron uptake, and methionine synthesis compared to the WT when grown in whole blood.

DNase footprinting revealed an IscR Motif II binding site in the intergenic region between *hmuR* and *hmuSTUV* that contains six of the nine bases found to be important for IscR binding (33). This and data from the β-galactosidase assays suggested that Apo-IscR may drive transcription from the intergenic promoter between *hmuR* and *hmuSTUV*. We predicted that a Δ*iscR* mutant would be defective in heme uptake as *hmuTUV* has been shown to be required for utilization of hemin (9). However, we observed that a Δ*iscR* mutant has no defect in growth in hemin as the only iron source. We also showed that although IscR binds to the intergenic region between *hmuR* and *hmuSTUV*, IscR cannot itself drive transcription from this promoter. Given these finding, we now predict that under conditions where IscR is highly expressed, such as during aerobic growth, oxidative stress, and/or iron limitation, high levels of Apo- or Holo-IscR bind this site to prevent repression by another transcriptional regulator (18-20, 39). This mode of regulation is not unlike the IscR regulation of the *sodA* promoter in *E. coli*. The *sodA* promoter unresponsive to IscR levels in *in vitro* transcription assays and IscR is thought to compete with Fur to prevent repression (18, 40). Additionally, given the recent research showing the requirement of molecular O_2 for the function of HmuS, a role for IscR in leading to increased expression from the intergenic promoter between *hmuR* and *hmuSTUV* in response to increasing O_2 concentrations seems logical (13). The lack of Fur binding

to the intergenic promoter between *hmuR* and *hmuSTUV* suggests that IscR is not competing with Fur at this promoter. Currently, we are interested in identifying other transcriptional regulators that interact with this promoter region to better understand how environmental signals regulate the *hmuRSTUV* operon in *Yersinia pseudotuberculosis*.

We also performed survival curves using sheep's whole blood, a heme-rich medium. While we observed a role for IscR for survival of *Y. pseudotuberculosis* in blood, we did not observe a defect for the Δ*hmuRSTUV* or Δ*hmuSTUV* mutants (data not shown). This may stem from the lack of iron starvation of the mutants before the survival assays in whole blood were performed. Indeed, to observe the Δ*iscR* growth defect in M9 media plus hemin, the bacteria had to be iron-starved prior to hemin exposure (data not shown). These results suggest that the Δ*iscR* survival defect in blood is independent of its defect in hemin utilization. Additionally, we ruled out any contribution of IscR control of the T3SS to survival in blood, as two different T3SS mutants did not display survival defects in blood. Furthermore, a mutant lacking *phoP* was not defective in survival in blood, indicating that growth inside blood-borne leukocytes is not essential for *Y. pseudotuberculosis* survival in blood. Our transcriptome analysis revealed an upregulation of several genes involved in oxidative stress in the Δ*iscR* mutant, including *ter* genes, putative oxidoredutases, and *katA*. The *ter* operon was named for its involvement in resistance to the highly toxic oxyanion tellurite; however, the Ter system has been suggested to detoxify antimicrobial compounds during oxidative stress (41). Catalase A, encoded by *katA,*

is best characterized in the bacterial pathogen *Pseudomonas aeruginosa*, where it plays an important role in oxidative stress resistance during infection and, interestingly, is regulated by IscR (42). These data suggest the intriguing possibility that IscR control of stress resistance genes is required for survival in blood.

In addition to upregulation of oxidative stress genes, we found that *emrR* is upregulated in a Δ*iscR* mutant grown in blood. Recently, research in *E. coli* has suggested that EmrR represses the efflux pump EmrAB under oxidative stress conditions, and that this may serve to increase the total glutathione (GSH) in the cell (43). Studies have shown that the *isc*-encoded protein IscU catalyzes the formation of [2Fe-2S] clusters in the presence of GSH (44). We hypothesize that a Δ*iscR* mutant expresses high levels of the *isc* operon due to derepression from inactivation of IscR (45). This potentially leads to an increased need for cysteine for a sulfur source for [2Fe-2S] clusters and a decreased ability to produce GSH under harsh conditions, as GSH production requires cysteine. Accordingly, the *metE* gene that encodes the folate-independent conversion of homocysteine to methionine is downregulated in the Δ*iscR* mutant, suggesting that all homocystine in the cell is being converted to cysteine to meet GSH and [2Fe-2S] needs instead of methionine. In line with this hypothesis, GSH levels are decreased in a Δ*iscR* mutant in *Comamonas testosteroni* S44 under oxidative stress conditions (46).

Several genes upregulated in the Δ*iscR* mutant in blood were found to be involved iron uptake genes, including *hmuR*, the putative ferric siderophore receptor YPTB0792, and *bdf*. In *Yersinia pestis*, all of these genes have been shown to be part

of the Fur regulon, suggesting derepression of Fur in the Δ*iscR* mutant grown in whole sheep's blood, compared to the WT strain (38). Indeed, we also observed that the Fur-controlled promoter upstream of *hmuR* has increased activity in a Δ*iscR* mutant. Given that depression of Fur occurs when intracellular iron levels are low, this suggests that a Δ*iscR* mutant has low intracellular iron levels. Increased expression of Fur-regulated iron uptake systems in the Δ*iscR* mutant may be due to constant depletion of intracellular iron due to increased [2Fe-2S] cluster biogenesis.

In summary, we provide evidence of regulation of the *hmuRSTUV* locus by both Fur and IscR. We show that Fur directly binds to the promoter upstream of *hmuR* whereas IscR binds to the intergenic region between *hmuR* and *hmuSTUV*. However, our data suggest that IscR works to prevent repression of the intergenic promoter by a transcriptional regulator distinct from Fur. Our data indicates that the *hmu* system is controlled by at least three different transcriptional regulators, perhaps enabling control of heme uptake in response to several environmental signals. Additionally, we suggest that deletion of IscR leads to global dysregulation of iron and sulfur metabolism. This contributes to defective survival of the Δ*iscR* mutant in blood, and may partly explain the severe virulence defect of the *Y. pseudotuberculosis* Δ*iscR* mutant.

REFERENCES

1. **Posey JE, Gherardini FC.** 2000. Lack of a role for iron in the Lyme disease pathogen. Science **288:**1651-1653.

2. **Weinberg ED.** 1978. Iron and infection. Microbiol Rev **42:**45-66.

3. **Cassat JE, Skaar EP.** 2013. Iron in infection and immunity. Cell Host Microbe **13:**509-519.

4. **Robins-Browne RM, Prpic JK.** 1985. Effects of iron and desferrioxamine on infections with *Yersinia enterocolitica*. Infect. Immun. **47:**774-779.

5. **Burrows TW, Jackson S.** 1956. The virulence-enhancing effect of iron on nonpigmented mutants of virulent strains of *Pasteurella pestis*. Br J Exp Pathol **37:**577-583.

6. **Perry RD, Bobrov AG, Fetherston JD.** 2015. The role of transition metal transporters for iron, zinc, manganese, and copper in the pathogenesis of *Yersinia pestis*. Metallomics **7:**965-978.

7. **Bearden SW, Fetherston JD, Perry RD.** 1997. Genetic organization of the yersiniabactin biosynthetic region and construction of avirulent mutants in *Yersinia pestis.* Infect. Immun. **65:**1659-1668.

8. **Choby JE, Skaar EP.** 2016. Heme Synthesis and Acquisition in Bacterial Pathogens. J. Mol. Biol. **428:**3408-3428.

9. **Hornung JM, Jones HA, Perry RD.** 1996. The *hmu* locus of *Yersinia pestis* is essential for utilization of free haemin and haem--protein complexes as iron sources. Mol. Microbiol. **20:**725-739.

10. **Thompson JM, Jones HA, Perry RD.** 1999. Molecular characterization of the hemin uptake locus (*hmu*) from *Yersinia pestis* and analysis of hmu mutants for hemin and hemoprotein utilization. Infect. Immun. **67:**3879-3892.

11. **Stojiljkovic I, Hantke K.** 1992. Hemin uptake system of *Yersinia enterocolitica*: similarities with other TonB-dependent systems in gram-negative bacteria. EMBO J. **11:**4359-4367.

12. **Stojiljkovic I, Hantke K.** 1994. Transport of haemin across the cytoplasmic membrane through a haemin-specific periplasmic binding-protein-dependent transport system in *Yersinia enterocolitica*. Mol. Microbiol. **13:**719-732.

13. **Onzuka M, Sekine Y, Uchida T, Ishimori K, Ozaki SI.** 2017. HmuS from *Yersinia pseudotuberculosis* is a non-canonical heme-degrading enzyme to acquire iron from heme. Biochim. Biophys. Acta.

14. **Skaar EP.** 2010. The battle for iron between bacterial pathogens and their vertebrate hosts. PLoS Pathog **6:**e1000949.

15. **Troxell B, Hassan HM.** 2013. Transcriptional regulation by Ferric Uptake Regulator (Fur) in pathogenic bacteria. Front Cell Infect Microbiol **3:**59.

16. **Jacobi CA, Gregor S, Rakin A, Heesemann J.** 2001. Expression analysis of the yersiniabactin receptor gene fyuA and the heme receptor hemR of *Yersinia enterocolitica in vitro* and *in vivo* using the reporter genes for green fluorescent protein and luciferase. Infect. Immun. **69:**7772-7782.

17. **Miller HK, Kwuan L, Schwiesow L, Bernick DL, Mettert E, Ramirez HA, Ragle JM, Chan PP, Kiley PJ, Lowe TM, Auerbuch V.** 2014. IscR is essential for *Yersinia pseudotuberculosis* type III secretion and virulence. PLoS Pathog **10:**e1004194.

18. **Giel JL, Rodionov D, Liu M, Blattner FR, Kiley PJ.** 2006. IscR-dependent gene expression links iron-sulphur cluster assembly to the control of O2-regulated genes in Escherichia coli. Mol. Microbiol. **60:**1058-1075.

19. **Wu Y, Outten FW.** 2009. IscR controls iron-dependent biofilm formation in *Escherichia coli* by regulating type I fimbria expression. J. Bacteriol. **191:**1248-1257.

20. **Yeo WS, Lee JH, Lee KC, Roe JH.** 2006. IscR acts as an activator in response to oxidative stress for the suf operon encoding Fe-S assembly proteins. Mol. Microbiol. **61:**206-218.

21. **Cheng LW, Anderson DM, Schneewind O.** 1997. Two independent type III secretion mechanisms for YopE in Yersinia enterocolitica. Mol. Microbiol. **24:**757-765.

22. **Bliska JB, Guan KL, Dixon JE, Falkow S.** 1991. Tyrosine phosphate hydrolysis of host proteins by an essential *Yersinia* virulence determinant. Proc Natl Acad Sci U S A **88:**1187-1191.

23. **Durand EA, Maldonado-Arocho FJ, Castillo C, Walsh RL, Mecsas J.** 2010. The presence of professional phagocytes dictates the number of host cells targeted for Yop translocation during infection. Cell. Microbiol. **12:**1064-1082.

24. **Balada-Llasat JM, Mecsas J.** 2006. *Yersinia* has a tropism for B and T cell zones of lymph nodes that is independent of the type III secretion system. PLoS Pathog **2:**e86.

25. **Auerbuch V, Golenbock DT, Isberg RR.** 2009. Innate immune recognition of *Yersinia pseudotuberculosis* type III secretion. PLoS Pathog **5:**e1000686.

26. **Miller HK, Schwiesow L, Au-Yeung W, Auerbuch V.** 2016. Hereditary Hemochromatosis Predisposes Mice to *Yersinia pseudotuberculosis* Infection Even in the Absence of the Type III Secretion System. Front Cell Infect Microbiol **6:**69.

27. **Warrens AN, Jones MD, Lechler RI.** 1997. Splicing by overlap extension by PCR using asymmetric amplification: an improved technique for the generation of hybrid proteins of immunological interest. Gene **186:**29-35.

28. **Andrews HL, Vogel JP, Isberg RR.** 1998. Identification of linked *Legionella pneumophila* genes essential for intracellular growth and evasion of the endocytic pathway. Infect. Immun. **66:**950-958.

29. **Merriam JJ, Mathur R, Maxfield-Boumil R, Isberg RR.** 1997. Analysis of the *Legionella pneumophila fliI* gene: intracellular growth of a defined mutant defective for flagellum biosynthesis. Infect. Immun. **65:**2497-2501.

30. **Uliczka F, Pisano F, Kochut A, Opitz W, Herbst K, Stolz T, Dersch P.** 2011. Monitoring of gene expression in bacteria during infections using an adaptable set of bioluminescent, fluorescent and colorigenic fusion vectors. PLoS One **6:**e20425.

31. **Nesbit AD, Fleischhacker AS, Teter SJ, Kiley PJ.** 2012. ArcA and AppY antagonize IscR repression of hydrogenase-1 expression under anaerobic

conditions, revealing a novel mode of O2 regulation of gene expression in *Escherichia coli*. J. Bacteriol. **194:**6892-6899.

32. **Schwartz CJ, Giel JL, Patschkowski T, Luther C, Ruzicka FJ, Beinert H, Kiley PJ.** 2001. IscR, an Fe-S cluster-containing transcription factor, represses expression of *Escherichia coli* genes encoding Fe-S cluster assembly proteins. Proc Natl Acad Sci U S A **98:**14895-14900.

33. **Nesbit AD, Giel JL, Rose JC, Kiley PJ.** 2009. Sequence-specific binding to a subset of IscR-regulated promoters does not require IscR Fe-S cluster ligation. J. Mol. Biol. **387:**28-41.

34. **Raymond B, Young JC, Pallett M, Endres RG, Clements A, Frankel G.** 2013. Subversion of trafficking, apoptosis, and innate immunity by type III secretion system effectors. Trends Microbiol. **21:**430-441.

35. **Schindler MK, Schutz MS, Muhlenkamp MC, Rooijakkers SH, Hallstrom T, Zipfel PF, Autenrieth IB.** 2012. *Yersinia enterocolitica* YadA mediates complement evasion by recruitment and inactivation of C3 products. J. Immunol. **189:**4900-4908.

36. **Skurnik M, Toivanen P.** 1992. LcrF is the temperature-regulated activator of the *yadA* gene of *Yersinia enterocolitica* and *Yersinia pseudotuberculosis.* J. Bacteriol. **174:**2047-2051.

37. **Grabenstein JP, Marceau M, Pujol C, Simonet M, Bliska JB.** 2004. The response regulator PhoP of *Yersinia pseudotuberculosis* is important for replication in macrophages and for virulence. Infect. Immun. **72:**4973-4984.

38. **Gao H, Zhou D, Li Y, Guo Z, Han Y, Song Y, Zhai J, Du Z, Wang X, Lu J, Yang R.** 2008. The iron-responsive Fur regulon in *Yersinia pestis*. J. Bacteriol. **190:**3063-3075.

39. **Rajagopalan S, Teter SJ, Zwart PH, Brennan RG, Phillips KJ, Kiley PJ.** 2013. Studies of IscR reveal a unique mechanism for metal-dependent regulation of DNA binding specificity. Nat. Struct. Mol. Biol. **20:**740-747.

40. **Beauchene NA, Myers KS, Chung D, Park DM, Weisnicht AM, Keles S, Kiley PJ.** 2015. Impact of Anaerobiosis on Expression of the Iron-Responsive Fur and RyhB Regulons. MBio **6:**e01947-01915.

41. **Taylor DE.** 1999. Bacterial tellurite resistance. Trends Microbiol. **7:**111-115.

42. **Kim SH, Lee BY, Lau GW, Cho YH.** 2009. IscR modulates catalase A (KatA) activity, peroxide resistance and full virulence of *Pseudomonas aeruginosa* PA14. J Microbiol Biotechnol **19:**1520-1526.

43. **Sakamoto A, Terui Y, Yoshida T, Yamamoto T, Suzuki H, Yamamoto K, Ishihama A, Igarashi K, Kashiwagi K.** 2015. Three members of polyamine modulon under oxidative stress conditions: two transcription factors (SoxR and EmrR) and a glutathione synthetic enzyme (GshA). PLoS One **10:**e0124883.

44. **Qi W, Li J, Chain CY, Pasquevich GA, Pasquevich AF, Cowan JA.** 2012. Glutathione complexed Fe-S centers. J. Am. Chem. Soc. **134:**10745-10748.

45. **Giel JL, Nesbit AD, Mettert EL, Fleischhacker AS, Wanta BT, Kiley PJ.** 2013. Regulation of iron-sulphur cluster homeostasis through transcriptional

control of the Isc pathway by [2Fe-2S]-IscR in Escherichia coli. Mol. Microbiol. **87:**478-492.

46. **Liu H, Zhuang W, Zhang S, Rensing C, Huang J, Li J, Wang G.** 2015. Global Regulator IscR Positively Contributes to Antimonite Resistance and Oxidation in *Comamonas testosteroni* S44. Front Mol Biosci **2:**70.

CHAPTER 4

Characterization of IscR Motif II *lcrF* Promoter Mutants in *Yersinia pseudotuberculosis*

By Leah Schwiesow, Patricia J Kiley, and Victoria Auerbuch

INTRODUCTION

The type III secretion system (T3SS) is a needle-like injectisome that delivers bacterial effector proteins directly into the host cytosol (1). In the three pathogenic *Yersinia* species, *Yersinia pestis*, *Yersinia enterocolitca*, and *Yersinia pseudotuberculosis*, the T3SS is essential for full virulence (2). The T3SS enables *Yersinia* species to dampen the host immune response and evade phagocytosis. However, expression of the T3SS could also be potentially detrimental for the bacteria (3). For example, it is well documented that induction of the T3SS leads to growth arrest *in vitro* (4). Additionally, the innate immune system can recognize several components of the *Yersinia* T3SS (5, 6). Accordingly, the expression of the T3SS is tightly regulated (3, 4).

The *Yersinia* T3SS is encoded on a 70 kB virulence plasmid termed pYV. The master regulator of the *Yesinia* T3SS, LcrF, is encoded on this virulence plasmid and is the only known transcriptional activator of downstream T3SS components, including T3SS machinery and effector proteins (4). LcrF is thermoregulated at both the transcriptional and translational levels (4). At 25°C, the histone like protein YmoA blocks transcription of *lcrF* transcription. However, upon shift to 37°C, YmoA is cleaved by proteases to allow *lcrF* transcription (7-9). Additionally, a thermoswitch in the *lcrF* mRNA only allows for translation at 37°C (7). In addition to thermoregulation, the response regulator of the Rcs two component system, RcsB, has been shown to directly bind to the *lcrF* promoter, suggesting a role for extracytoplasmic stress in the regulation of the T3SS (10).

We previously demonstrated that the transcriptional regulator IscR binds to a Motif II site in the promoter region of *lcrF* and regulates its transcription in *Yersinia pseudotuberculosis* (11). IscR has been extensively characterized in *E.coli*, where its DNA-binding activity is modulated based on the coordination of a [2Fe-2S] cluster (12-14). When IscR is bound to a [2Fe-2S] cluster and in its Holo- form, it can bind both a Motif I site and a Motif II site; however, clusterless IscR, or Apo-IscR, can only bind a Motif II site (12-14). As iron starvation, oxidative stress, and oxygen limitation affect the Holo-IscR/Apo-IscR ratio, these environmental cues are thought to have a direct effect on gene expression through IscR in *E. coli* (15-17). The effect of oxygen levels, oxidative stress or iron limitation on the T3SS or IscR has not been demonstrated in *Yersinia pseduotuberculosis*.

In this study, we set out to assess the importance of correct IscR-mediated control on the T3SS. We created mutations in the IscR Motif II binding site in the *lcrF* promoter region that either abolish all IscR binding or switch the control of the *lcrF* promoter from a Motif II site to a Motif I site. We characterized the functionality of the T3SS in both of these mutants *in vitro* and in a mouse model of *Yersinia* infection *in vivo*. We demonstrate that an *lcrF* promoter mutant that abolishes all IscR binding is defective in type III secretion *in vitro* and has a virulence defect *in vivo*. We also show that a promoter mutant that switches IscR *lcrF* promoter control from a Motif II site to a Motif I site secretes normally under standard *in vitro* conditions, but has a virulence defect *in vivo*.

MATERIALS AND METHODS

Bacterial Strains, plasmids, and growth conditions. All strains used in this study are listed in Table 1. Bacterial strains were grown in 2XYT at 26°C with shaking at 250 rpm. Where stated, Yop synthesis was induced via back-dilution of cultures into low calcium 2XYT media (2XYT plus 20 mM $MgCl_2$ and 20 mM sodium oxalate) to an OD_{600} of 0.2 grown for 1.5 hr at 26°C/shaking followed by 37°C shaking as previously described (18).

Table 1. Strains Used In This Study

Strain	Background	Mutation(s)	Reference
WT	IP2666	Naturally lacks full length YopT	(19)
Δ*iscR*	IP2666	Δ*iscR*	(11)
IscR Binding Null	IP2666	Abolishes IscR binding to the *lcrF* promoter	This study
IscR Binding Motif I	IP2666	Changes IscR Motif II binding site in *lcrF* promoter to IscR Motif I binding site	This study
pYV-	IP2666	Δ*yscBL* pYV cured	(20)

Construction of *Y. pseudotuberculosis* mutant strains. The IscR Binding Null mutant and IscR Binding Motif I mutant were generated via splicing by overlap extension (21). Primer pairs F5lcrF/R5Null and F3Null/R3lcrF (Table 2) were used to amplify ~1000 bp 5' and 3' of the IscR Motif II Site in the *lcrF* promoter for the IscR Binding Null Mutant. Primer pairs F5lcrF/R5MotifI and F3MotifI/R3lcrF (Table 2) were used to amplify ~1000 bp 5' and 3' of the IscR Motif II Site in the *lcrF*

promoter for the IscR Motif I Mutant. Amplified PCR fragments served as templates in an overlap extension PCR using the outside primers F5lcrF and R3lcrF. Nucleotide changes within the internal primers allowed for amplification of *lcrF* promoter sequence target containing sequences coding for substitutions to create the IscR Binding Null mutant and the IscR Binding Motif I mutant.

The resulting ~2 kb fragments were cloned into the TOPO TA cloning vector (Invitrogen) and further subcloned into a BamHI-digested pSR47s suicide plasmid (λpir-dependent replicon, kanamycin^R (Kan^R), *sacB* gene conferring sucrose sensitivity) (22, 23). Recombinant plasmids were transformed into *E. coli* S17-1 λpir competent cells and later introduced into *Y. pseudotuberculosis* IP2666 via conjugation. The resulting Kan^R, irgansan^R (*Yersinia* selective antibiotic) integrants were grown in the absence of antibiotics and plated on sucrose-containing media to select for clones that had lost *sacB* (and by inference, the linked plasmid DNA). Kan^S, sucrose^R, congo red-positive colonies were screened by PCR and sequencing to identify correct mutations within the *lcrF* promoter.

Table 2. *Y. pseudotuberculosis* primers used in this study

Name	Primer Sequence (5'-3')	Reference
F5lcrF	ATGATGGGATCCTTAGTAAGCTGATGCTAATCC	This Study
R5Null	TGTATAAATCCTTTGAAATCGCATCATATATTCCTAATAT	This Study
F3Null	GATTTCAAAGGATTTATACAGTATGGTAATTGTATTTCT	This Study
R5MotifI	TTCCCGAGTAAATTGGTCAACTATAAATCGCATCATA	This Study

F3MotifI	TATAGTTGACCAATTTACTCGGGAATTGTATTTCTCCTG	This Study
R3lcrF	ATGATGGGATCCGGCCATCTTGTGAATGCTCAAC	This Study

***Y. pseudotuberculosis* Growth Curves.** *Y. pseudotuberculosis* strains were cultured overnight in 2xYT at 26°C and sub-cultured to an OD_{600} of 0.2 in 20 mL of either high calcium (2XYT plus 5 mM $CaCl_2$) or low calcium 2XYT (2XYT plus 20 mM $MgCl_2$ and 20 mM sodium oxalate). Cultures were incubated at either 26°C or 37°C with shaking at 250 rpm and OD_{600} was measured every hour for 9 hr**.**

Type III Secretion Assay. Visualization of T3SS cargo secreted into culture was performed as previously described (24). Briefly, *Y. pseudotuberculosis* was grown in Low-Ca^{2+} 2XYT (2YXT with 20 mM $MgCl_2$ and 20 mM sodium oxalate) for 1.5 hrs at 26°C followed by growth for 1.5 hrs at 37°C. Cultures were normalized by OD_{600} and pelleted at 13,200 rpm for 10 min at room temperature. Supernatants were removed and proteins were precipitated by addition of trichloroacetic acid (TCA) at a final concentration of 10%. Samples were incubated on ice for 20 min and were pelleted at 13,200 rpm for 15 min at 4°C. Resulting pellets were washed twice with ice-cold 100% EtOH and subsequently resuspended in final sample buffer (FSB) containing 20% dithiothreitol (DTT). Samples were boiled for 5 min prior to running on a 12.5% SDS PAGE gel.

Mouse Infections. All animal use procedures were in strict accordance with the NIH *Guide for the Care and Use of Laboratory Animals* and were approved by the UC Santa Cruz Institutional Animal Care and Use Committee. Eleven to twelve-

week-old 129S6/SvEvTac mice from Jackson labs were used for oral infections using a bread feeding method described in Bou Ghanem et al, 2013 (25). Briefly, the night before infection, mice to be infected were withheld food. The morning of infection, 2 X 10^8 CFU of *Y. pseudotuberculosis* was resuspended in 2 µL 1X PBS and 3 µL melted salted butter. The 5 µL mixture was then pipetted onto a 2 mm X 2 mm cube of white bread. Each mouse was fed an infected bread piece. After bread feeding, mice were given food and water *ad libitum* and were euthanized 5 days post infection. Peyer's patches, mesenteric lymph nodes, spleens, and livers were isolated and homogenized for 30 s in PBS followed by serial dilution and plating on LB supplemented with 1 µg/mL irgasan for CFU determination.

Cytokine Profiling. Cytokine measurements were performed as previously described (26). Briefly, previously frozen Peyer's patch and mesenteric lymph node homogenates from mice infected with 2 × 10^8 CFU of WT, Δ*iscR*, IscR Binding Null, or IscR Binding Motif I *Y. pseudotuberculosis* were thawed on ice and centrifuged at 13,000 rpm for 1 min. The mouse inflammatory cytometric bead array kit (BD Biosciences) was used to detect IL-12p70, TNF-α, IFN-γ, MCP-1, IL-10, and IL-6 according to the manufacturer's protocol, with the following exceptions: the amount of antibody-conjugated beads was decreased to 4 µl each with 20 µl of sample/standard and 20 µl of detection reagent per reaction. Data were acquired and analyzed using a BD FACS LSRII flow cytometer and BD analysis software, respectively. Individual cytokine concentrations in pg/ml were plotted against CFU per gram of liver tissue determined at the time of organ harvest.

RESULTS

IscR binding to the *lcrF* promoter is important for *Y. pseudotuberculosis* Ysc T3SS function. We mutated residues important for IscR binding in the IscR Motif II binding site of the *lcrF* promoter (Figure 1A). Studies in *E .coli* have demonstrated that mutation of these four residues within an IscR Motif II site should abolish IscR binding (14). To determine if abolishment of IscR binding in the *lcrF* promoter leads to alterations in T3SS function, we visualized the secretome of this IscR Binding Null mutant. The IscR Binding Null mutant was observed to be dramatically defective in secretion of T3SS cargo compared to the WT strain (Figure 1B). This data suggest that IscR binding to the *lcrF* promoter is important for proper T3SS function.

To further assess the importance of IscR-mediated control of the *lcrF* promoter, we replaced the IscR Motif II site in the *lcrF* promoter with the IscR Motif I site upstream of the *iscRSUA* operon in *E. coli* and visualized the secretome of this IscR Motif I mutant (Figure 1A) (13). This mutation should switch control of the *lcrF* from Apo- and Holo- IscR to Holo-IscR exclusively, as Apo-IscR cannot bind a Motif I site (12). The IscR Motif I mutant showed no difference in secretion of T3SS cargo compared to the WT strain (Figure 1B). These data suggest that Holo-IscR can drive *lcrF* transcription and that at least some Holo-IscR is present in *Y. pseudotuberculosis* under aerobic, iron replete culture conditions.

To ensure that lack of type III secretion did not result from a growth defect in the IscR Binding Null mutant, we performed growth curves at 37°C in low and high calcium 2xYT. All strains grew similarly under high calcium 2xYT condition (Figure

A

	Sequence 5'-3'
WT *lcrF* Motif II Site	TAAAACCATATATACAGTATGGTAATTGT
IscR Binding Null Mutant	TCAAAGGATTTATACAGTATGGTAATTGT
IscR Motif I Mutant	TATAGTTGACCAATTTACTCGGGAATTGT

B

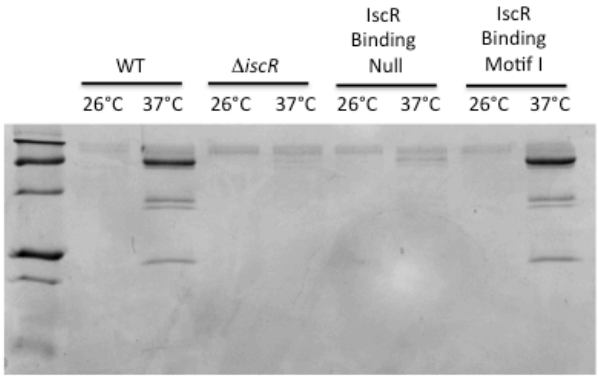

Figure 1. Ability of IscR Motif II *lcrF* promoter mutants to secrete T3SS cargo. **(A)** Sequences of the WT *lcrF* Motif II site, the IscR Binding Null Mutant site, and the IscR Motif I Mutant site. Nucleotides denoted in red represent mutations from the WT IscR Motif II site in the *lcrF* promoter. **(B)** *Y. pseudotuberculosis* IP2666 wild type (WT), *iscR* deletion (Δ*iscR*), IscR Binding Null Mutant, and IscR Motif I strains were grown in 2xYT low calcium media at 26° or 37°C to induce type III secretion in the absence of host cells. Proteins in the bacterial culture supernatant were precipitated and visualized alongside a protein molecular weight marker (L) on a polyacrylamide gel using commassie blue. Sample loading was normalized for OD_{600} of each culture.

2A). Under low calcium 2xYT conditions, the IscR Binding Null mutant grew better than the WT strain, while the IscR Motif I mutant and WT strain grew similarly (Figure 2B). These data are consistent with a T3SS defect in the IscR Binding Null mutant, as WT *Yersinia* display growth restriction upon T3SS expression (27, 28). Additionally, this result is consistent with previous reports that type III secretion requires millimolar concentrations of calcium to grow at 37°C (29, 30).

IscR Binding *lcrF* promoter mutants are defective in colonizing a mouse model of infection. Based on the knowledge that the T3SS is an important virulence determinant for *Y. pseudotuberculosis in vivo*, we investigated whether abolishment of IscR binding to the *lcrF* promoter or altered IscR *lcrF* binding would lead to decreased infectious capacity. Using a bread feeding protocol to better mimic natural *Y. pseudotuberculosis* infection, we infected mice with $2x10^8$ *Y. pseudotuberculosis* WT, Δ*iscR*, IscR Binding Null mutant, or the IscR Binding Motif I mutant. At 5 days post bread feeding, the Δ*iscR*, IscR Binding Null mutant, and the IscR Motif I Binding mutants had significant defects in colonizing the spleen and liver, but were not defective in colonizing the Peyer's patches or mesenteric lymph nodes (Figure 3). The virulence defect of a Δ*iscR* strain has been demonstrated previously (11). These data suggest that IscR binding to a Motif II Site in the *lcrF* promoter is important for full virulence of *Y. pseudotuberculosis in vivo*.

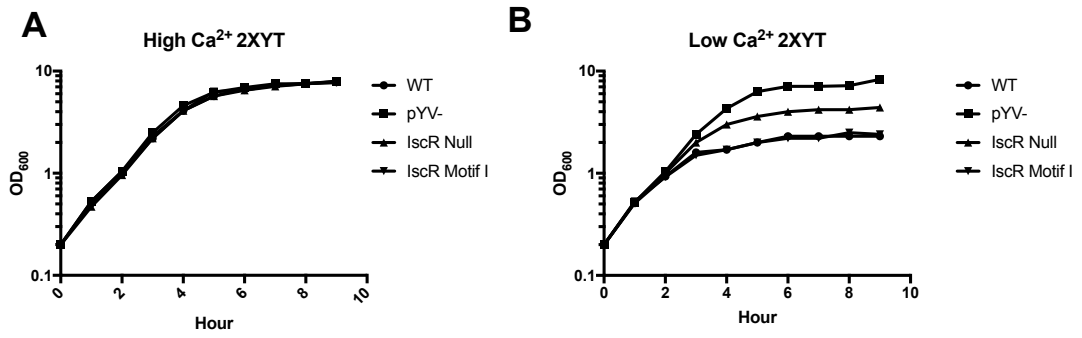

Figure 2. Growth of IscR Motif II *lcrF* mutants under low and high calcium conditions. The *Y. pseudotuberculosis* WT, pYV-, IscR Binding Null and IscR Motif I mutant were grown **(A)** in 2XYT supplemented with 5mM $CaCl_2$ (High Ca^{2+}2XYT) at 37°C or **(B)** in Low Ca^{2+} 2XYT at 37°C. Optical density of the cultures were monitored at 600 nm every hour for 9 h. Data is representative of two independent experiments.

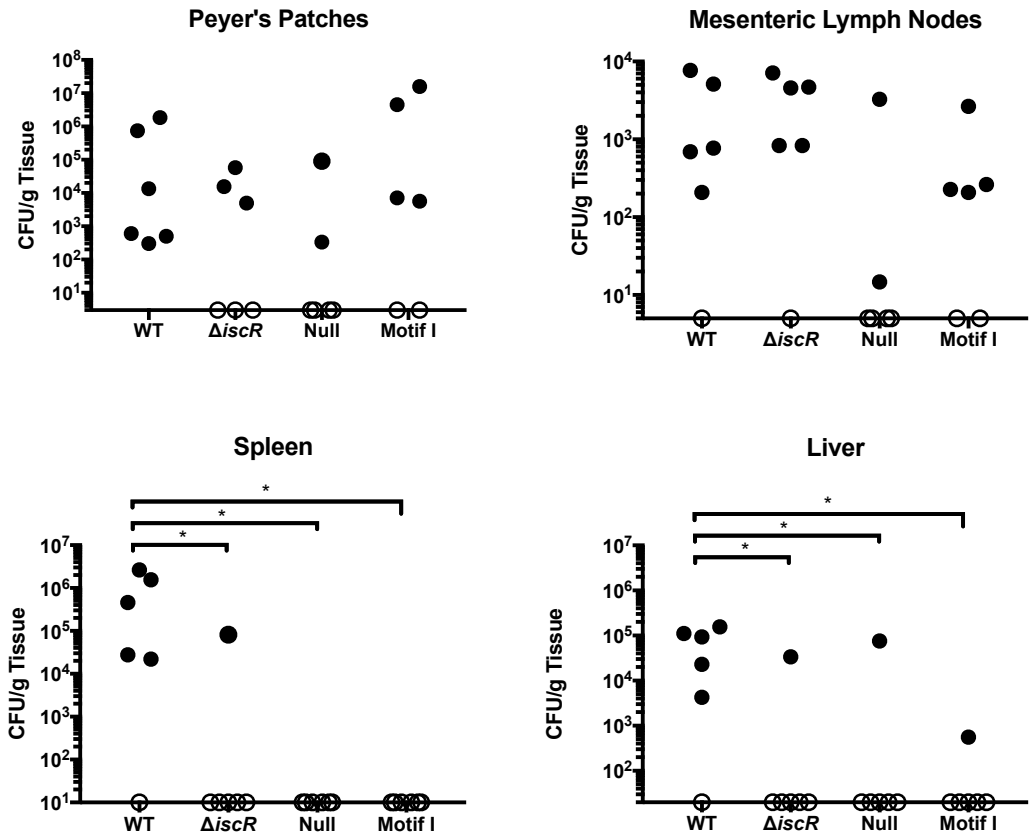

Figure 3. Virulence of IscR Motif II *lcrF* promoter mutants in a mouse model of *Yersinia pseudotuberculosis* infection. Mice were infected with 2×10^8 CFU of WT, Δ*iscR*, IscR Binding Null mutant, or the IscR Motif I mutant via bread feeding. At 5 days post-inoculation, the Peyer's patches (PP), mesenteric lymph nodes (MLN), spleens and livers were collected, homogenized and CFU were determined. Each symbol represents one animal. Unfilled symbols indicate that CFU were below the limit of detection. The data presented are from two independent experiments. *$p<0.05$, as determined by a Kruskal-Wallis rank sum test.

Cytokine profiling suggests that IscR *lcrF* promoter mutants induce normal inflammatory cytokine production *in vivo*. We were surprised that an IscR Motif I Binding mutant is able to secrete T3SS cargo normally *in vitro* but has a virulence defect in a mouse model of infection. The balance of Apo-IscR and Holo-IscR is thought to change in response to oxygen limitation, oxidative stress, and iron limitation (15-17). The IscR Motif I Binding mutant should drive transcription of *lcrF* under conditions in which Holo-IscR is the predominant form of IscR in the cell, such as under anaerobic, iron replete conditions (13, 14, 31). Given this, we hypothesized that we would observe increased type III secretion in gut-associated tissues with lower oxygen tension, and that this may lead to decreased cytokine production in gut associated tissues, as several T3SS effectors dampen the host immune response (32). However, we observed no difference in cytokine secretion of TNFα, IL-6, or MCP-1 between Peyer's Patch or mesenteric lymph node tissue infected the WT strain or the IscR Motif I Binding mutant, where cytokine levels correlated with bacterial burden (Figure 4). This data suggests an alternative model for the virulence defect of the IscR Motif I Binding mutant.

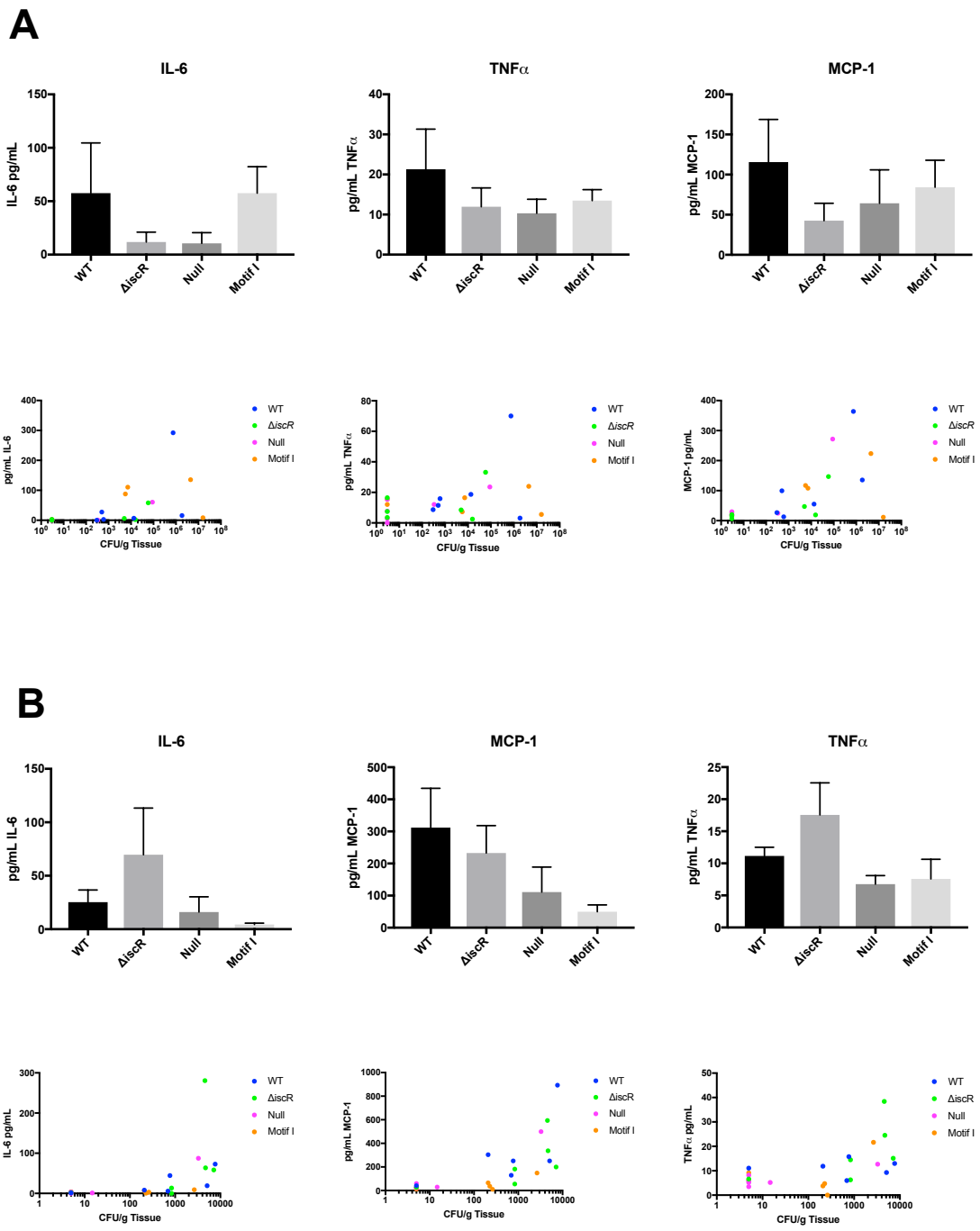

Figure 4. Secretion of IL-6, TNFα, and MCP-1 in Peyer's patches and mesentenic lymph nodes infected with IscR Motif II *lcrF* promoter mutants. WT mice were infected with 2x10^8 WT, Δ*iscR*, IscR Binding Null or IscR Motif I *Y.*

pseudotuberculosis via bread feeding and tissues harvested 5 days post-inoculation. Flow cytometry-based ELISA was used to measure levels of the cytokines IL-6, and TNF-α and the chemokine MCP-1 from **(A)** Peyer's patch and **(B)** mesenteric lymph node homogenates. Bar graphs are representative of total cytokine secretion and error bars represent standard error of the mean, N=6 mice per group. No significant differents between groups were detected using One-way ANOVA. Scatter plots are representative of cytokine secretion normalize to CFU/g tissue, N=6 mice per group.

DISCUSSION

In this study, we characterize two separate IscR Motif II *lcrF* promoter mutants. The IscR Binding Null mutant had a dramatic defect in secretion of T3SS cargo *in vitro* and displayed a virulence defect *in vivo*. The IscR Motif I mutant showed no defect in secretion of T3SS cargo, however, this mutant displayed a virulence defect *in vivo*. Collectively, these findings indicate that IscR binding to a Motif II site in the *lcrF* promoter is essential for complete virulence.

Both Holo- and Apo- IscR are predicted to bind the Motif II site within the *lcrF* promoter (12, 14). Based on previous work in *E.coli*, conditions of aerobic growth, iron limitation, or high oxidative stress lead to increased IscR levels in the cell through derepression of the *iscRSUA* operon (15-17, 33). Increased IscR levels under these conditions are predicted to lead to an increase of *lcrF* expression and T3SS gene expression Conversely, conditions of anaerobic growth, high iron, or low oxidative stress should lead to a decrease in T3SS expression due to decreased levels of IscR through repression of the *iscRSUA* operon by Holo-IscR (15-17, 33). We hypothesized that there should be more Apo-IscR than Holo-IscR in the cell under normal lab conditions of aerobic growth in iron replete media. We expected an IscR Motif I mutant to show decreased secretion of T3SS cargo under these conditions because Apo-IscR cannot bind a Motif I site (12). However, we observed that the IscR Motif I mutant displayed no defect in secretion of T3SS cargo, suggesting that is enough Holo-IscR in the cell to drive T3SS expression under these conditions.

Yersinia pseudotuberculosis is ingested through contaminated food or water. Once in the gut, the bacteria bind to the luminal surface of M cells to transverse the intestinal barrier into the underlying Peyer's patches (34). From there, it is thought that *Yersinia pseudotuberculosis* travels to the mesenteric lymph nodes and deeper tissues such as the spleen and liver (35-37). However, other research has suggested that *Yersinia pseudotuberculosis* can transverse the intestinal barrier independently of M cells (38). Additionally, the pool of *Yersinia pseudotuberculosis* in the gut that disseminates to deeper tissues crosses the gut barrier independently of the M cells (38). Both of our IscR Motif II *lcrF* promoter mutants showed no significant defect in colonizing the Peyer's patches and mesenteric lymph nodes but showed significant defects in colonizing the spleen and liver. These data lead to the intriguing possibility that IscR may contribute to M-cell independent dissemination of *Y. pseudotuberculosis* from the gut. Alternatively, IscR may be required for *Y. pseudotuberculosis* growth or survival in the spleen and liver once dissemination has occurred.

Previously, we demonstrated that a Δ*iscR* mutant was defective in colonizing the Peyer's patches, mesenteric lymph nodes, liver and spleen in a mouse model of infection using orogastric inoculation (11). We hypothesized that IscR controls processes other than the T3SS that were important for virulence, as research has demonstrated that the T3SS is not a requirement for persistence in the mesenteric lymph nodes (7, 11, 39, 40). We characterized the IscR Binding Null mutant to determine the effect of IscR on the T3SS independent of other potential factors that

IscR could be controlling. However, when we utilized a bread feeding model of infection, we observed no difference in colonization of the Peyer's patches and mesenteric lymph nodes between the Δ*iscR* mutant, the IscR binding Null mutant, or IscR Motif I mutant. This difference in colonization between the two models is unclear, but suggests that the main effect of IscR on virulence may be through the control of the T3SS, and not through IscR control of other virulence factors.

Throughout its infection cycle, *Yersinia pseudotuberculosis* experiences changes in oxygen availability, reactive oxygen species (ROS), and iron limitation. The lumen of the gut is completely anaerobic, while oxygen levels increase as the bacteria move closer to the intestinal barrier (41). Additionally, within the host iron is sequestered away from the bacteriairon is sequestered away from bacteria (42). Furthermore, phagocytes and intestinal epithelial cells produce reactive oxygen species (ROS), although ROS production can be inhibited by *Yersinia* T3SS effector proteins (43-45). Therefore, we postulate that under condition where Apo-IscR is the predominant form (low iron, high oxygen tension, and/or high ROS levels), IscR may drive LcrF expression only in the WT bacteria but not in the IscR Motif I mutant. Because the T3SS inhibits multiple host defense mechanisms (5, 32), this would then lead to differences in the immune response to these two strains. While we did not observe differences in TNF-a, IL-6, or MCP-1 expression in the Peyer's patches or MLNs during infection with the *lcrF* promoter mutants and WT bacteria, in the future it will be necessary to analyze other aspects of the immune response to *Yersinia*, such as inhibition of phagocytosis or ROS production by macrophages and neutrophils.

REFERENCES

1. **Deng W, Marshall NC, Rowland JL, McCoy JM, Worrall LJ, Santos AS, Strynadka NCJ, Finlay BB.** 2017. Assembly, structure, function and regulation of type III secretion systems. Nat. Rev. Microbiol. **15:**323-337.
2. **Coburn B, Sekirov I, Finlay BB.** 2007. Type III secretion systems and disease. Clin. Microbiol. Rev. **20:**535-549.
3. **Plano GV, Schesser K.** 2013. The *Yersinia pestis* type III secretion system: expression, assembly and role in the evasion of host defenses. Immunol. Res. **57:**237-245.
4. **Schwiesow L, Lam H, Dersch P, Auerbuch V.** 2015. *Yersinia* Type III Secretion System Master Regulator LcrF. J. Bacteriol. **198:**604-614.
5. **Chung LK, Park YH, Zheng Y, Brodsky IE, Hearing P, Kastner DL, Chae JJ, Bliska JB.** 2016. The *Yersinia* Virulence Factor YopM Hijacks Host Kinases to Inhibit Type III Effector-Triggered Activation of the Pyrin Inflammasome. Cell Host Microbe **20:**296-306.
6. **Ratner D, Orning MP, Proulx MK, Wang D, Gavrilin MA, Wewers MD, Alnemri ES, Johnson PF, Lee B, Mecsas J, Kayagaki N, Goguen JD, Lien E.** 2016. The *Yersinia pestis* Effector YopM Inhibits Pyrin Inflammasome Activation. PLoS Pathog **12:**e1006035.
7. **Bohme K, Steinmann R, Kortmann J, Seekircher S, Heroven AK, Berger E, Pisano F, Thiermann T, Wolf-Watz H, Narberhaus F, Dersch P.** 2012.

Concerted actions of a thermo-labile regulator and a unique intergenic RNA thermosensor control *Yersinia* virulence. PLoS Pathog **8:**e1002518.

8. **King JM, Schesser Bartra S, Plano G, Yahr TL.** 2013. ExsA and LcrF recognize similar consensus binding sites, but differences in their oligomeric state influence interactions with promoter DNA. J. Bacteriol. **195:**5639-5650.

9. **Jackson MW, Silva-Herzog E, Plano GV.** 2004. The ATP-dependent ClpXP and Lon proteases regulate expression of the *Yersinia pestis* type III secretion system via regulated proteolysis of YmoA, a small histone-like protein. Mol. Microbiol. **54:**1364-1378.

10. **Li Y, Hu Y, Francis MS, Chen S.** 2015. RcsB positively regulates the *Yersinia* Ysc-Yop type III secretion system by activating expression of the master transcriptional regulator LcrF. Environ. Microbiol. **17:**1219-1233.

11. **Miller HK, Kwuan L, Schwiesow L, Bernick DL, Mettert E, Ramirez HA, Ragle JM, Chan PP, Kiley PJ, Lowe TM, Auerbuch V.** 2014. IscR is essential for *Yersinia pseudotuberculosis* type III secretion and virulence. PLoS Pathog **10:**e1004194.

12. **Rajagopalan S, Teter SJ, Zwart PH, Brennan RG, Phillips KJ, Kiley PJ.** 2013. Studies of IscR reveal a unique mechanism for metal-dependent regulation of DNA binding specificity. Nat. Struct. Mol. Biol. **20:**740-747.

13. **Giel JL, Nesbit AD, Mettert EL, Fleischhacker AS, Wanta BT, Kiley PJ.** 2013. Regulation of iron-sulphur cluster homeostasis through transcriptional

control of the Isc pathway by [2Fe-2S]-IscR in *Escherichia coli*. Mol. Microbiol. **87:**478-492.

14. **Nesbit AD, Giel JL, Rose JC, Kiley PJ.** 2009. Sequence-specific binding to a subset of IscR-regulated promoters does not require IscR Fe-S cluster ligation. J. Mol. Biol. **387:**28-41.

15. **Giel JL, Rodionov D, Liu M, Blattner FR, Kiley PJ.** 2006. IscR-dependent gene expression links iron-sulphur cluster assembly to the control of O2-regulated genes in *Escherichia coli*. Mol. Microbiol. **60:**1058-1075.

16. **Yeo WS, Lee JH, Lee KC, Roe JH.** 2006. IscR acts as an activator in response to oxidative stress for the suf operon encoding Fe-S assembly proteins. Mol. Microbiol. **61:**206-218.

17. **Wu Y, Outten FW.** 2009. IscR controls iron-dependent biofilm formation in *Escherichia coli* by regulating type I fimbria expression. J. Bacteriol. **191:**1248-1257.

18. **Cheng LW, Anderson DM, Schneewind O.** 1997. Two independent type III secretion mechanisms for YopE in *Yersinia enterocolitica*. Mol. Microbiol. **24:**757-765.

19. **Bliska JB, Guan KL, Dixon JE, Falkow S.** 1991. Tyrosine phosphate hydrolysis of host proteins by an essential *Yersinia* virulence determinant. Proc Natl Acad Sci U S A **88:**1187-1191.

20. **Auerbuch V, Golenbock DT, Isberg RR.** 2009. Innate immune recognition of *Yersinia pseudotuberculosis* type III secretion. PLoS Pathog **5:**e1000686.

21. **Warrens AN, Jones MD, Lechler RI.** 1997. Splicing by overlap extension by PCR using asymmetric amplification: an improved technique for the generation of hybrid proteins of immunological interest. Gene **186:**29-35.

22. **Andrews HL, Vogel JP, Isberg RR.** 1998. Identification of linked *Legionella pneumophila* genes essential for intracellular growth and evasion of the endocytic pathway. Infect. Immun. **66:**950-958.

23. **Merriam JJ, Mathur R, Maxfield-Boumil R, Isberg RR.** 1997. Analysis of the *Legionella pneumophila* fliI gene: intracellular growth of a defined mutant defective for flagellum biosynthesis. Infect. Immun. **65:**2497-2501.

24. **Kwuan L, Adams W, Auerbuch V.** 2013. Impact of host membrane pore formation by the *Yersinia pseudotuberculosis* type III secretion system on the macrophage innate immune response. Infect. Immun. **81:**905-914.

25. **Bou Ghanem EN, Myers-Morales T, D'Orazio SE.** 2013. A mouse model of foodborne *Listeria monocytogenes* infection. Curr Protoc Microbiol **31:**9B 3 1-9B 3 16.

26. **Auerbuch V, Isberg RR.** 2007. Growth of *Yersinia pseudotuberculosis* in mice occurs independently of Toll-like receptor 2 expression and induction of interleukin-10. Infect. Immun. **75:**3561-3570.

27. **Sheridan JJ, Logue CM, McDowell DA, Blair IS, Hegarty T.** 1998. A study of the growth kinetics of *Yersinia enterocolitica* serotype O:3 in pure and meat culture systems. J. Appl. Microbiol. **85:**293-301.

28. **Goverde RL, Kusters JG, Huis in 't Veld JH.** 1994. Growth rate and physiology of *Yersinia enterocolitica*; influence of temperature and presence of the virulence plasmid. J Appl Bacteriol **77:**96-104.

29. **Kupferberg LL, Higuchi K.** 1958. Role of calcium ions in the stimulation of growth of virulent strains of *Pasteurella pestis*. J. Bacteriol. **76:**120-121.

30. **Higuchi K, Kupferberg LL, Smith JL.** 1959. Studies on the nutrition and physiology of *Pasteurella pestis*. III. Effects of calcium ions on the growth of virulent and avirulent strains of Pasteurella pestis. J. Bacteriol. **77:**317-321.

31. **Santos JA, Pereira PJ, Macedo-Ribeiro S.** 2015. What a difference a cluster makes: The multifaceted roles of IscR in gene regulation and DNA recognition. Biochim. Biophys. Acta.

32. **Bliska JB, Wang X, Viboud GI, Brodsky IE.** 2013. Modulation of innate immune responses by *Yersinia* type III secretion system translocators and effectors. Cell. Microbiol. **15:**1622-1631.

33. **Schwartz CJ, Giel JL, Patschkowski T, Luther C, Ruzicka FJ, Beinert H, Kiley PJ.** 2001. IscR, an Fe-S cluster-containing transcription factor, represses expression of Escherichia coli genes encoding Fe-S cluster assembly proteins. Proc Natl Acad Sci U S A **98:**14895-14900.

34. **Clark MA, Hirst BH, Jepson MA.** 1998. M-cell surface beta1 integrin expression and invasin-mediated targeting of *Yersinia pseudotuberculosis* to mouse Peyer's patch M cells. Infect. Immun. **66:**1237-1243.

35. **Mecsas J, Bilis I, Falkow S.** 2001. Identification of attenuated *Yersinia pseudotuberculosis* strains and characterization of an orogastric infection in BALB/c mice on day 5 postinfection by signature-tagged mutagenesis. Infect. Immun. **69:**2779-2787.

36. **Pepe JC, Miller VL.** 1993. *Yersinia enterocolitica* invasin: a primary role in the initiation of infection. Proc Natl Acad Sci U S A **90:**6473-6477.

37. **Carter PB.** 1975. Pathogenecity of *Yersinia enterocolitica* for mice. Infect. Immun. **11:**164-170.

38. **Barnes PD, Bergman MA, Mecsas J, Isberg RR.** 2006. *Yersinia pseudotuberculosis* disseminates directly from a replicating bacterial pool in the intestine. J. Exp. Med. **203:**1591-1601.

39. **Crimmins GT, Mohammadi S, Green ER, Bergman MA, Isberg RR, Mecsas J.** 2012. Identification of MrtAB, an ABC transporter specifically required for *Yersinia pseudotuberculosis* to colonize the mesenteric lymph nodes. PLoS Pathog **8:**e1002828.

40. **Balada-Llasat JM, Mecsas J.** 2006. *Yersinia* has a tropism for B and T cell zones of lymph nodes that is independent of the type III secretion system. PLoS Pathog **2:**e86.

41. **Marteyn B, Scorza FB, Sansonetti PJ, Tang C.** 2011. Breathing life into pathogens: the influence of oxygen on bacterial virulence and host responses in the gastrointestinal tract. Cell. Microbiol. **13:**171-176.

42. **Cassat JE, Skaar EP.** 2013. Iron in infection and immunity. Cell Host Microbe **13:**509-519.

43. **Rauch I, Deets KA, Ji DX, von Moltke J, Tenthorey JL, Lee AY, Philip NH, Ayres JS, Brodsky IE, Gronert K, Vance RE.** 2017. NAIP-NLRC4 Inflammasomes Coordinate Intestinal Epithelial Cell Expulsion with Eicosanoid and IL-18 Release via Activation of Caspase-1 and -8. Immunity **46:**649-659.

44. **Brodsky IE, Palm NW, Sadanand S, Ryndak MB, Sutterwala FS, Flavell RA, Bliska JB, Medzhitov R.** 2010. A *Yersinia* effector protein promotes virulence by preventing inflammasome recognition of the type III secretion system. Cell Host Microbe **7:**376-387.

43. **Bliska JB, Black DS.** 1995. Inhibition of the Fc receptor-mediated oxidative burst in macrophages by the *Yersinia pseudotuberculosis* tyrosine phosphatase. Infect. Immun. **63:**681-685.

44. **Ruckdeschel K, Roggenkamp A, Schubert S, Heesemann J.** 1996. Differential contribution of *Yersinia enterocolitica* virulence factors to evasion of microbicidal action of neutrophils. Infect. Immun. **64:**724-733.

45. **Songsungthong W, Higgins MC, Rolan HG, Murphy JL, Mecsas J.** 2010. ROS-inhibitory activity of YopE is required for full virulence of *Yersinia* in mice. Cell. Microbiol. **12:**988-1001.